June 2009

UNIVERSITY OF CANTERBURY
Te Whare Wānanga o Waitaha
CHRISTCHURCH NEW ZEALAND

The Synthesis and Configuration of Some Polydentate Amino Acid Complexes of Cobalt(III)

A thesis submitted in partial fulfilment of the requirements

for the Degree of

Master of Science

in **Biochemistry**

at the

University of Canterbury

by

Sarah Mary Wilson-Coutts

“Don’t synthesise anything I wouldn’t synthesise.”

Michael Flanders, *At the Drop of Another Hat*, 1963

ABSTRACT

This thesis reports a study of polydentate amino acid complexes of cobalt(III). The complexes prepared during this project have been characterized by a range of techniques, including $^{13}C\{^{1}H\}$ and ^{1}H NMR spectroscopy, UV-visible spectroscopy, infra-red spectroscopy, elemental analysis and single crystal X-ray structure determination. A total of seven single crystal X-ray structure determinations have been performed during these studies.

The imino acid polydentate complex, $[Co(Aim_2trien)]_2[ZnCl_4]$, was reduced to the corresponding amino acid complex, $[Co(A_2trien)]Cl$, where as many as ten diastereoisomers could be formed due to the formation of new stereogenic centres. The crude product of these reactions was a mixture of isomers, according to $^{13}C\{^{1}H\}$ NMR data. These isomers were separated using ion-exchange chromatography. The major isomer (**I1**), a minor isomer (**I2a**) and a half reduced complex (**I4a**) from the $[Co(A_2trien)]Cl$ reduction and separation experiment were characterised. The predominant isomers produced were found to have had the proton on the α-carbon atoms positioned on the amine face of each amino acid ligand fragment.

To investigate the ratio of the isomers formed by the initial borohydride reduction, an isomerisation study of the major isomer of the $[Co(A_2trien)]^+$ complex (**I1**) was performed. This study hoped to establish the degree to which the distribution of isomers was a result of dynamic equilibrium. Experiments on a small scale showed the initial isomer distribution to be similar to that obtained from the borohydride reduction reaction. However, prolonged exposure to the carbonate buffer (≈ two weeks) resulted in isomers not previously seen. Experiments on a large scale were performed to establish whether the results were consistent. The materials from both the two hour and two week experiments were mixtures of isomers by $^{13}C\{^{1}H\}$ NMR spectroscopy and were separated using ion-exchange chromatography. ^{1}H NMR data of the two hour experiment showed only epimerisation of the amine proton adjacent to the α-carbon atom. Therefore the isomers produced from the isomerisation of **I1** have the same configuration of the proton on the α-carbon atoms, which is on the amine face of each amino acid chelate ring. ^{1}H NMR data from the two week experiment resulted in new isomers not previously seen as both

the amine proton and the proton on the α-carbon atom have been epimerised. The polyamine wrapping around the central metal ion may also have changed in some cases. It would appear, from the ^{1}H NMR data that the methyl group signals of these isomers fall in two distinct clusters; a cluster at δ 1.50-1.65 ppm and a cluster at δ 1.40-1.49 ppm. From these results, and the results of Chapter Two, it has been calculated that there is at least 92% facial selectivity for the amine face of the molecule during the initial borohydride reduction reactions. This may be due to a di-hydrogen bonding interaction between an adjacent amine proton and a hydride of the borohydride, which directs the attack.

Following on from this study, a new range of imino and amino acid complexes were synthesised using different tetraamine and pentaamine cobalt(III) complexes. X-ray quality crystals of $[Co(Aim_2 2,2,3\text{-tet})][ClO_4]$ and $[Co(Aim_2 2,3,2\text{-tet})][ClO_4]$ were obtained and solved with assistance from Dr. Chris Fitchett and Dr. Jennifer Burgess. Borohydride reductions were performed on the $[Co(Aim_2 2,2,3\text{-tet})]^{+}$ and $[Co(Aim_2 2,3,2\text{-tet})]^{+}$ systems. The products were a mixture of isomers according to ^{1}H and $^{13}C\{^{1}H\}$ NMR spectroscopy. The results from the ^{1}H NMR experiments showed similarity between the $[Co(A_2 2,3,2\text{-tet})]^{+}$ and $[Co(A_2 trien)]^{+}$ systems, where three major stereoisomers were present in solution. Analogous results for the asymmetric $[Co(A_2 2,2,3\text{-tet})]^{+}$ system were also observed. Preliminary attempts have been made to separate these isomers using ion-exchange chromatography.

ACKNOWLEDGEMENTS

My utmost thanks to my Supervisor, Assoc. Prof. Richard Hartshorn, for his constant encouragement, patience and guidance.

Sincere thanks to Dr. Chris Fitchett, Dr. Matt Polson, Dr. Jan Wikaira, Prof. Peter Steel and Dr. Jennifer Burgess for their expertise and assistance with the X-ray crystallography. Special mention must be made to Chris and Jeni for their time in helping prepare the structures in this work and dealing with CIF checks.

Thanks are also due to Dr. Marie Squire for her assistance with the NMR experiments and performing the Mass. Spec. experiments;

Thanks to Emeritus Professor Don House, for providing the tetraamine complexes used in Chapter Four.

Thanks also to the technical staff in the Department of Chemistry, particularly Wayne Mackay**,** Robert McGregor, Robert Stainthorpe and Archna Tandon.

To the past and present members of '*Team Hartshorn*' – thank you all for providing many happy times.

To my wonderful parents, Alister and Lavina Coutts, and also my brilliant Nana, Mary Wilson; thank you for your constant love and support.

Finally, my heartfelt thanks to my partner, Maurice Barnes. Without your unwavering support and love, I would have never have made it this far.

TABLE OF CONTENTS

ABBREVIATIONS

2,2,3-tet	*N*-(2-aminoethyl)-N′-(3-aminopropyl)ethane-1,2-diamine
2,3,2-tet	*N*,*N*'-bis(2-aminoethyl)propane-1,3-diamine
3,2,3-tet	*N*,*N*'-bis-(3-aminopropyl)ethane-1,2-diamine
$^{13}C\{^{1}H\}$	Proton decoupled Carbon-13 NMR
A	alanine
AA	amino acid
adj	adjacent
CIP	Cahn, Ingold and Prelog
cpg	cyclopropylglycine
dil.	dilute
E	glutamic acid
f or fac	facial
gCOSY	gradient selected COrrelation SpectroscopY
HSQCAD	Heteronuclear Single Quantum Coherence ADiabatic
I1	[Co(A_2trien)]Cl – Band 1; the major isomer
I2	[Co(A_2trien)]Cl – Band 2
I2a	[Co(A_2trien)]Cl – Band 2; a minor isomer
I3	[Co(A_2trien)]Cl – Band 3
I4a	[Co(AimAtrien)]Cl – a half reduced isomer

IR	Infra-Red frequency light
LiBKPA	Lithium 5-bromo-2-oxopentanoate
Lit.	Literature
m or mer	meridional
MHz	megahertz
NMR	Nuclear Magnetic Resonance
ppm	parts per million
R_1	Refinement factor
str	stretch
T	Temperature
tetraen	tetraethylenepentaamine
TMPS	3-(trimethylsilyl)propane-1-sulfonic acid
trien	*N*,*N*'-bis(2-aminoethyl)ethane-1,2-diamine
UV	Ultra-Violet light
vis.	Visible
Z	number of asymmetric units per cell
δ	chemical shift
ε_{max}	extinction coefficient at maximum absorbance
λ_{max}	wavelength at maximum absorbance
μ(Mo-Kα)	absorption coefficient

CHAPTER ONE

INTRODUCTION

1.1 GENERAL INTRODUCTION

What is coordination chemistry? Simply defined, coordination chemistry is the study of coordination complexes. Coordination complexes (also known as coordination entities) are described as "an assembly consisting of a central atom (usually metallic) to which is attached a surrounding array of other groups of atoms (ligands)".[1]

Coordination complexes were not formally 'discovered' until 1798, with Tassaert's accidental discovery of hexaamminecobalt(III) chloride ($CoCl_3 \cdot 6NH_3$).[2] It was not until 1869 that the first structural theory was developed by Blomstrand and Jørgensen, to explain the existence of such a compound. This theory was known as the 'chain theory'.

One idea behind the 'chain theory' was Blomstrand's belief that ammonia molecules were 'quinquvalent' – that is, with five atoms attached.[3] It was also believed that elements had only one type of valence, and so Blomstrand and Jørgensen suggested that the cobalt(III) metal ion could only have three bonds attached. In order to account for reactivities of the complexes, Jørgensen determined that those chloride ions held 'farther' from the central metal ion would precipitate immediately from silver nitrate ($AgNO_3$), and so were bonded through the ammonia chains such as the example of $CoCl_3 \cdot 6NH_3$ (Figure 1-1).[2]

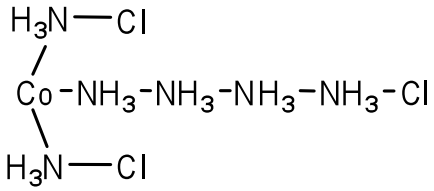

Figure 1-1: Blomstrand-Jørgensen representation of $CoCl_3 \cdot 6NH_3$

In 1893, Alfred Werner published a seminal article on the geometry of cobalt(III) complexes, such as $[Co(NH_3)_6]Cl_3$.[4] He proposed that the ligands were oriented around the central metal atom in an octahedral geometry (Figure 1-2).[3]

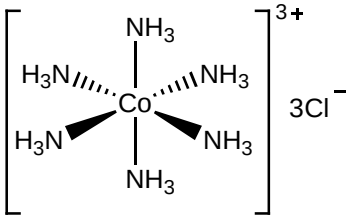

Figure 1-2: $[Co(NH_3)_6]Cl_3$ - in an octahedral coordination fashion

Werner also proposed that the existence of the *praseo* and *violeo* salts (*trans* and *cis* stereoisomers) of $[Co(en)_2Cl_2]^+$ was a consequence of the octahedral geometry of the complexes (Figure 1-3).

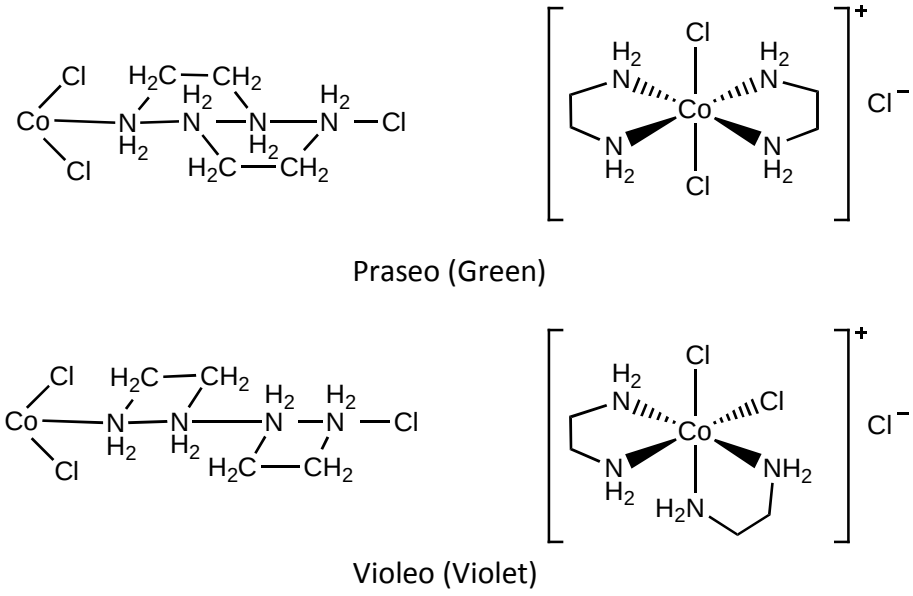

Figure 1-3: Jørgensen's and Werner's formulae for *praseo* and *violeo* ethane-1,2-diamine isomers. Jørgensen representation is on the left; Werner, on the right

By 1902, Werner had formulated the idea of 'principal and auxiliary valence'; the auxiliary valence (or coordination number) is the number of atoms or ligands attached to the central ion; while "dissociated ions... satisfy the principle valence of the central atom".[5] Werner synthesised a range of novel cobalt(III) complexes to validate his hypothesis. Jørgensen was convinced that the chain theory still accounted for the range of complexes seen, based on the varying chain lengths of the complex and precipitation of the halogens with $AgNO_3$.[5] He also criticized Werner for "predicting the existence of compounds, which were unknown", referring in particular to the "violeo" $[Co(NH_3)_4Cl_2]^+$ salts.[6] It was not until a preparation by

Werner, of *cis*-$[Co(NH_3)_4Cl_2]Cl$ in 1907 that Jørgensen conceded that this compound was “a necessary consequence” of Werner’s coordination theory.[3]

Werner’s work in this area resulted in a Nobel prize in chemistry "in recognition of his work on the linkage of atoms in molecules by which he has thrown new light on earlier investigations and opened up new fields of research especially in inorganic chemistry" and also acceptance of his coordination theory.

1.2 NOMENCLATURE AND CONFIGURATION

It was Werner who first used the *cis* and *trans* nomenclature to describe the position of ligands around the central cobalt atom, and hence the two different isomers. In 1926, Mann and Pope synthesised a series of bis(triaminopropane)-cobalt complexes “in which molecules of the aliphatic triamine have replaced the six molecules of ammonia in $[Co(NH_3)_6]Cl$”.[7] Using Werner’s octahedral configuration, Mann and Pope postulated that the complexes should exist in three isomeric forms; where “in the first two forms…the three amino groups are attached to the three corners of a triangular octahedron face” and “in the third form…the three amino groups being thus attached to the three corners of the square cross-section of the octahedron”. This initial stereochemical description formed the basis of the *fac* and *mer* descriptors (Figure 1-4).[8]

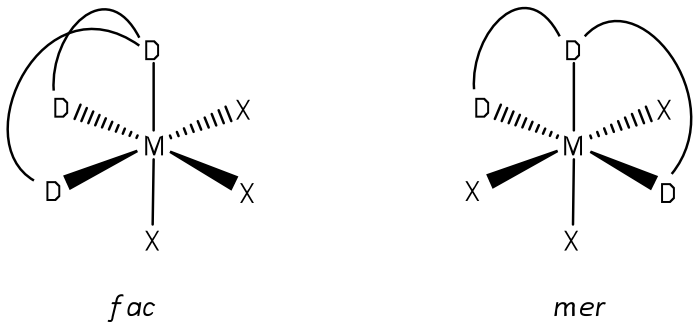

Figure 1-4: Schematic of *fac* and *mer* descriptors

The work described in this thesis involved the synthesis of complexes with polydentate ligands. As such, there are a range of different stereoisomers that could be formed, so a way

to easily describe the different isomers was required. Historically, the conventions used for the different isomers generated in inorganic complexes were primarily used to distinguish the products from different synthetic routes, where there was little or no knowledge of the stereochemistry. Complexes with linear polyamine chains, such as dichlorido *N*,*N'*-bis(2-aminoethyl)ethane-1,2-diaminecobalt(III) complexes, use the descriptors α and β, arising from the spectroscopic properties.[9] The wrapping of the linear backbone around the coordination sites can also result in the descriptors Λ and Δ provided the system is sufficiently closely related to that of a tris(bidentate) octahedral complex (Figure 1-5).

The term "configuration" defines "the arrangements of atoms of a molecular entity in space that distinguishes stereoisomers, the isomerism between which is not due to conformation differences".[10] Configuration can also be split into two classes; absolute configuration, and relative configuration.

Absolute configuration is "the spatial arrangement of the atoms of a chiral molecular entity (or group) and its stereochemical description e.g. *R* or *S* ".[10]

Relative configuration is "the configuration of any stereogenic (asymmetric) centre with respect to any other *stereogenic* centre contained within the same molecular entity. Unlike absolute configuration, relative configuration is reflection-invariant. Relative configuration, distinguishing diastereoisomers, may be denoted by the configurational descriptors ***R****, ***R**** (or *l*) and ***R****, ***S**** (or *u*) meaning, respectively, that the two centres have identical or opposite configurations. For molecules with more than two asymmetric centres the prefix *rel*- may be used in front of the name of one enantiomer where *R* and *S* have been used. If any centres have known absolute configuration then only ***R**** and ***S**** can be used for the relative configuration".[10]

The initial problem faced by inorganic chemists is having a nomenclature and configuration system that allows immediate distinction between diastereoisomers of complexes, without being cumbersome and without the need for illustration.

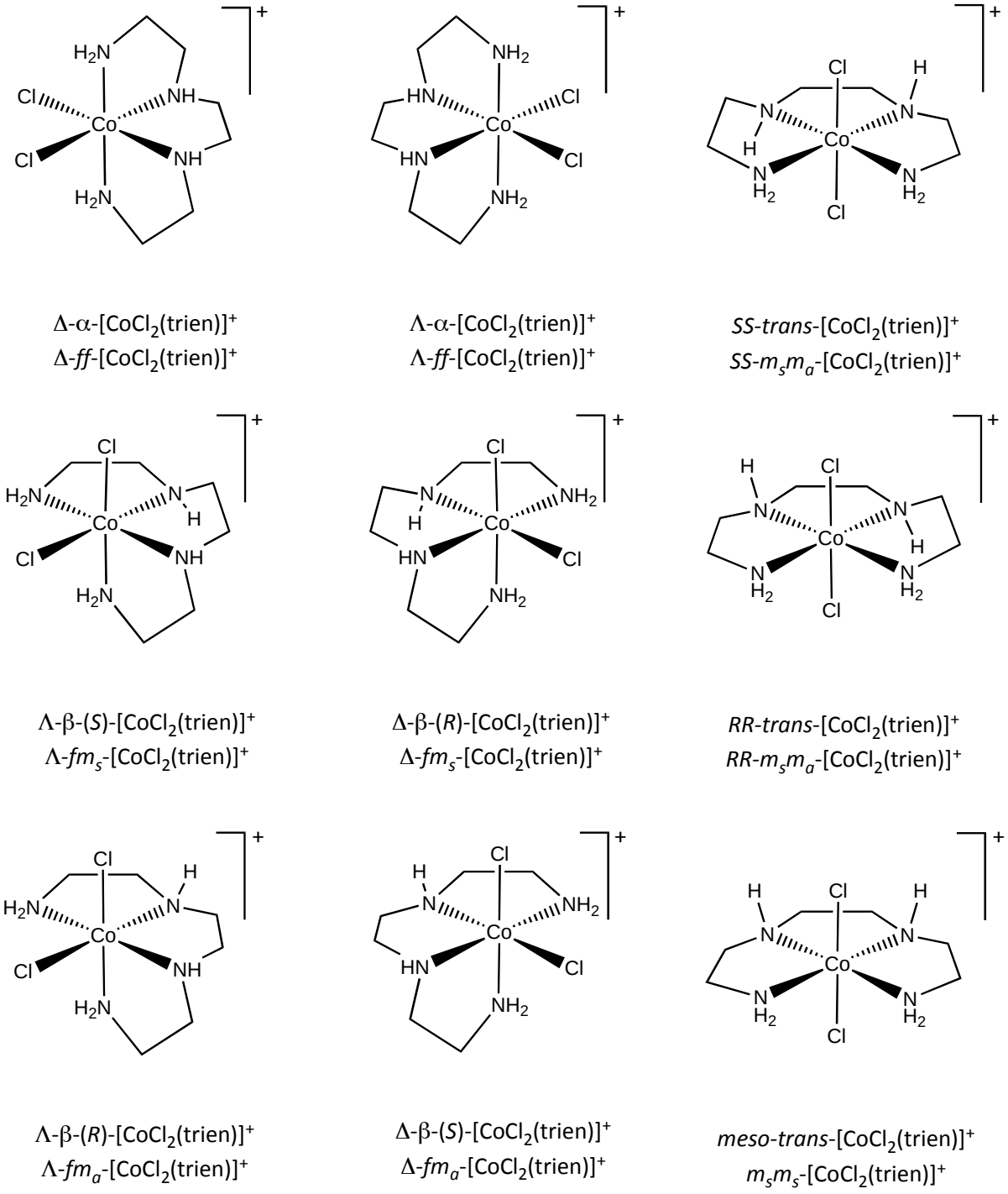

Figure 1-5: The nine isomers of $[Co(trien)Cl_2]^+$ and two nomenclature systems.

In 2005, IUPAC published their most recent recommendations for nomenclature of inorganic chemistry.[1] To describe the configuration of coordination complexes, three issues must be considered;

1) the coordination geometry – the number and location of donor atoms
2) relative configuration – where the ligands are placed relative to each other around the central metal ion
3) absolute configuration – which enantiomer is being identified

Once the coordination geometry has been determined (e.g. *OC*-6 for an octahedron) the next step is to identify which ligands occupy certain coordination positions, *i.e.* identifying the relative configuration. A *configuration index* is used to label the positions of the ligating atoms on the corner points of the polyhedra (vertices). The donor atoms are assigned priority numbers based on the rules developed by Cahn, Ingold and Prelog (CIP).[11] Simplistically, donor atoms of higher atomic number have higher priority than those of lower atomic number.

In an octahedral system, there are two digits that determine the configuration index. The first digit is the priority number of the ligating atom *trans* to the ligating atom with priority number 1. This defines the reference axis. The second digit is the priority number of the ligating atom *trans* to the most preferred ligating atom in the plane perpendicular to the reference axis (Figure 1-6).

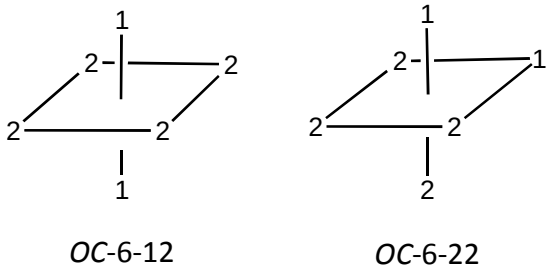

Figure 1-6: Example of an octahedral complex of the form $[MA_4B_2]$ with the configuration index assigned (where A and B have CIP priority 2 and 1 respectively)

In order to distinguish between enantiomers, there are two systems used for this purpose. The *R/S* convention is applied to tetrahedral centres (Figure 1-7). If the priority of the remaining three substituents decreases in clockwise direction, it is labelled *R* (for *Rectus*), if it decreases in counterclockwise direction, it is *S* (for *Sinister*).

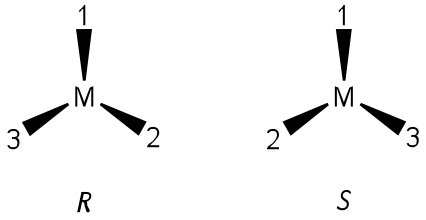

Figure 1-7: The *R* and *S* convention for tetrahedral centres

The *C/A* convention applies to other polyhedra. The atoms in the coordination plane perpendicular to the reference axis are viewed from the ligating atom with the highest priority. The sequence is then compared (Figure 1-8). The structure is assigned *C* (for clockwise) or *A* (for anticlockwise).

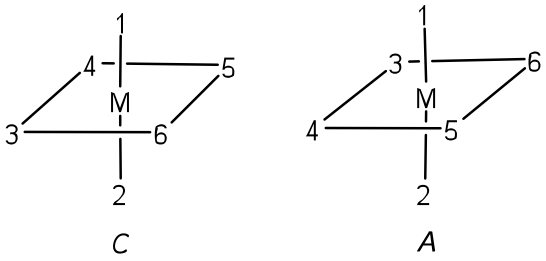

Figure 1-8: The *C* and *A* convention for octahedral centres

These IUPAC conventions allow absolute configurations to be assigned for complexes. Unfortunately configuration indices for closely related complexes can be rather different and thereby obscure interpretation of the stereochemical course of a reaction.

In 1998, Hartshorn and House published an article to propose a new nomenclature system for distinguishing diastereoisomers that result from wrapping polydentate ligands around octahedral metal ions.[12] To allow the reader to readily visualize the wrapping of the ligand segment around the central metal atom, the conventional *facial* and *meridional* designators have been used. If the spatial arrangement of atoms on central donors needs to be described, the symbols *s* (for *syn*) and *a* (for *anti*) are used. Using this nomenclature, the reader can easily envisage the wrapping of the ligand around the central metal ion, and the

diastereoisomer that is being described (Figure 1-9). Such descriptions may make the stereochemical course of a reaction more obvious.

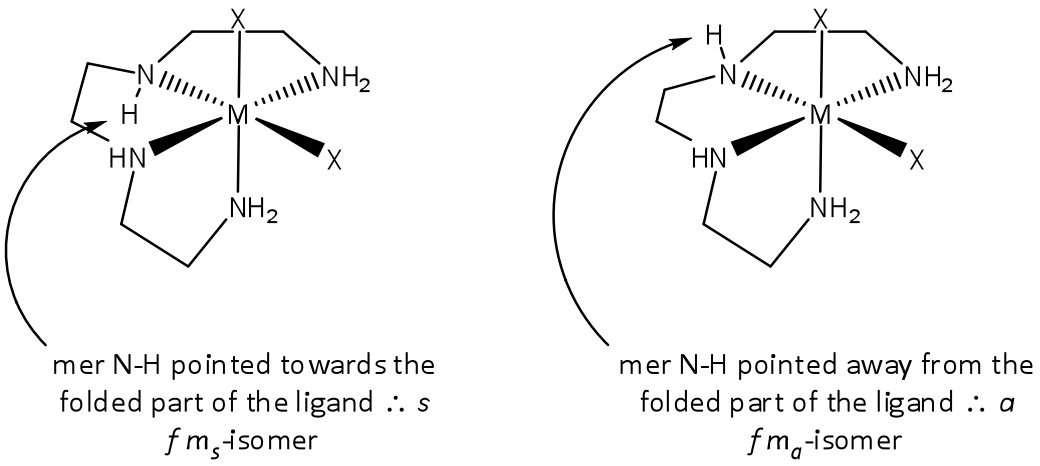

Figure 1-9: Description of *syn* and *anti* subscripts to indicate the location of substituents of meridional donor groups[12]

Complex polydentate ligands generally have abbreviated names to simplify discussion, and also provide a shorthand name for molecular formulae. The *N*,*N*'-bis(2-aminoethyl)ethane-1,2-diamine ligand is normally abbreviated to "trien". This in turn allows the complex *N*,*N*'-bis(2-aminoethyl)ethane-1,2-diaminedichloridocobalt(III) monocation to be simplified in a formula to $[Co(trien)Cl_2]^+$.

Work in this thesis involves the synthesis of complexes of polydentate ligands. The abbreviations used to describe these ligands have been previously described.[13] However, a brief explanation of the nomenclature follows.

For example, consider the nomenclature for the $[Co(A_2trien)]^+$ complex (1) shown in Figure 1-10.

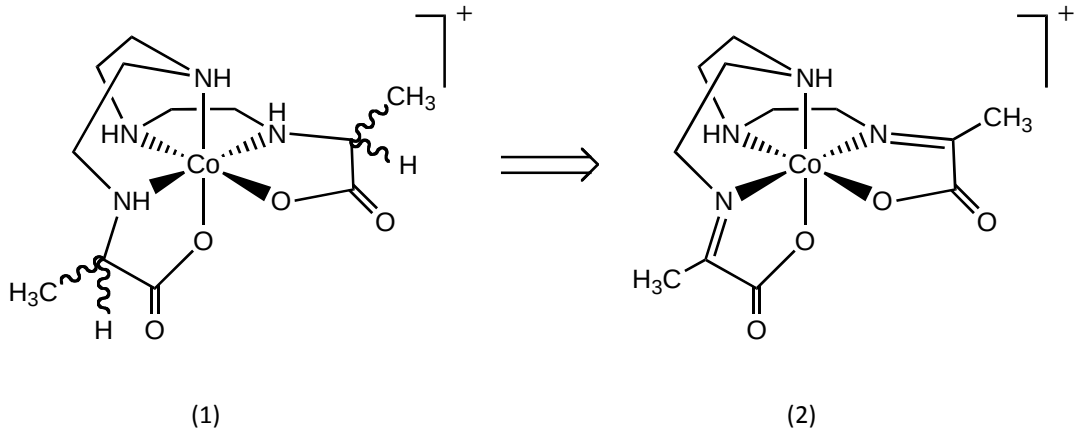

(1) (2)

Figure 1-10: Retrosynthesis of $[Co(A_2trien)]^+$ (1) from $[Co(Aim_2trien)]^+$ (2)

Abbreviations for the amino acid ligand are constructed from the accepted single letter abbreviation for the related amino acid (*e.g.* A = alanine, E = glutamic acid), followed by the accepted abbreviation for the polyamine to which the residue is fused. The abbreviation 'im' indicates that the residue is at the imine oxidation level.

1.3 COBALT(III) CHEMISTRY

The cobalt(III) ion is an ideal metal ion for the study of inorganic reaction mechanisms, configuration and stereochemistry, due to the characteristic properties found for most of its complexes: inertness; octahedral coordination; diamagnetism and colour.

1.3.1 INERTNESS

A definition of chemical inertness is 'stable and unreactive under specified conditions'.[10] Cobalt(III) is an example of a strong field d^6 octahedral complex, and, when complexed in the +3 oxidation state, is normally inert. Because octahedral cobalt(III) complexes are inert, structural assignment and configurations can be made with greater confidence, as processes such as ligand substitution and/or interconversion do not occur sufficiently rapidly to confuse such assignments. Research in this thesis also relies on the inertness of cobalt(III)

due to the need to separate and characterise many of the stereoisomers that are being studied. If the complexes were not inert, the stereoisomers may interconvert before they could be characterised.

1.3.2 OCTAHEDRAL COORDINATION

"Six coordination is the most common arrangement for electronic configurations ranging from d^0 to d^9"[14] and for metals in the +3 oxidation state, they are almost exclusively found in an octahedral geometry (Figure 1-11).[14] Because of this coordination geometry, and due to the inertness of the cobalt(III) ion, the wrapping of ligands around the central metal atom is well defined.

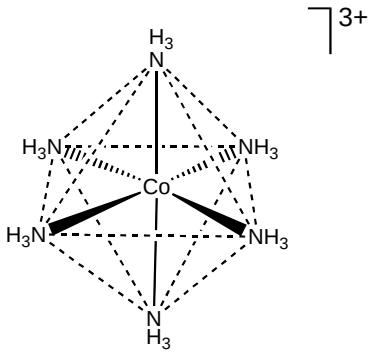

Figure 1-11: The $[Co(NH_3)_6]^{3+}$ complex, showing octahedral coordination (in solid bonds and wedges), the dashed lines indicating the faces of the octahedron

1.3.3 DIAMAGNETISM

Another key characteristic of most cobalt(III) complexes is diamagnetism. This property allows the complexes to be monitored and studied using nuclear magnetic resonance (NMR) spectroscopy techniques. For example, information from ^{1}H and $^{13}C\{^{1}H\}$ spectra allows determination of what functional groups are present (for example, the assignment of primary, secondary and tertiary amines can be deduced based on chemical shift data for the adjacent carbon atoms). By using NMR spectroscopy, the course and completeness of a reaction can be monitored. For example, using $^{13}C\{^{1}H\}$ NMR spectroscopy, the imine carbon atom chemical shift (generally found at ≈160-180 ppm) displacement to the amine carbon atom

chemical shift (found at ≈40-65 ppm, depending on coordination) is a useful indicator on whether a desired reduction reaction has been completed. Use of two-dimensional NMR spectroscopy techniques allows greater certainty in structural assignments, particularly when the reactions have resulted in isomerised complexes.

1.3.4 COLOUR

The colour of transition metal complexes (and in this case, specifically, cobalt(III)) is a function of the ligands that are attached to the central metal ion. By changing a ligand, there is a change of colour. For example, $[Co(NH_3)_6]^{3+}$ is a yellow/orange colour and absorbs at around 475 nm. If one ligand is exchanged for, in this example, a chloride, then the resulting $[Co(NH)_5Cl]^{2+}$ complex is a purple colour and has a visible absorption maximum at 530nm. Such changes allow reactions (and resulting compounds) to be monitored by UV-visible spectroscopy. It also provides a qualitative handle on whether a reaction has occurred.

1.4 AMINO ACID COMPLEXES

1.4.1 PREVIOUS RESEARCH

The interconversion of amino acids and α-keto acids is a reaction catalysed by transanimases in biological systems. For example, the enzyme glutamate:alanine aminotransferase catalyses the transfer of an amino group from alanine to α-ketoglutarate, the products of this reversible transamination reaction being pyruvate and glutamate.

Initial studies of pentaammine and tetraammine amino acid complexes can be traced back to 1965.[15]

Amino acid complexes were synthesised by Harrowfield and Sargeson in order to investigate ‘metal-template’ reactions, where the coordination of an amino acid fragment occurs *via* an intramolecular condensation reaction, shown in Figure 1-12.[16]

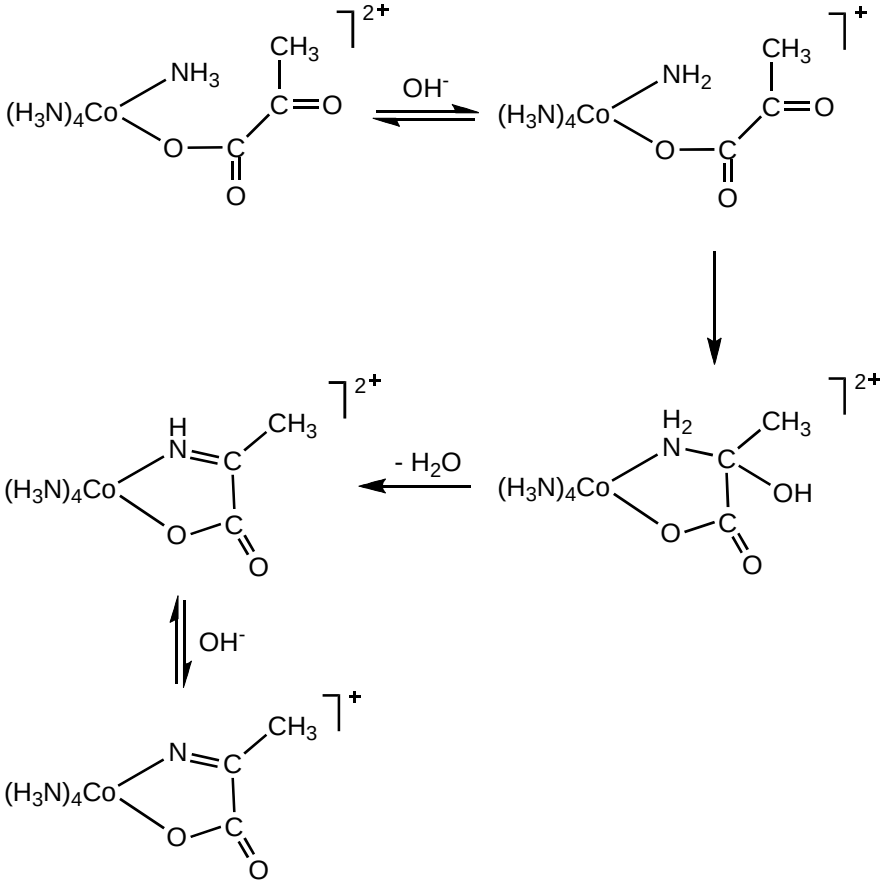

Figure 1-12: Schematic of intramolecular imine formation *via* a metal-template reaction

Research from this area led to studies of the regio- and stereoselectivity in coordination of amino acids, focussing on areas such as proton exchange, carbinolamine formation, mutarotation and selectivity of borohydride reduction.[13, 17-25]

In view of the complexity of the system, the synthesis of specific polydentate amino acid complexes needs some degree of diastereoselectivity, and stereoselectivity in order to limit the number of isomers produced. By using conditions (and reagents) that exhibit such selectivity, the synthesis and characterization of particular isomers of the resulting compounds would be greatly helped.

1.4.2 Synthesis of the Amino Acid Complexes

Previous research by Hartshorn *et al.* focused on the synthesis of polydentate amino acids *via* imines.[13] The imine intermediates were obtained by coordination and condensation of various keto acids with a cobalt complex with a polyamine backbone, such as that of *N*,*N'*-bis(2-aminoethyl)ethane-1,2-diamine (trien) (Figure 1-13). Due to the imine bond preferentially being held in a planar conformation, this limits the number of stereoisomers formed (the preference for imine planarity is discussed in Section 1.4.3).

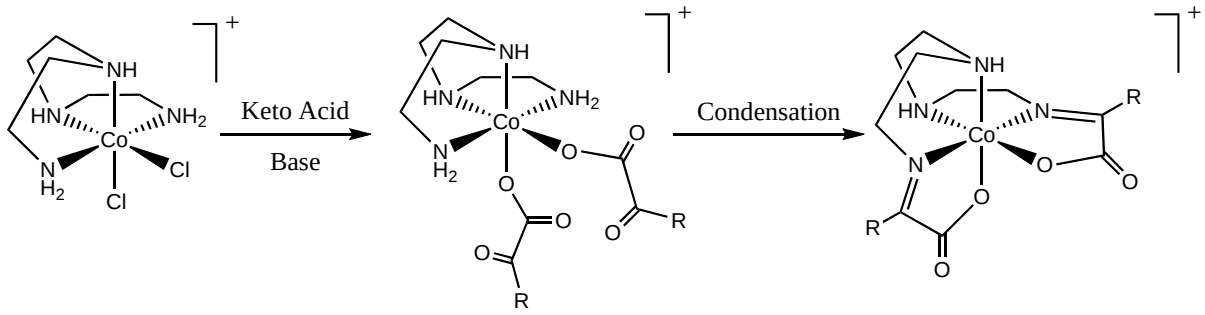

Figure 1-13: Coordination and condensation of a keto acid

Imine reduction with borohydride is a straight-forward reaction with much precedent in the literature.[13, 16, 25] In this case however, it results in a significant increase in configurational complexity. The resulting complexity from the borohydride reduction is due to the formation of four new stereogenic centres in addition to the pre-existing stereogenic centre at the cobalt(III) ion (Figure 1-14).

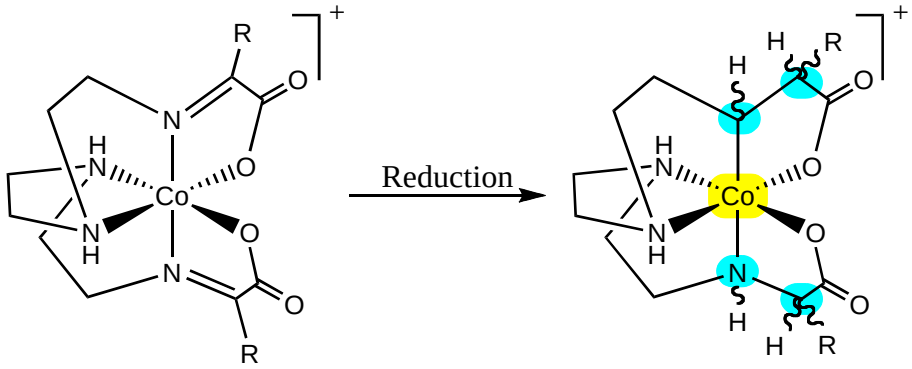

Figure 1-14: Reduction of the imine forms the amino acid complex; stereogenic centres in the resulting complex are highlighted; the new stereogenic centres are highlighted in blue, while the pre-existing stereogenic centre is highlighted in yellow

The reduction reaction involving a tetraamine backbone may result in as many as 2^5 stereoisomers. However, with a symmetrical tetraamine, such as *N*,*N'*-bis(2-aminoethyl)ethane-1,2-diamine complexes (Figure 1-14), only twenty stereoisomers (or ten pairs of enantiomers) are able to be formed. Which isomers may be produced is discussed in detail in Chapter Two.

Previous preliminary studies show that only a few of the possible diastereoisomers are produced in any significant amount from the system shown in Figure 1-14. [26, 27]

A possible explanation for this observation is the mechanism by which borohydride acts. It is well documented in the literature that borohydride reacts typically in an *anti* fashion across a double bond.[28] This would limit the diastereoisomers formed, but other factors may also be involved and one goal of this project is to examine this possibility.

A study by Pearce *et al.* [25] of reduction by dithionite and borohydride of coordinated α-imino acids demonstrated that borohydride reduction occurred preferentially *via* hydride attack on the more hindered face of the imino-acidato ligand (Figure 1-15), leading to more of one diastereoisomer being produced.

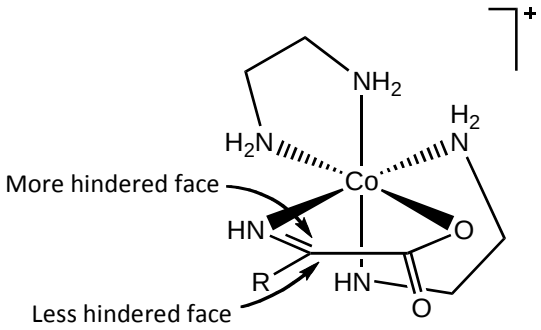

Figure 1-15: Schematic of the hydride attack on the imine

The idea of selectivity based on steric constraints, such as in the bis(1,2-ethanediamine) system shown above, may also provide some understanding of the selectivity shown in polyamine cobalt(III) systems, but it was unclear why attack should be favoured from the more hindered face.

1.4.3 Stereochemical Control of the Condensation Reaction and Imine Planarity

As mentioned earlier the imino acid complexes have generally been synthesised *via* a 'template reaction' (Figure 1-16).

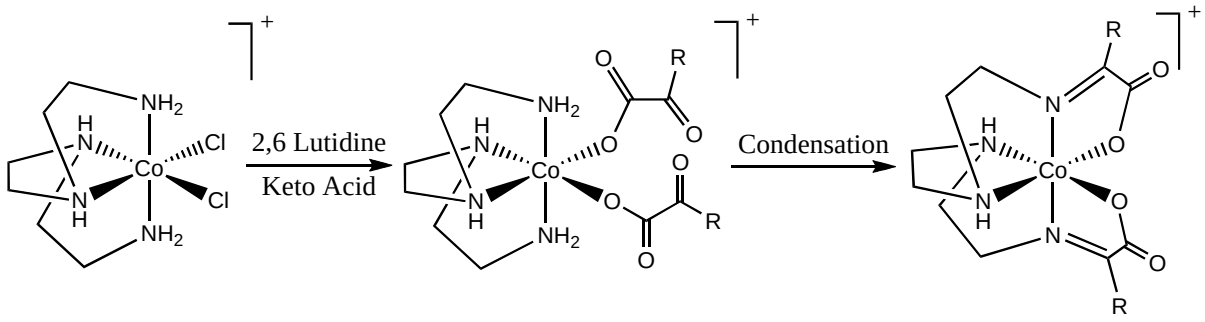

Figure 1-16: The coordination and condensation of a keto acid to form the imino acid complex

This particular reaction was of interest regarding possible stereoselectivity of the coordinating amino acid fragment. Further work by Sargeson *et al.* investigated the condensation reaction of $[Co(tren)Cl(NH_2CH_2CH(OH)_2)]^{2+}$, with the chloride ion *trans* to a primary amine group. It was observed that the reaction was completely stereoselective for the amine *trans* to the coordinated chloride (Figure 1-17). Proton exchange at this centre occurs ≈100-fold faster than a similar primary amine centre *cis* to the coordinated chloride.[29]

Such an observation regarding the relative acidities of primary amines led to further investigation of this, in particular regarding the preferred geometry of the resulting imine from condensation reactions, such as the work from Engelhardt *et al.* [22]

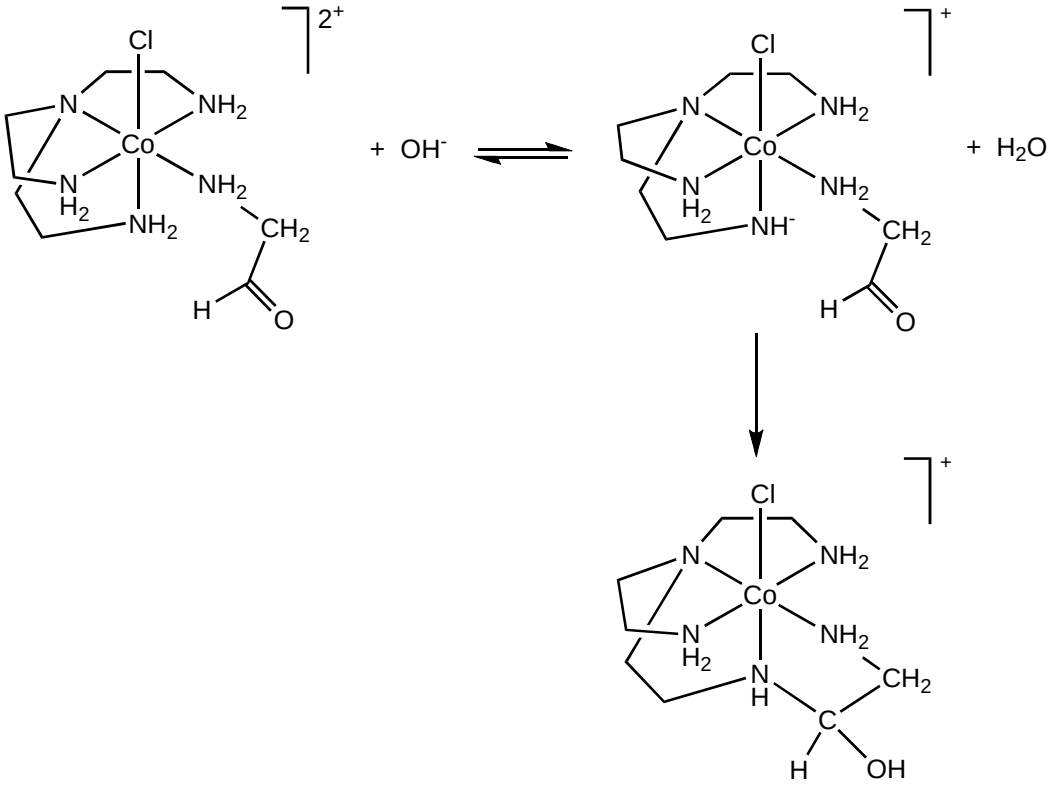

Figure 1-17: Condensation reaction of $[Co(tren)Cl(NH_2CH_2CH(OH)_2)]_2^+$, forming the carbinolamine intermediate

In 2001, Browne *et al.* [24] reinvestigated the reaction between a coordinated aminoacetaldehyde and a metal complex, in this case $[Co(trien)Cl_2]^+$. Reports of one of the complexes that had been isolated from the Engelhardt study suggested that the imine adopted an "angular" geometry (Figure 1-18), where the imine nitrogen atom and the two adjacent amine donors adopt a facial disposition around the cobalt(III) ion.[22, 24]

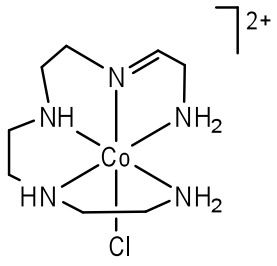

Figure 1-18: *ffm*$_s$-$[Co(tetraenim)Cl]^{2+}$; note the angular imine *trans* to the chloride ligand

The initial assignment of the "angular" imine was the subject of the re-investigation. Under aqueous conditions, imines are susceptible to hydrolysis, however, when coordinated to an

inert cobalt(III) ion, the bond is stabilised. Such stability may arise from the chelate effect (where the stability of a complex containing chelate rings is enhanced compared to similar complexes without chelate rings).[30] Possible back donation of π electrons between the cobalt(III) ion and the imine nitrogen may result in a synergistic effect, where the filled π* orbitals reduces susceptibility to nucleophilic attack.[26]

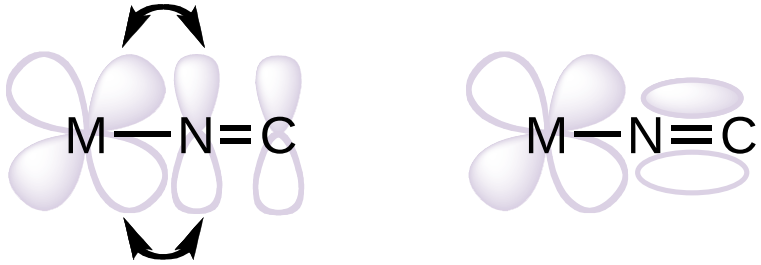

A B

Figure 1-19: Diagrams showing π symmetry orbitals. Metal d-orbital- π* overlap is shown in A and the d-orbital and π orbital in B (note that overlap is not possible in this case because the π orbital is between the C and N atoms)

The greater the overlap of the π orbitals for an imine results in greater thermodynamic stability (Figure 1-19). If the imine is twisted from a planar geometry, the reduced overlap of the π orbitals will lead to a reduction of thermodynamic stability. Therefore an imine in a meridional geometry (with respect to the two neighbouring atoms) will possess the greatest π orbital overlap.

By re-examining the reaction of *ffm*$_s$-[Co(tetraenim)Cl]$^{2+}$, Browne *et al.* [24] were able to confirm that the site of the initial reaction was at the primary amine group *trans* to the chloride ion, however the dehydration of the carbinolamine intermediate could not proceed, due to the 'angular' imine. It was shown that the ligand is able to rearrange due to aquation, and subsequently allow formation of a planar imine. Due to the ligand rearrangement, the elimination reaction can then proceed.

1.5 WORK DESCRIBED IN THIS THESIS

Chapter two of this work reports on the separation and characterisation of polydentate amino acid cobalt(III) complexes. As part of this study, further work on the imine synthesis and borohydride reduction on the [Co(Aim$_2$trien)]Cl system is described. The separation and characterisation of some isomers of the [Co(A$_2$trien)]$^+$ system is also described.

Chapter three of this work is an extension of the results from the borohydride reduction. It is possible that the amine proton and α-carbon protons may subsequently exchange under mildly basic reaction conditions and this has been investigated. After purification and characterization of the major isomer (**I1**), isomerisation studies were performed by re-dissolving **I1** in a basic solution to investigate whether epimerization occurs. This will allow examination of whether the isomer distribution from the borohydride reduction is a result of stereoselective reaction or subsequent equilibration.

Chapter four extends the chemistry from Chapter Two, by using different polyamine backbones on the cobalt(III) complexes, which are then used in the intramolecular condensation reaction with pyruvic acid. The imine synthesis and borohydride reduction on the imino acid complexes are described.

Chapter five suggests possible future avenues for work on this project.

1.6 REFERENCES

[1] N. G. Connelly, T. Damhus, R. M. Hartshorn, and A. T. Hutton, 'Nomenclature of Inorganic Chemistry : IUPAC recommendations ', RSC Publishing, 2005.

[2] F. Basolo and R. C. Johnson, 'Coordination chemistry : the chemistry of metal complexes', W. A. Benjamin, 1964.

[3] G. B. Kauffman, 'Inorganic coordination compounds', Heyden, 1981.

[4] A. Werner, *Zeitschrift fuer Anorganische Chemie* 1893, **3**, 267.

[5] G. B. Kauffman, A. Werner, American Chemical Society. Division of Inorganic Chemistry., and American Chemical Society. Division of the History of Chemistry., 'Werner centennial : a symposium', American Chemical Society, 1967.

[6] J. C. Bailar and D. H. Busch, 'The chemistry of coordination compounds', Reinhold, 1956.

[7] F. G. Mann and W. J. Pope, *Journal of the Chemical Society*, 1926, 2675.

[8] Y. Saito, *Top. Stereochem.*, 1978, **10**, 95.

[9] A. M. Sargeson and G. H. Searle, *Inorganic Chemistry*, 1965, **4**, 45.

[10] A. D. McNaught and A. Wilkinson, 'Compendium of Chemical Terminology : IUPAC recommendations', Blackwell Science, 1997.

[11] R. S. Cahn, C. Ingold, and V. Prelog, *Angewandte Chemie-International Edition*, 1966, **5**, 385.

[12] R. M. Hartshorn and D. A. House, *Journal of the Chemical Society-Dalton Transactions*, 1998, 2577.

[13] J. M. W. Browne, J. Wikaira, C. M. Fitchett, and R. M. Hartshorn, *Journal of the Chemical Society-Dalton Transactions*, 2002, 2227.

[14] D. F. Shriver and P. W. Atkins, 'Inorganic chemistry', Oxford University Press, 2002.

[15] J. Fujita, T. Yasui, and Y. Shimura, *Bulletin of the Chemical Society of Japan*, 1965, **38**, 654.

[16] J. M. Harrowfield and A. M. Sargeson, *Journal of the American Chemical Society*, 1974, **96**, 2634.

[17] D. A. Buckingham, L. G. Marzilli, and A. M. Sargeson, *Journal of the American Chemical Society*, 1967, **89**, 5133.

[18] A. R. Gainsford and A. M. Sargeson, *Australian Journal of Chemistry*, 1978, **31**, 1679.

[19] A. R. Gainsford, R. D. Pizer, A. M. Sargeson, and P. O. Whimp, *Journal of the American Chemical Society*, 1981, **103**, 792.

[20] P. J. Lawson, M. G. McCarthy, and A. M. Sargeson, *Journal of the American Chemical Society*, 1982, **104**, 6710.

[21] P. A. Sutton and D. A. Buckingham, *Accounts of Chemical Research*, 1987, **20**, 357.

[22] L. M. Engelhardt, A. R. Gainsford, G. J. Gainsford, B. T. Golding, J. M. Harrowfield, A. J. Herlt, A. M. Sargeson, and A. H. White, *Inorganic Chemistry*, 1988, **27**, 4551.

[23] D. A. Buckingham, I. Stewart, and P. A. Sutton, *Journal of the American Chemical Society*, 1990, **112**, 845.

[24] J. M. W. Browne, J. Wikaira, and R. M. Hartshorn, *Journal of the Chemical Society-Dalton Transactions*, 2001, 3513.

[25] D. A. Pearce, R. M. Hartshorn, and A. M. Sargeson, *Journal of the Chemical Society-Dalton Transactions*, 2002, 1747.

[26] J. M. Browne, 'Intramolecular condensation reactions of cobalt(III) complexes : a thesis submitted in partial fulfilment of the requirements for the degree of Master of Science in Chemistry at the University of Canterbury', 2000.

[27] L. C. Marsh, 'B.Sc. Hons. Report; Department of Chemistry, University of Canterbury', 2001.

[28] M. Smith and J. March, 'March's advanced organic chemistry : reactions, mechanisms, and structure', John Wiley, 2001.

[29] B. T. Golding, J. M. Harrowfield, and A. M. Sargeson, *Journal of the American Chemical Society*, 1974, **96**, 3003.

[30] J. Ribas Gispert, 'Coordination chemistry', Wiley-VCH, 2008.

CHAPTER TWO

POLYDENTATE AMINO ACID COMPLEXES - SEPARATION AND CHARACTERISATION OF ISOMERS

2.1 INTRODUCTION

Previous work by Hartshorn *et al.* showed that coordinated amino acids, which are part of a polydentate framework, form stable metallocyclic compounds following radiation.[1, 2] This project arose from attempts to prepare new polydentate amino acid complexes that might be useful for further study of the photochemical reactions.

The syntheses of these amino acid complexes relies on keto acid substitution onto the polyamine cobalt(III) complex followed by an intramolecular condensation reaction and then reduction with borohydride (Figure 2-1).

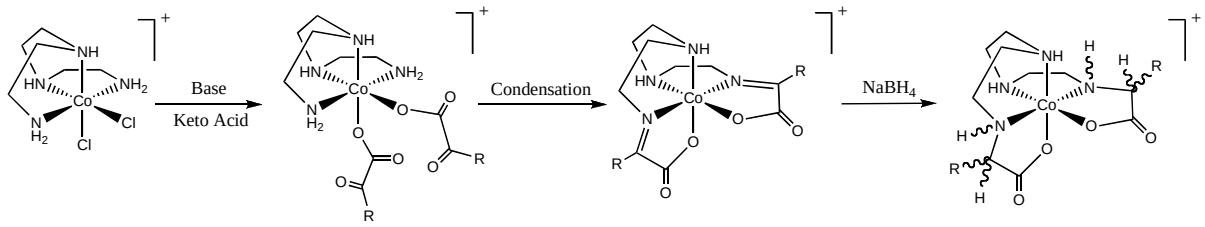

Figure 2-1: An example of a double intramolecular condensation and reduction reaction of $[Co(trien)Cl_2]^+$ and a keto acid

The intramolecular condensation reaction is a facile process provided it can result in a planar imine group. In other cases, however, isomerisation of the polyamine backbone may occur to allow a planar imine to form.[3] Due to the driving force for the imine formed to be held in a planar conformation, the condensation reaction is stereoselective. Other isomers of the dichloride starting material, such as *fm*$_s$-, *fm*$_a$-, *m*$_s$*m*$_a$-, and *m*$_s$*m*$_s$- give the diimine complex shown above.

The final step, formation of the amino acid complexes, is a simple reduction reaction using sodium borohydride. The reduction of the imine is achieved though hydride attack on the α-carbon atom, with protonation of the amine. The hydride may attack from either one of the two faces of each imine, and the face chosen determines the configuration at the α-carbon atom in the initial product. Protonation of the nitrogen atom can also occur on either face.

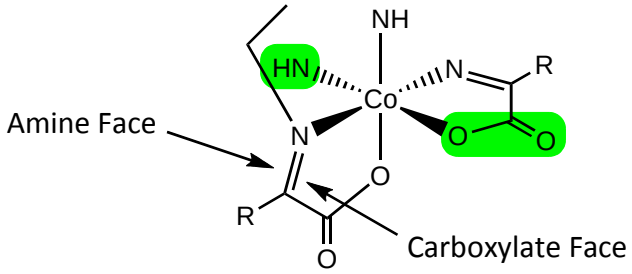

Figure 2-2: Schematic of possible directions of BH_4^- attack

The highlighted functional groups (Figure 2-2) are used to identify the faces. Some atoms and bonds are omitted for clarity.

The reduction reaction of [Co(Aim$_2$trien)]Cl generates four new stereogenic centres, indicated in blue in Figure 2-3, in addition to the one already present (at the cobalt centre, indicated in yellow).

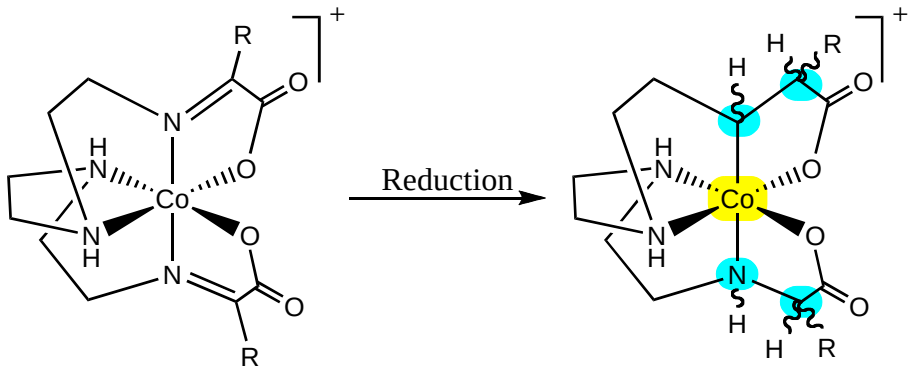

Figure 2-3: Reduction of the imino acid complex to the amino acid complex. New stereogenic centres are highlighted in blue

In all, there are twenty stereoisomers that could be formed (Figure 2-4) without altering the wrapping of the initial polyamine portion of the ligand. This is discussed further in section 2.4.3.

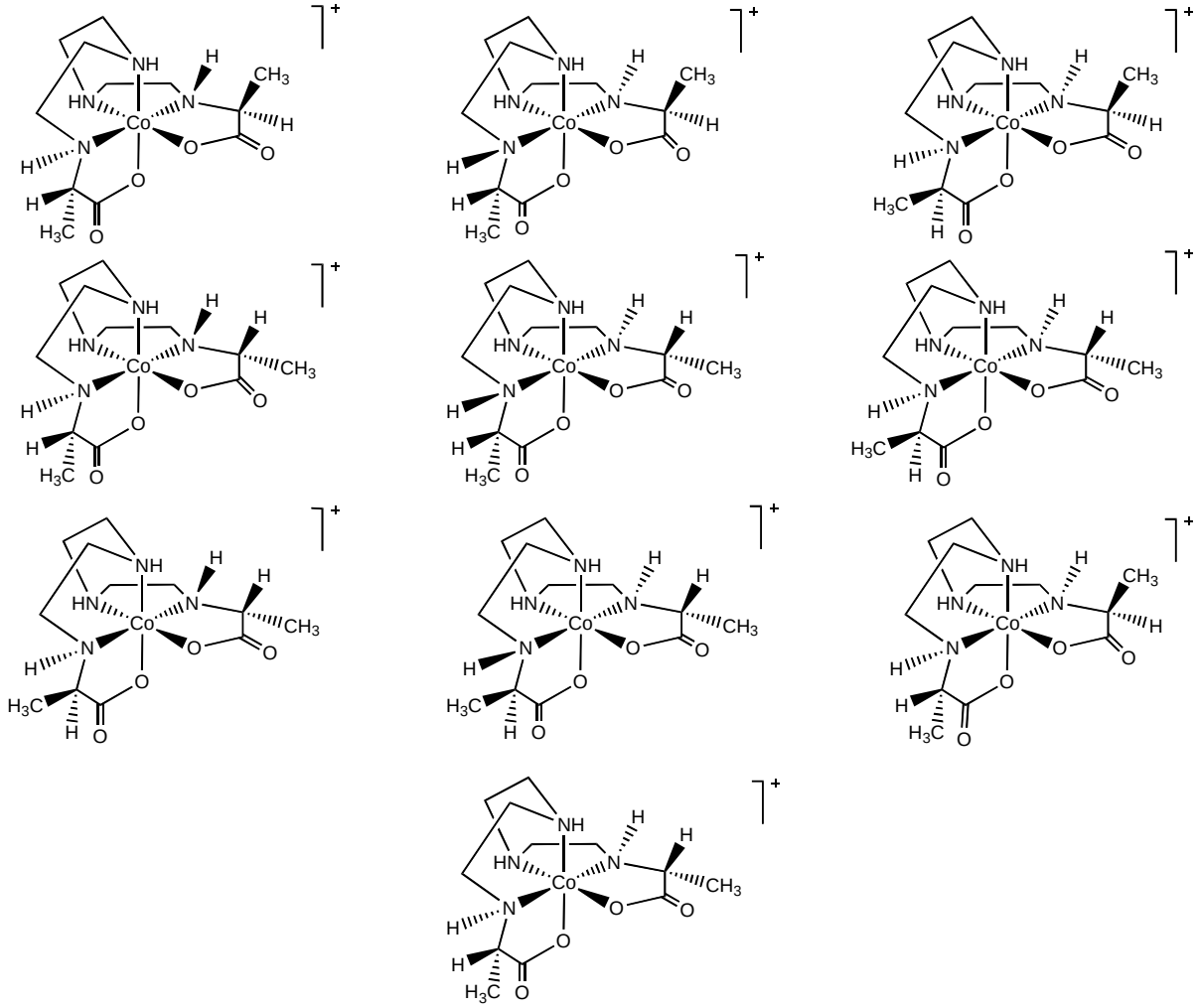

Figure 2-4: The ten diastereoisomers formed from the reduction reaction. The remaining ten stereoisomers are each an enantiomer of one of these shown

A preliminary study of this system has shown that only a few of the isomers are formed in any significant amount.[4]

The goal of this work was to identify and characterise the principal stereoisomers that resulted from the borohydride reduction reaction. By studying this, it is hoped that an understanding of why the hydride attack is selective might be achieved, and to learn about the level of control that may be able to be exerted on the chemistry of the imine ligand as a result of it being bound to the metal centre.

This chapter therefore describes the synthesis of cobalt(III) amino acid complexes with a *N*,*N'*-bis(2-aminoethyl)ethane-1,2-diamine backbone and the separation and characterisation of the isomers formed from this reaction.

2.2 EXPERIMENTAL

2.2.1 MATERIALS

Reagents and solvents were obtained from Sigma Aldrich or Merck and were of reagent grade or better and were used without further purification, unless stated otherwise. Distilled H_2O was used unless stated otherwise.

[Co(tetraen)Cl]$ZnCl_4$,[5] *ff*-[Co(trien)Cl_2]Cl,[6] *mffm*-[Co(Aim$_2$trien)]$_2$[$ZnCl_4$],[3] *mffm*-[Co(Aimtetraen)]$ZnCl_4$,[3] and LiBKPA[7-10] were prepared according to literature methods.

Dowex 50WX2-200 (cation exchange resin), Dowex 50WX2-400 (cation exchange resin) and SP Sephadex C25 ion exchange resins were obtained from Sigma Aldrich. Column dimensions are given as (height x diameter).

2.2.2 INSTRUMENTATION/MEASUREMENTS

^{1}H, gCOSY and HSQCAD experiments were all recorded on a Varian INOVA 500 spectrometer at 23℃, operating at 500 MHz. The INOVA was equipped with a variable temperature and inverse-detection 5 mm probe or a triple-resonance indirect detection PFG probe. The ^{13}C{^{1}H} NMR spectra were recorded on either a Varian UNITY 300 NMR spectrometer equipped with a variable temperature direct broadband 5 mm probe, at 23℃, operating at 75 MHz or on a Varian INOVA 500 spectrometer at 23℃, operating at 125 MHz, using a 5mm variable temperature switchable PFG probe. Chemical shifts are expressed in parts per million (ppm) on the δ scale and were referenced to the appropriate solvent peaks: DMSO-d_6 referenced to CD_3(C**H**D_2)SO at δ_H 2.50 (^{1}H) and (**C**D_3)$_2$SO at δ_C 39.6 (^{13}C). As reference in D_2O and DCl (99% D, 35 wt. % in D_2O), 3-(trimethylsilyl)propane-1-sulfonic acid (TMPS) or 3-(trimethylsilyl)propionic acid-d_4 sodium salt was used as an internal standard (δ_H 0 (^{1}H); δ_C 0 (^{13}C)).

Infrared spectra were obtained using a Shimadzu 8201PC Series FTIR using diffuse reflectance method in solid KBr.

High Resolution Electrospray Ionisation Mass Spectra (HRESIMS) were recorded on a Micromass LCT spectrometer using a probe voltage of 3200V, an operating temperature of 150°C and a source temperature of 80°C. The carrier solvent was 50:50 CH_3CN/H_2O at 20 μL/minute. Typically, 10 μL of a 10 μg/mL solution was injected. Leucine enkephalin was used as the lock mass internal standard.

UV-visible spectra were recorded on a Varian CARY Probe 50 UV-vis. spectrophotometer, or a Varian CARY 100 UV-vis. spectrophotometer.

Evaporations were performed using a Büchi rotary evaporator equipped with either a diaphragm vacuum pump or a water aspirator pump (pressure $\approx$ 15 torr) and with a water bath temperature of 40°C unless otherwise stated.

Elemental analyses were performed by the Campbell Microanalytical Laboratory at the University of Otago.

2.2.3 PREPARATIONS

2.2.3.1 SYNTHESIS OF THE IMINES

mffm-[Co(Aim$_2$trien)]$_2$[ZnCl$_4$]

mffm-[Co(Aim$_2$trien)]$_2$[ZnCl$_4$] was prepared according to the literature method[3] except in a larger scale reaction, with comparable results. _ff_-[Co(trien)Cl$_2$]Cl (2.34 g, 7.6 mmol), pyruvic acid (2.66 g, 30 mmol), 2,6-lutidine (3.20 g, 30 mmol) and 400 mL of methanol were heated at reflux for 24 hours. Methanolic ZnCl$_2$ (ZnCl$_2$ (1.04 g, 7.6 mmol) in 15 mL of methanol) was added dropwise to the hot solution and heated at reflux for a further 1 hour. The solution was cooled at room temperature for 48 hours during which time an orange precipitate formed. The volume was reduced to 100 mL on a rotary evaporator at 40°C, cooled at -10°C and filtered under suction to give an orange microcrystalline powder.

Yield: 2.58 g, (89.74%). $^{13}C\{^1H\}$ NMR (ppm); 182.9 (C=N), 175.8 (COOM), 57.9, 56.9, 55.7 (CH_2NH_2), 21.1 (CH_3).

mffm-[Co(Eim$_2$trien)]Cl

_ff_-[Co(trien)Cl$_2$]Cl (0.93 g, 3 mmol), α-ketoglutaric acid (2.20 g, 15 mmol), LiOH (0.73 g, 15 mmol) and 250 mL of methanol were heated at reflux for 18 hours. Methanolic ZnCl$_2$ (ZnCl$_2$ (0.62 g, 4.5 mmol) in 30 mL of methanol) was added dropwise to the hot solution and left to cool to room temperature during which time a red/orange precipitate formed. The solution was filtered under suction to give a red/orange powder.

Yield: 0.68 g, (33.80%). This crude material was found to contain impurities and so purification was conducted using ion-exchange chromatography.

mffm-[Co(Eim$_2$trien)]$_2$ZnCl$_4$ (0.68 g, 1.02 mmol) was dissolved in 500 mL of H_2O and was adsorbed onto a H^+- Dowex 50WX2-400 column (24 x 5 cm). The column was washed with H_2O (1 L) and eluted with 0.2 M HCl (11 L). The orange eluate was taken to dryness by rotary evaporation at 40°C.

Yield: 0.46 g, (91.20%). Anal. Calcd. for $C_{16}H_{24}ClCoN_4O_8 \cdot 3H_2O$: C, 35.02; H, 5.51; N, 10.21. Found C, 35.46; H, 5.24; N, 9.90. Absorption spectrum λ_{max}, (ε_{max}): 456 nm (144 M^{-1} cm^{-1}). IR (str): 3062 cm^{-1}, 2880 cm^{-1}, 1677 cm^{-1}. HRESIMS: *m/z* = 458.9 ($[M\text{-}Cl]^+$ 100%), 460.1 ($[M\text{-}Cl]^+$ 20%), 460.9 ($[M\text{-}Cl]^+$ ≈2%). $^{13}C\{^1H\}$ NMR (ppm); 181.4 (C=N), 176.1 (COOH), 172.5 (COOM), 55.7, 54.6, 53.6 (CH_2NH_2), 29.9, 27.7 (methylene CH_2).

[Co(Aimtetraen)][$ZnCl_4$]

[Co(Aimtetraen)][$ZnCl_4$] was prepared according to the literature method[3] except in a larger scale reaction, with comparable results. [Co(tetraen)Cl][$ZnCl_4$] (2.47 g, 5.0 mmol), pyruvic acid (1.0 g, 11.3 mmol), 2,6-lutidine (0.62 g, 5.8 mmol) and 220mL of methanol were heated at reflux for 48 hours, during which time a orange precipitate formed. The solution was cooled to room temperature, followed by cooling to -10°C. The solution was filtered under suction to give an orange powder.

Yield: 2.31 g, (88.0%). $^{13}C\{^1H\}$ NMR (ppm); 184.1 (C=N), 175.8 (COOM), 59.4, 56.8, 56.5, 55.7, 54.9, 53.0, 52.6, 51.0 (CH_2NH_2), 21.6 (CH_3).

[Co(cpgimtetraen)][$ZnCl_4$]

[Co(tetraen)Cl][$ZnCl_4$] (0.30 g, 0.61 mmol), LiBKPA (0.17 g, 0.85 mmol), 2,6-lutidine (0.10 g, 0.93 mmol) and 70 mL of methanol were heated at reflux for 24 hours, during which time an orange precipitate formed. The solution was left to cool to room temperature, and the solution was filtered under suction to give an orange crystalline powder.

Yield: 0.10 g, (29.51%); Anal. Calcd. for $C_{13}H_{26}Cl_4CoN_5O_2Zn \cdot H_2O$: C, 27.46; H, 4.96; N, 12.32. Found: C, 27.10; H, 4.57; N, 11.76. Absorption spectrum λ_{max}, (ε_{max}): 465 nm (216 M^{-1} cm^{-1}). IR (str) 3500 cm^{-1}, 3219 cm^{-1}, 1670 cm^{-1}. $^{13}C\{^1H\}$ NMR (ppm); 184.4 (C=N), 173.3 (COOM), 59.2, 56.4, 56.0, 55.1, 54.2, 52.6, 52.2, 50.5 (CH_2NH_2), 20.5, 14.5, 14.1 (cpg CH_2).

2.2.3.2 REDUCTION OF THE IMINE COMPLEXES

Reduction of *mffm*-[Co(Aim$_2$trien)]$_2$[ZnCl$_4$]

mffm-[Co(Aim$_2$trien)]$_2$[ZnCl$_4$] (2.38 g, 5.33 mmol) was dissolved in 250mL of carbonate buffer (2.12 g K_2CO_3 and 2.09 g $KHCO_3$ in 500mL H_2O). $NaBH_4$ (1.01 g, 26.7 mmol) was added and stirred constantly for 5 minutes. The orange solution was adsorbed onto a Na^+-form Dowex column (10 x 10 cm) under suction, followed by carbonate buffer (250 mL). The column was initially washed with H_2O (≈2 L), after which the red band was ready to be eluted with aqueous HCl (0.3 M, ≈3 L). The red eluate was taken to dryness on a rotary evaporator at 40°C. The product was shown to be a mixture of components (by $^{13}C\{^1H\}$ NMR).

Yield: 6.03 g. (The crude material was contaminated with NaCl.)

Reduction of [Co(Aimtetraen)]ZnCl$_4$

[Co(Aimtetraen)]ZnCl$_4$ (1.00 g, 1.92 mmol) was dissolved in 250 mL of carbonate buffer (2.12 g K_2CO_3 and 2.09 g $KHCO_3$ in 500 mL of H_2O). $NaBH_4$ (0.72 g, 19.2 mmol) was added and stirred constantly for 5 minutes. The red/pink solution was adsorbed onto a Na^+-form Dowex column (10 x 10 cm) under suction, followed by carbonate buffer (250 mL)The column was initially washed with H_2O (3 L), after which the red/pink band was ready to be eluted with aqueous HCl (0.1 M, 2 L; 3 M, 2 L). The red/pink eluate was taken to dryness on a rotary evaporator at 40°C.

Yield: 1.02 g. (The crude material was contaminated with NaCl.)

2.2.3.3 ISOLATION OF THE ISOMERS

***mffm*-[Co(A$_2$trien)]Cl**

Crude *mffm*-[Co(A$_2$trien)]Cl (6.00 g, 15.67 mmol, contaminated with NaCl) was dissolved in acidified H_2O (pH ≈ 3, 2 L) and adsorbed onto a H^+-Dowex column (50 x 5 cm). The column was eluted with aqueous HCl (0.2 M, 20 L). During the elution three bands developed. The

first band (purple) and the second band (red) were collected and the third band (orange) was finally eluted with aqueous HCl (3 M, 1 L). All eluates were taken to dryness on a rotary evaporator at 40°C. Bands 2 and 3 contained a mixture of isomers, according to the $^{13}C\{^{1}H\}$ NMR data. The second band was dissolved in aqueous H_2O and loaded onto a SP C-25 sephadex column (43 x 3.5 cm) and eluted with $NaH_2PO_4{\cdot}2H_2O$ (0.05 M, 20 L) to separate the two isomers. However, the separation was unsuccessful.

mffm-[Co(A_2trien)]Cl – Band 1; major isomer (**I1**);

Yield: 1.63 g. Anal. Calcd. for $C_{12}H_{24}ClCoN_4O_4{\cdot}2.5H_2O$: C, 34.01; H, 5.95; N, 13.22. Found: C, 34.26; H, 6.79; N, 12.76. Absorption spectrum λ_{max}, (ε_{max}): 486 nm (26 M^{-1} cm^{-1}).IR (str): 1664 cm^{-1}, 1487 cm^{-1}. HRESIMS: *m/z* = 347.1 ($[M\text{-}Cl]^+$ 100%), 348.1 ($[M\text{-}Cl]^+$ 15%), 349.1 ($[M\text{-}Cl]^+$ ≈2%). $^{13}C\{^{1}H\}$ NMR (ppm); 187.1 (C=O), 64.4, 60.9, 58.3, 53.3 (CH_2NH_2), 17.9 (CH_3).

[Co(A_2trien)]Cl – Band 2; minor isomers (**I2**);

Yield: 0.28 g. Absorption spectrum λ_{max}, (ε_{max}): 456 nm (154 M^{-1} cm^{-1}). IR (str): 1623 cm^{-1}, 1461 cm^{-1}. HRESIMS: *m/z* = 347.3 ($[M\text{-}Cl]^+$ 100%), 348.3 ($[M\text{-}Cl]^+$ 45%), 349.3 ($[M\text{-}Cl]^+$ 10%). $^{13}C\{^{1}H\}$ NMR (ppm); 190.6, 187.8, 186.8, 186.5 (C=O), 64.2, 63.9, 63.4, 60.7, 60.1, 56.5, 56.3, 55.3, 54.5, 52.0, 51.9, 47.6 (CH_2NH_2), 17.7, 17.6, 17.5, 16.6 (CH_3).

[Co(A_2trien)]Cl – Band 3; minor isomers (**I3**);

Yield: 0.03 g. $^{13}C\{^{1}H\}$ NMR (ppm); 188.1, 188.0, 184.2, 179.6 (C=O), 61.5, 61.2, 60.6, 57.9, 53.6, 51.8, 49.0, 44.7 (CH_2NH_2), 18.3, 14.9, 14.8, 13.7 (CH_3).

2.2.3.4 PREPARATION OF THE HALF-REDUCED ISOMER [Co(AimAtrien)]Cl

In one instance, borohydride reduction did not go to completion and resulted in a 'half-reduced isomer (Band 2; **I4a**).

mffm-[Co(Aim_2trien)]$_2$[$ZnCl_4$] (2.38 g, 5.33 mmol) was dissolved in 250mL of carbonate buffer (2.12 g K_2CO_3 and 2.09 g $KHCO_3$ in 500mL H_2O). $NaBH_4$ (1.01 g, 26.7 mmol) was added and stirred constantly for 5 minutes. The orange solution was adsorbed onto a

Na^+-form Dowex column (10 x 10 cm) under suction, followed by carbonate buffer (250 mL). The column was initially washed with H_2O (≈2 L), after which the red band was ready to be eluted with aqueous HCl (0.3 M, ≈3 L). The red eluate was taken to dryness on a rotary evaporator at 40°C. The product was a mixture of components (by $^{13}C\{^1H\}$ NMR).

Crude *mffm*-[Co(A_2trien)]Cl (6.00 g, 15.67 mmol, contaminated with NaCl) was dissolved in acidified H_2O (pH ≈ 3, 2 L) and adsorbed onto a H^+-Dowex column (50 x 5 cm). The column was eluted with aqueous HCl (0.2 M, 20 L). During the elution three bands developed. The first band (purple) and the second band (red) were collected and the third band (orange) was finally eluted with aqueous HCl (3 M, 1 L). All eluates were taken to dryness on a rotary evaporator at 40°C.

Band 1 was the major isomer (**I1**) according to the $^{13}C\{^1H\}$ NMR and ^1H NMR data.

Band 2 was a half reduced isomer (**I4a**) according to the $^{13}C\{^1H\}$ NMR and ^1H NMR data.

NMR spectra (such as ^1H NMR and $^{13}C\{^1H\}$ NMR) were not obtained for band 3 (**I4b**) as there was only a very small amount of this material in comparison to other bands.

2.2.4 CRYSTAL STRUCTURE DETERMINATIONS

Information on the setup of the X-Ray system can be found in Appendix I. Reference numbers (*e.g.* **2.10**, **2.11** etc) for each structure are provided, referring to the tables in Appendix I

mffm-[Co(Eim$_2$trien)]Cl (2.10)

Crystals of *mffm*-[Co(Eim$_2$trien)]Cl (red blocks) were grown by slow evaporation of an aqueous solution of *mffm*-[Co(Eim$_2$trien)]Cl in aqueous hydrochloric acid (0.2 M).

Crystal Data:

$C_{16}H_{27.8}N_4O_{9.9}ClCo$, M =529.00, Monoclinic, a = 23.5815(11) Å, b = 13.5077(5) Å, c = 14.2947(6) Å, α = 90, β= 105.8310(10), γ = 90, U = 4380.6(3) Å^3, T = 296(2), space group C2/c (no. 15), Z = 8, μ(Mo-Kα) = 0.966 mm^{-1}, 21713 reflections measured, 3855 unique (R_{int} = 0.0588) which were used in all calculations. The final $wR(F_2)$ was 0.1215 (all data), R_1 = 0.0456 (Final R indexes [I>2σ (I)]).

[Co(cpgimtetraen)]Cl (2.11)

Crystals of [Co(cpgimtetraen)]$ZnCl_4$ (red blocks) were grown by slow evaporation of an aqueous solution of [Co(cpgimtetraen)]$ZnCl_4$ in aqueous hydrochloric acid (0.2 M).

Crystal Data:

$C_{13}H_{25}N_5O_2ClCoZn$, M =443.13, Monoclinic, a = 9.5754(3) Å, b = 13.1438(4) Å, c = 16.1929(5) Å, α = 90, β= 95.9850(10), γ = 90, U = 2026.88(11) Å^3, T = 296(2), space group $P2_1/n$ (no. 14), Z = 4, μ(Mo-Kα) = 2.146, 10632 reflections measured, 4163 unique (R_{int} = 0.0215) which were used in all calculations. The final $wR(F_2)$ was 0.1206 (all data), R_1 = 0.0283 (Final R indexes [I>2σ (I)]).

***mffm*-[Co(A_2trien)]Cl – Band 1 - major isomer (I1) (2.12)**

Crystals of *mffm*-[Co(A_2trien)]Cl (red blocks) were grown by removal of solvent *in vacuo*.

Crystal Data:

$C_{12}H_{28}N_4O_6CoCl$, M =418.76, Monoclinic, a = 10.2882(17) Å, b = 12.738(2) Å, c = 13.267(2) Å, α = 90, β= 96.273(6), γ = 90, U = 1728.2(5) Å^3, T = 273(2), space group $P2_1/c$ (no. 14), Z = 4, μ(Mo-Kα) = 1.184 mm^{-1}, 8167 reflections measured, 2983 unique (R_{int} = 0.0776) which were used in all calculations. The final $wR(F_2)$ was 0.1188 (all data), R_1 = 0.0480 (Final R indexes [I>2σ (I)]).

***mffm*-[Co(A_2trien)]Cl - Band 2 – a minor isomer (I2a) (2.13)**

Crystals of *mffm*-[Co(A_2trien)]Cl (red blocks) were grown by removal of solvent *in vacuo*.

Crystal Data:

$C_{12}H_{20}N_4O_6ClCo$, M =410.70, Monoclinic, a = 7.5702(12) Å, b = 21.160(3) Å, c = 12.3205(19) Å, α = 90, β= 96.930(8), γ = 90, U = 1959.1(5) Å^3, T = 296(2), space group $P2_1/n$ (no. 14), Z = 4, μ(Mo-Kα) = 1.044 mm^{-1}, 36332 reflections measured, 3430 unique (R_{int} = 0.1258) which were used in all calculations. The final $wR(F_2)$ was 0.3617 (all data), R_1 = 0.1262 (Final R indexes [I>2σ (I)]).

mffm-[Co(AimAtrien)]Cl – half reduced isomer (I4a) (2.14)

Crystals of *mffm*-[Co(AimAtrien)]Cl (red blocks) were grown by vapour diffusion of acetone into a solution of *mffm*-[Co(AimAtrien)]Cl in aqueous hydrochloric acid (0.2 M)

Crystal Data:

$C_{10}H_{10}N_6O_6ClCo$, M =404.62, Monoclinic, a = 10.4102(6) Å, b = 12.7755(6) Å, c = 13.0729(6) Å, α = 90, β= 95.9870(10), γ = 90. U = 1729.15(15) Å^3, T = 296(2), space group $P2_1$ (no. 4), Z = 4, μ(Mo-Kα) = 1.185, 28026 reflections measured, 7965 unique (R_{int} = 0.0412) which were used in all calculations. The final $wR(F_2)$ was 0.1216 (all data), R_1 = 0.0399 (Final R indexes [I>2σ (I)]).

2.3 RESULTS

2.3.1 FORMATION OF THE IMINE COMPLEXES

$[Co(Aim_2trien)]_2[ZnCl_4]$, $[Co(Aimtetraen)][ZnCl_4]$ and $[Co(Eim_2trien)]_2[ZnCl_4]$ were prepared according to literature methods.[3] The $[Co(Eim_2trien)]_2[ZnCl_4]$ complex has been reported to be hygroscopic.[11] However when the reaction was scaled up (Section 2.2.3.1), the precipitate and subsequent powder was not hygroscopic. Due to contamination with 2,6-lutidine however, the material was dissolved in acidified H_2O and loaded onto an H^+-Dowex column. The resulting eluate ($[Co(Eim_2trien)]Cl$) was taken to near dryness on a rotary evaporator and crystals formed overnight.

2.3.1.1 SPECTROSCOPIC DATA FOR THE IMINE COMPLEXES

$^{13}C\{^1H\}$ NMR DATA

$^{13}C\{^1H\}$ NMR spectra were used as the primary spectroscopic tool for initial characterisations of the imine complexes, due to their simplicity. ^1H NMR spectroscopy was not used as a primary characterisation technique, as the congestion in the spectra for the methylene protons made assignment difficult. The spectra were consistent with literature values [3] and are shown in Table 1.

Complex	C=N (ppm)	CO_2Co (ppm)	CH_3 (ppm)	CHRNR'R"
$[Co(Aim_2trien)]^+$	182.9	175.8	21.1	57.9, 56.9, 55.7
$[Co(Eim_2trien)]^+$	181.4	172.5	N/A	55.7, 54.6, 53.6, 29.9, 27.7
$[Co(Aimtetraen)]^+$	184.1	175.8	21.6	59.4, 56.8, 56.5, 55.7, 54.9, 53.0, 52.6, 51.0
$[Co(cpgimtetraen)]^+$	184.4	173.3	N/A	59.2, 56.4, 56.0, 55.1, 54.2, 52.6, 52.2, 50.5

Table 1: $^{13}C\{^1H\}$ NMR data for the imine complexes

2.3.1.2 *Crystal Structure – [Co(Eim$_2$trien)]Cl (2.10)*

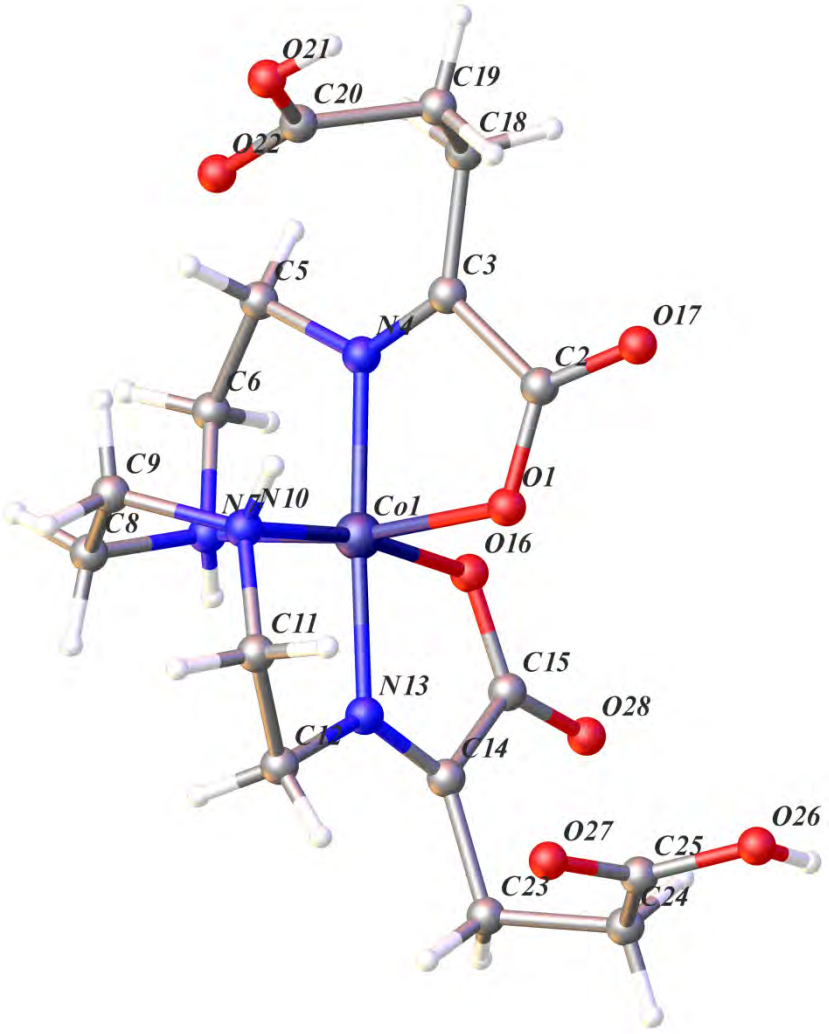

Figure 2-5: X-Ray crystal structure of [Co(Eim$_2$trien)]Cl (solvent molecules and counter-ion omitted for clarity)

Selected atomic distances (Å): Co1-O1, 1.916(2); Co1-N4, 1.879(3); Co1-N7, 1.933(3); Co1-N10, 1.932(3);Co1-N13, 1.879(3); Co1-O16, 1.916(2); C2-O17, 1.225(4); N4-C3, 1.274(4); N13-C14, 1.277(4). Other Nitrogen-Carbon bond lengths; 1.466(4)-1.500(4).

Selected bond angles (°): O1-Co1-O16, 90.13(9); N4-Co1-O1, 84.10(10); N4-Co1-N7, 86.35(11); N10-Co1-N7, 88.23(11); N13-Co1-N10, 86.98(11); N13-Co1-O16, 83.86(10); N4-Co1-N13, 176.59(11); C3-N4-C5, 127(3); C3-C18-C19, 111.2(3); O17-C2-O1, 125.1(3).

Selected torsion angles (°): C5-N4-C3-C18 2.15, C5-N4-C3-C2 178.19.

The space group is C2/c and the crystal system is monoclinic. The presence of imine bonds are confirmed by comparison of the bond lengths of C3-N4 (1.274 Å) and N13-C14 (1.277 Å) to other nitrogen-carbon bond lengths (~1.49 Å). These values are comparable to the values found for the analogous $[Co(Aim_2trien)]^+$ system, where the imine bond was measured as 1.28 Å and other nitrogen-carbon bond lengths (1.47-1.51 Å).[11]

The imine appears to be planar as the torsion angles around the imine bond are approximately 180° for *trans* substituents and approximately 0° for *cis* substituents. These values are also comparable to the $[Co(Aim_2trien)]^+$ system.

2.3.1.3 [Co(cpgimtetraen)]$ZnCl_4$ (2.11)

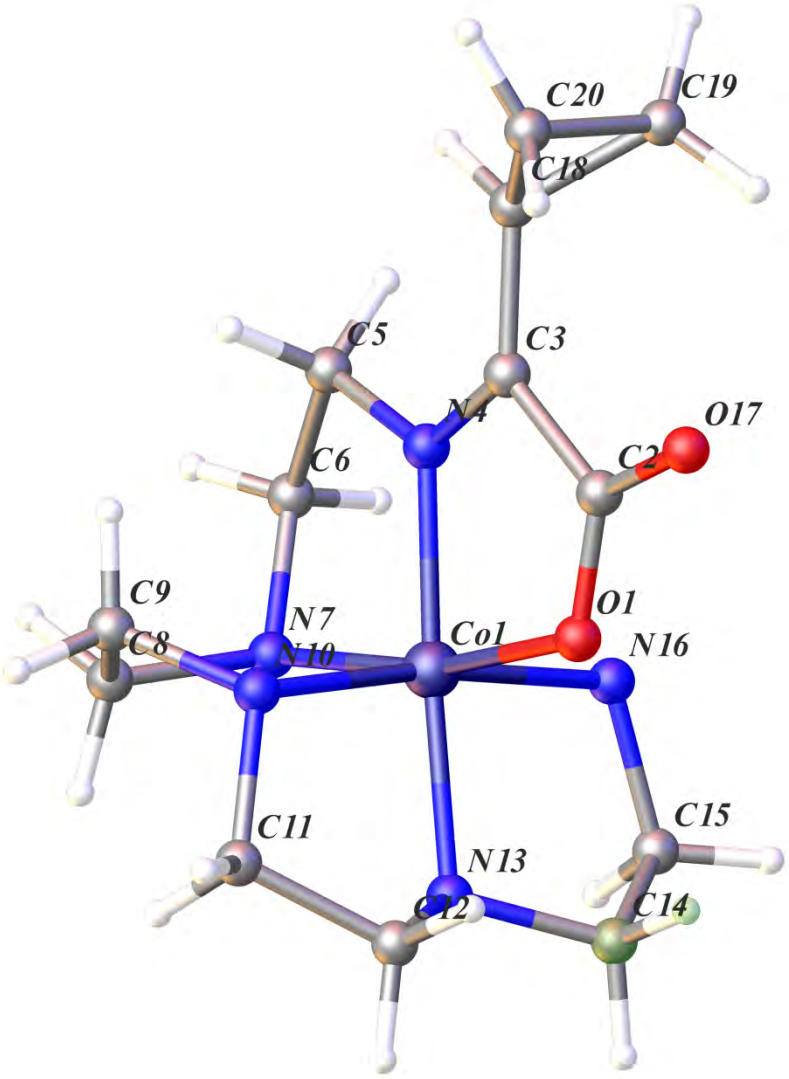

Figure 2-6: Crystal structure of [Co(cpgimtetraen)]$ZnCl_4$ (counter-ion is omitted for clarity)

Selected atomic distances (Å): Co1-O1, 1.9133(18); Co1-N4, 1.887(2); Co1-N7, 1.961(2); Co1-N10, 1.957(3); Co1-N13, 1.940(2); Co1-N16, 1.970(3); C2-O17, 1.223(3); N4-C3, 1.289(3). Other Nitrogen-Carbon bond lengths; 1.470(3)-1.515(3).

Selected bond angles (°): N4-Co1-O1, 82.87(8); N4-Co1-N7, 85.55(9); N10-Co1-N7, 87.08(10); N13-Co1-N10, 85.92(10); N13-Co1-N16, 85.58(10); O1-Co1-N16, 89.12(9); C3-N4-C5, 125.6(2); C3-C18-C19, 121.2(2); O17-C2-O1 123.4(2); N4-Co1-N13, 175.06(9).

Selected torsion angles (°): C5-N4-C3-C18 0.58, C5-N4-C3-C2 -178.04

The space group is $P2_1/n$ and the crystal system is monoclinic. The presence of imine bonds are confirmed by comparison of the bond length of C3-N4 (1.289 Å) to other nitrogen-carbon bond lengths (~1.47 Å). These bond lengths are comparable to the analogous $[Co(Aimtetraen)]^{2+}$ system, where the imine bond was measured as 1.28 Å compared to other nitrogen-carbon bond lengths (1.48-1.51 Å).[11]

The imine appears to be planar as the torsion angles around the imine bond are approximately 180° for *trans* substituents and approximately 0° for *cis* substituents. These values are also comparable to the $[Co(Aimtetraen)]^{2+}$ system.

2.3.2 BOROHYDRIDE REDUCTION OF $[Co(Aim_2trien)]^+$

2.3.2.1 SPECTROSCOPIC DATA FOR THE ISOMER MIXTURE - $[Co(A_2trien)]Cl$

Reduction of the $[Co(Aim_2trien)]^+$ complex using sodium borohydride in a HCO_3^-/CO_3^{2-} buffer generated multiple isomers. A $^{13}C\{^1H\}$ NMR spectrum of the crude isomer mixture was obtained (Figure 2-7). Multiple resonances in the methyl and carbonyl chemical shift range confirm the presence of numerous isomers in solution.

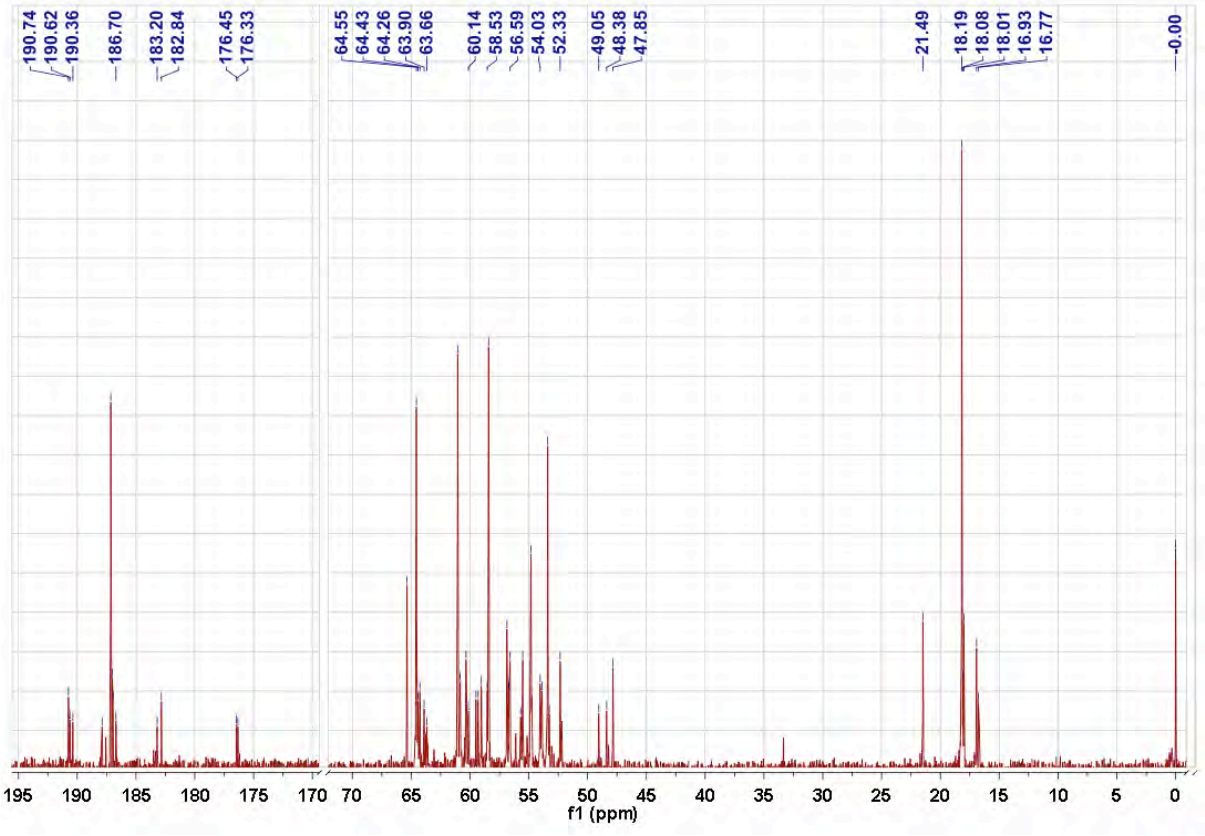

Figure 2-7: $^{13}C\{^1H\}$ NMR spectrum of the isomer mixture of $[Co(A_2trien)]^+$ complex obtained from BH_4^- reduction

The intensity of particular peaks may indicate the amount of certain isomers present. In $^{13}C\{^1H\}$ NMR spectroscopy, the relaxation times are longer, and integration of the peaks is not possible unless long delays are included in the pulse sequence. However, if the groups are related by symmetry or in a similar environment, they will relax at similar times. The relative peak heights observed in particular spectral regions may therefore correlate to the ratio of

particular isomers present. A ^{1}H NMR spectrum was obtained to better assess the distribution of isomers present in solution.

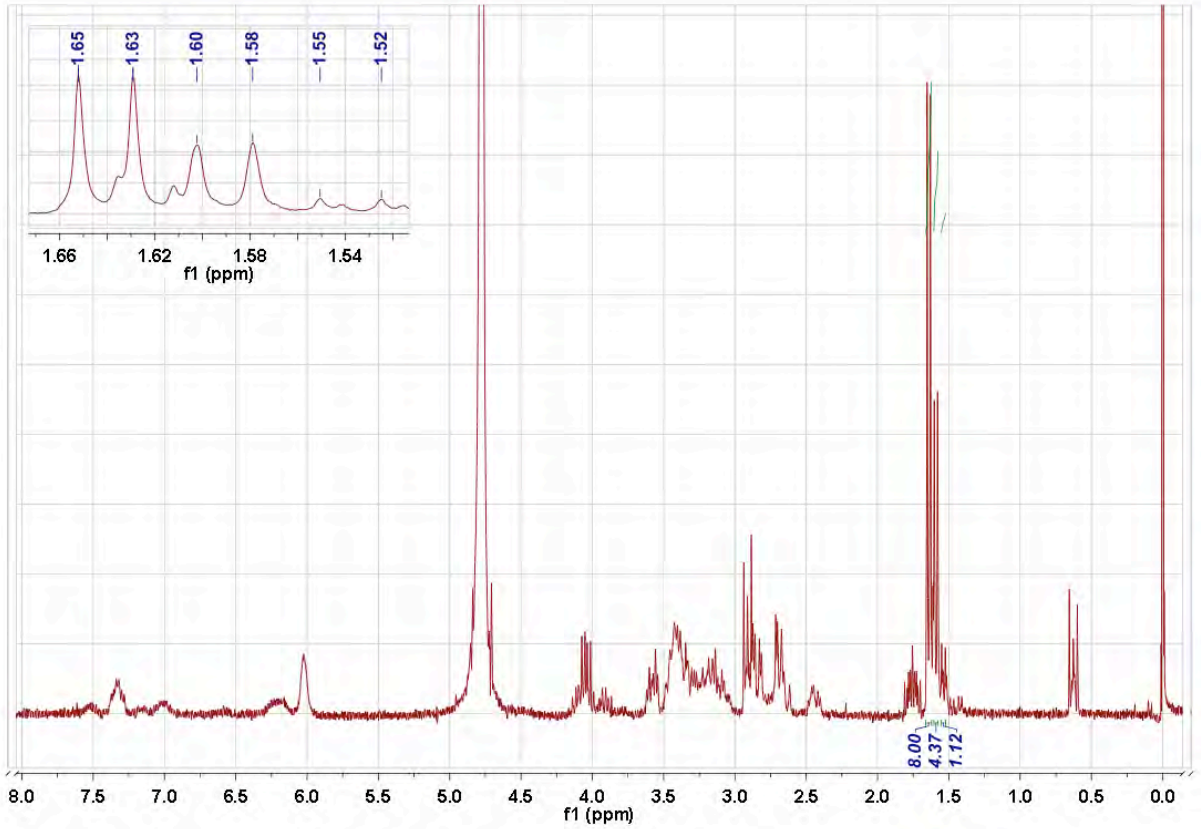

Figure 2-8: ^{1}H NMR spectrum of the isomer mixture of [Co(A_2trien)]Cl prior to ion-exchange chromatography, with an expansion of the methyl region (δ ≈1.50-1.60 ppm) showing the isomer chemical shifts, in the top left of the figure

The ^{1}H NMR spectrum (Figure 2-8) has a distinct cluster of doublets at approximately δ 1.5-1.6 ppm, where the integration of the peaks is approximately an 8:4:1 ratio. This would suggest that at least six stereoisomers (or three diastereoisomers) are formed in any significant yield. Separation of these isomers was attempted *via* ion exchange column chromatography (Figure 2-9).

Figure 2-9: H^+-Dowex column of [Co(A_2trien)]Cl – note the distinct separation of three bands

The separation on the H^+-Dowex column shows 3 distinct bands (Figure 2-9). Based on the mass isolated, the first band (**I1**) accounts for 85% of the total amount; the second band (**I2**) accounts for 14.5%, while the third band (**I3**) accounts for 0.5% of the total amount.

2.3.3 *Separation and Identification of the Major Isomer (I1)*

The first band to be collected and characterised is the major isomer **I1** (henceforth referred to as **I1**.

2.3.3.1 *Spectroscopic data for I1*

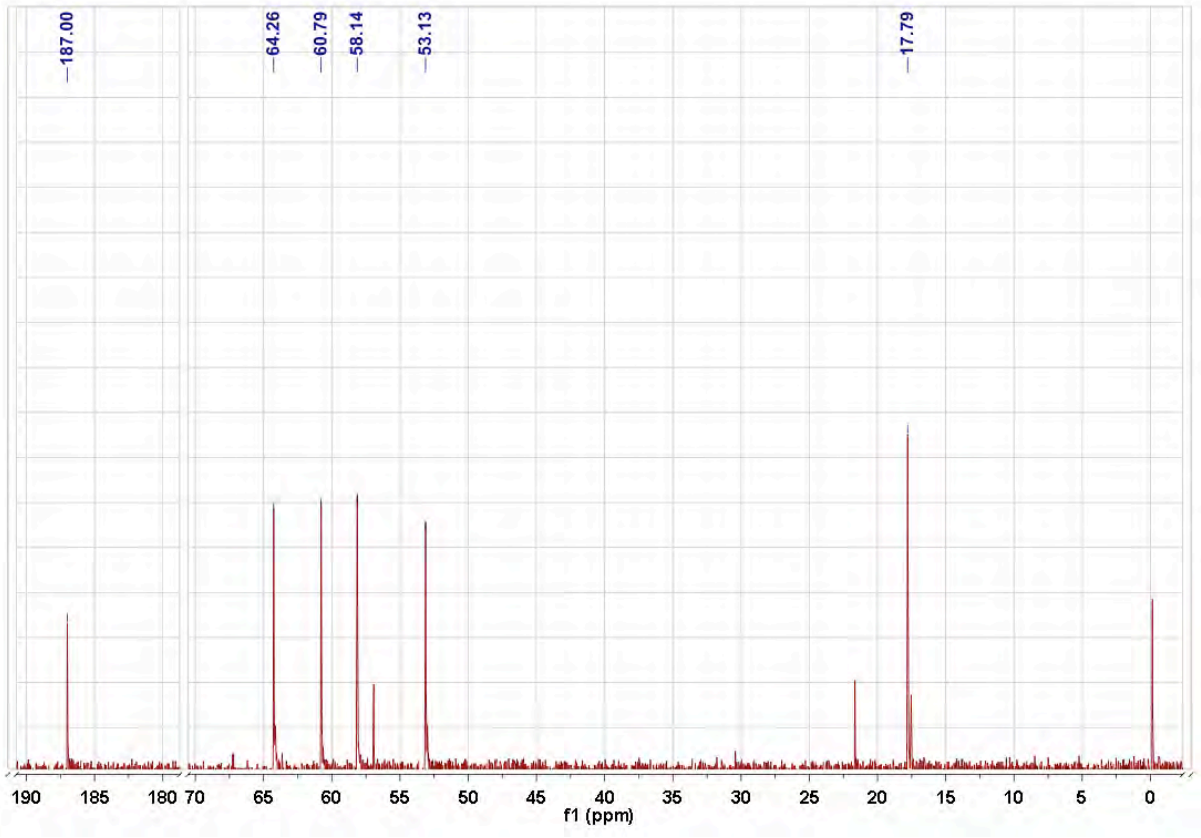

Figure 2-10: $^{13}C\{^{1}H\}$ NMR spectrum of I1 obtained from column chromatography. Unmarked peaks are assigned to the internal reference compound

A total of 6 signals are observed in the $^{13}C\{^{1}H\}$ NMR spectrum. **I1** is a symmetrical molecule.

The first signal to be assigned in the $^{13}C\{^{1}H\}$ NMR spectrum (Figure 2-10) was the methyl group at δ 17.8 ppm. The four signals at δ 53.1-64.2 ppm are the carbon atoms of the CH_2NH fragments and the α-carbon atom, while the carbonyl peak was assigned at δ 187 ppm.

gCOSY and HSQCAD spectroscopy allowed the ^{1}H NMR (Figure 2-11) spectrum of **I1** to be almost completely assigned.

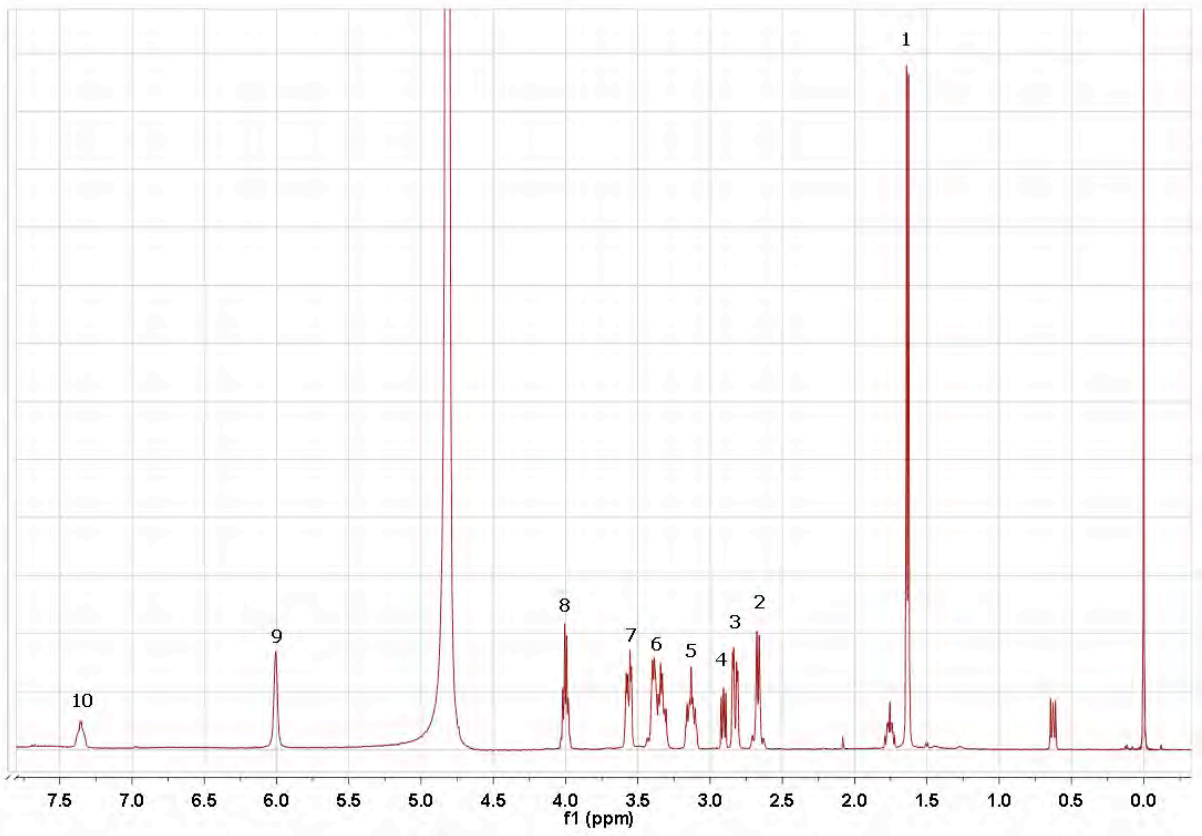

Figure 2-11: ^{1}H NMR spectrum of I1, with labelled peaks corresponding to the proton positions in the molecule (Figure 2-12)

It is not possible to assign particular protons in methylene groups with the available data.

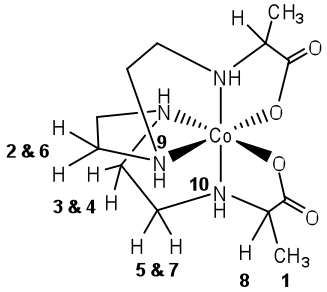

Figure 2-12: Chemdraw representation of I1. Labelled protons correlate to those shown in Figure 2-11

The coupling constant of proton 1 (the methyl group protons) and proton 8 (the proton on the α-carbon atom) is ^{3}J = 6.9 Hz.

2.3.3.2 CRYSTAL STRUCTURE – [Co(A_2trien)]Cl – MAJOR ISOMER – I1 (2.12)

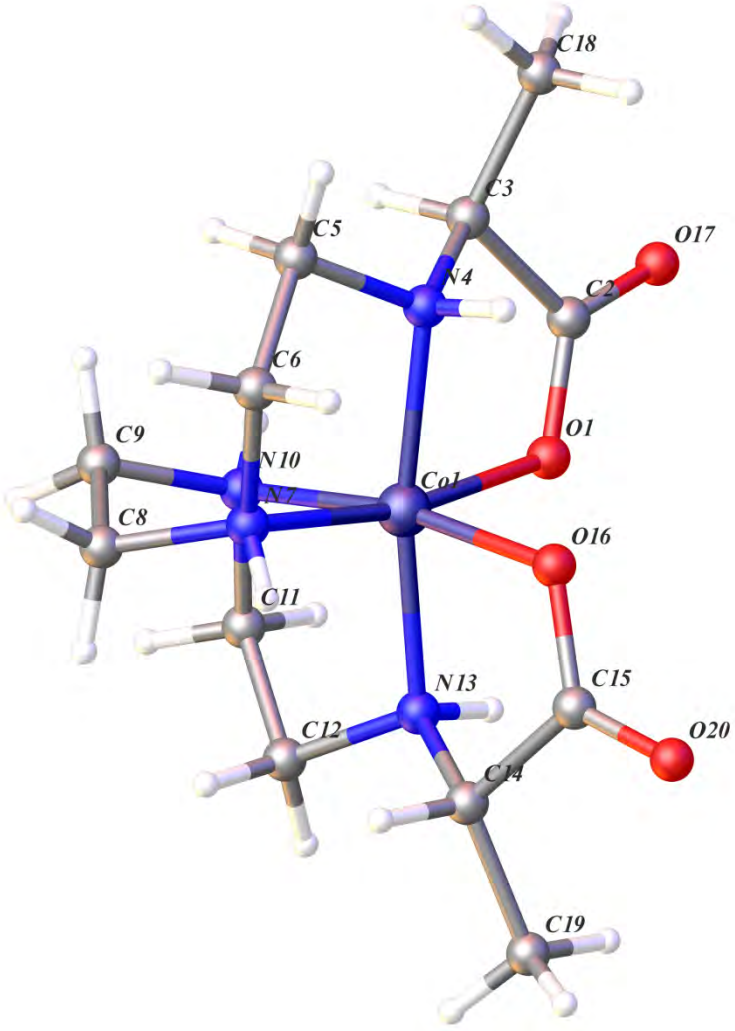

Figure 2-13: X-Ray crystal structure of the [Co(A_2trien)]Cl major isomer (I1) (solvent molecules and counter-ion omitted for clarity)

Selected atomic distances (Å): Co1-O1, 1.911(3); Co1-N4, 1.936(4); Co1-N7, 1.967(3); Co1-N10, 1.996(3); Co1-N13, 1.923(4); Co1-O16, 1.912(3); N4-C3, 1.480(5); C2-O17, 1.223(5); C3-C18, 1.513(6). Other Nitrogen-Carbon bond lengths; 1.478(5)-1.507(5).

Selected bond angles (°): O1-Co1-N4, 83.93(13); N4-Co1-N7, 86.36(15); N7-Co1-N10, 85.96(15); N13-Co1-N10, 86.72(15); O1-Co1-N13, 89.19(13); O1-Co1-O16, 91.17(12); C3-N4-C5, 118.4(3); N13-Co1-N4, 170.34(15).

Selected torsion angles (°): H-N4-C3-H, 169.45; H-N13-C14-H, 169.59

The space group is $P2_1/c$ and the crystal system is monoclinic.

Major features to note are the configuration of the hydrogen atoms on the N4-C3 and N13-C14 pairs. Consider the atoms N13-C14. The two hydrogen atoms are added during reduction of the double bond of N13-C14. The chelate ring of N13-C14 has the hydrogen atom of N13 on the carboxylate face of the ring, while the hydrogen atom on C14 is on the amine face of the chelate ring. The hydrogen atoms on N13 and C14 are in an *anti* conformation. The relative configuration of the N4-C3 hydrogen atoms is analogous.

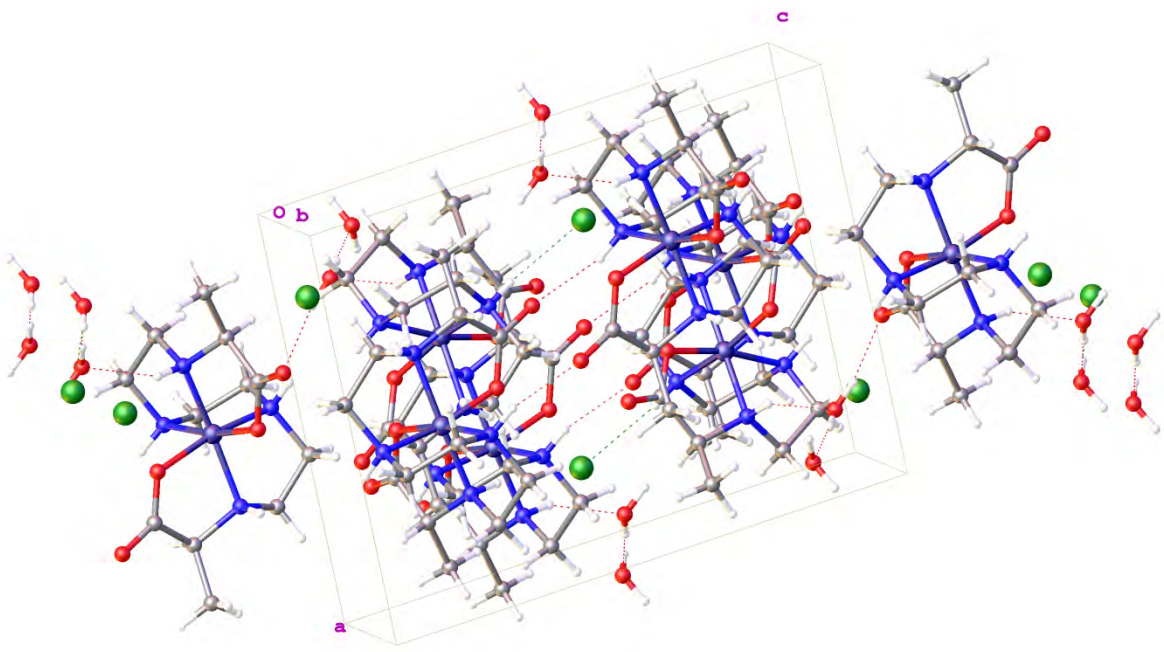

Figure 2-14: [Co(A_2trien)]Cl major isomer (I1)- packing extended outside the unit cell

Note the hydrogen bonding between adjacent amine protons and the carbonyl groups. There is also hydrogen bonding between the counter ions and amine protons. Some extended interactions with the water molecules outside the cell can also be observed.

2.3.4 *Separation of a Half-Reduced Isomer - [Co(AimAtrien)]Cl (I4a)*

2.3.4.1 *Spectroscopic data for [Co(AimAtrien)]Cl (I4a)*

In one case, a small amount of 'half reduced' complex, [Co(AimAtrien)]Cl, was obtained (**I4a**).

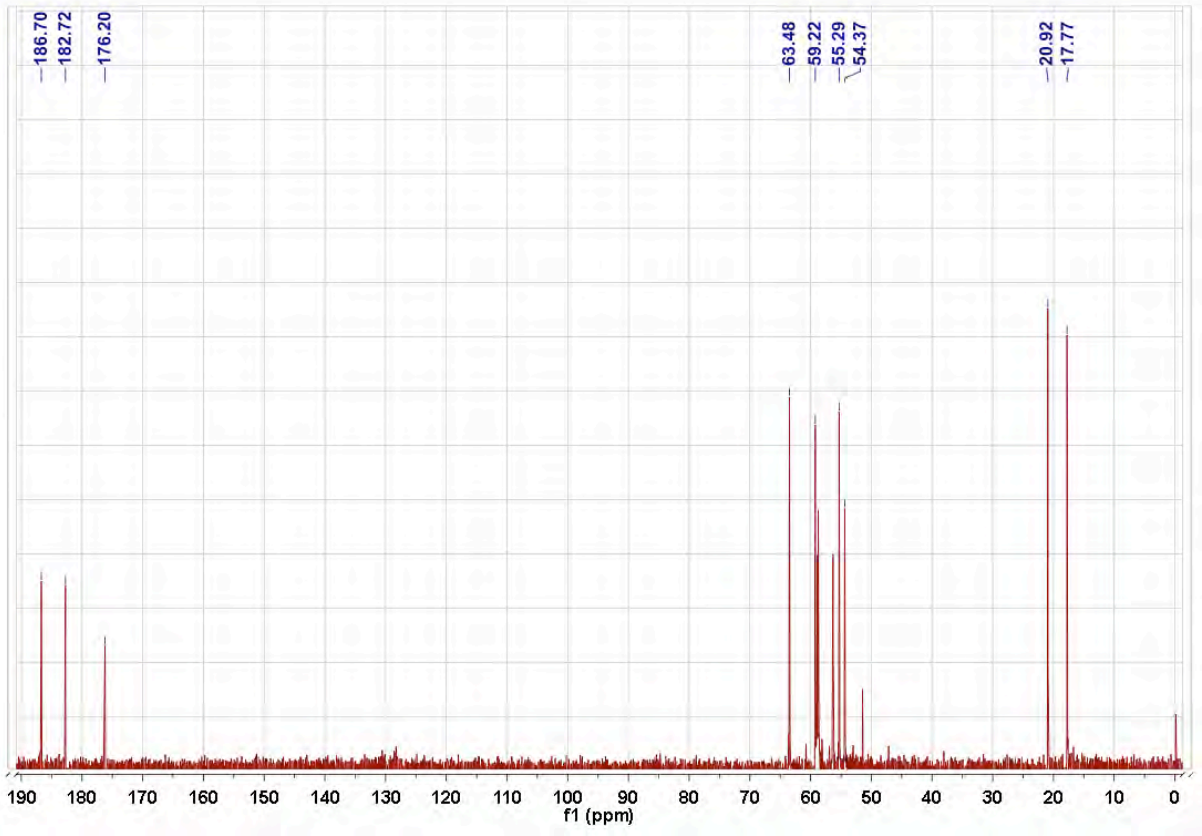

Figure 2-15: $^{13}C\{^{1}H\}$ NMR spectrum of the $[Co(AimAtrien)]^{+}$ half reduced isomer (I4a) obtained from column chromatography

To determine whether the chemical shifts seen in Figure 2-15 were the same as those in the $[Co(Aim_2trien)]^{+}$ complex, the chemical shifts of the methyl, carbonyl and imine groups in both $^{13}C\{^{1}H\}$ NMR spectra were compared (Figure 2-16).

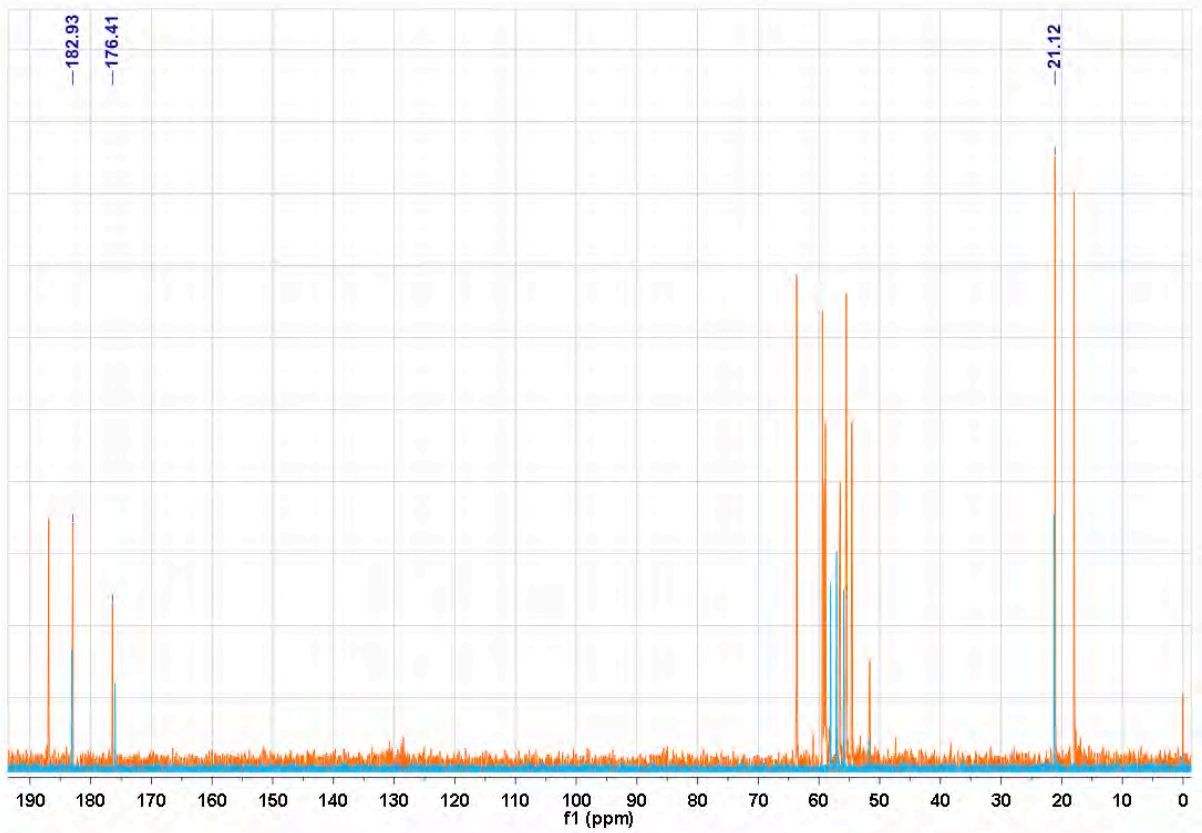

Figure 2-16: $^{13}C\{^{1}H\}$ NMR spectrum of the $[Co(AimAtrien)]^{+}$ half reduced isomer (I4a) obtained from column chromatography (in orange) and the $[Co(Aim_2trien)]^{+}$ complex (in blue)

The chemical shifts of the methyl, carbonyl and imine groups fall in the same region as the $[Co(Aim_2trien)]^{+}$ molecule, confirming the assignment of a half-reduced isomer.

The ^{1}H NMR spectrum of this species confirmed the presence of the half reduced isomer. A singlet peak at δ 2.64 ppm is the chemical shift of a proton adjacent to the imine carbon The doublet chemical shifts at δ 1.62 and δ 1.64 ppm are the same as those of **I1**. The ^{3}J coupling constant that links the methyl group protons with the proton on the α-carbon atom has been measured; ^{3}J = 6.9 Hz. This is also the same value as **I1**.

2.3.4.2 CRYSTAL STRUCTURE – [Co(AimAtrien)]$^{+}$ (I4a) - (2.13)

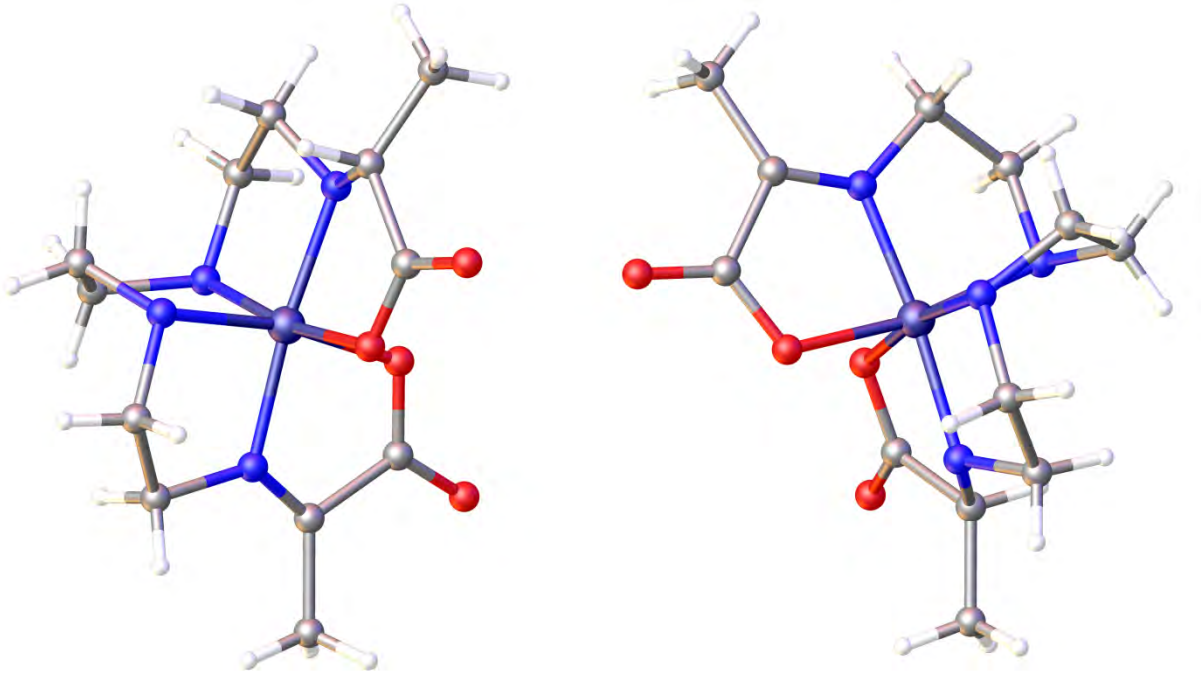

Figure 2-17: [Co(AimAtrien)]Cl - half reduced isomer (I4a) with two molecules in the asymmetric unit (solvent molecules and counter-ion omitted for clarity)

For clarity, only one molecule will be discussed.

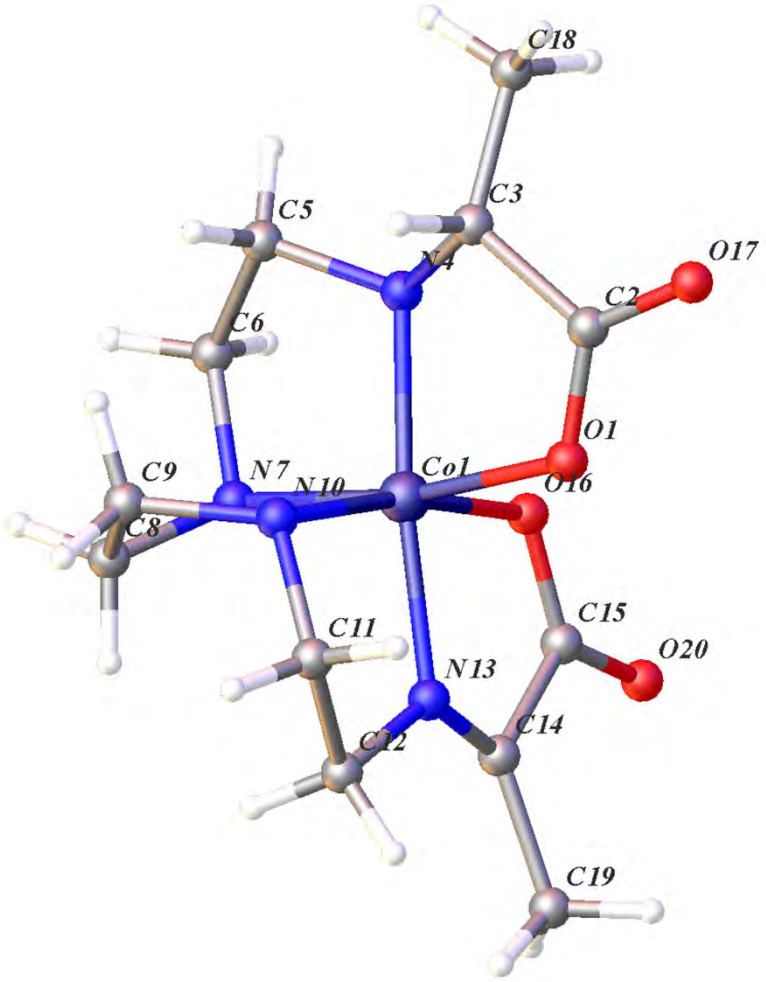

Figure 2-18: Close up view of [Co(AimAtrien)]Cl - half reduced isomer (I4a)

Selected atomic distances (Å) for the Co1 molecule: Co1-O1, 1.910(3); Co1-N4, 1.924(4); Co1-N7, 1.945(4); Co1-N10, 1.952(4); Co1-N13, 1.899(4); Co1-O16, 1.913(3); N4-C3, 1.417(5); N13-C14, 1.287(6); O17-C2, 1.229(5). Other Nitrogen-Carbon bond lengths: 1.459(6)-1.509(6).

Selected bond angles (°) for the Co1 molecule: O1-Co1-N4, 84.08(14); N4-Co1-N7, 86.98(16); N7-Co1-N10, 87.59(15); N13-Co1-N10, 85.80(15), N13-Co1-O16, 84.03(14); O1-Co1-O16, 90.43(13); N13-Co1-N4, 173.49(18); C3-N4-C5, 121.6(3); C14-N13-C12, 128.2(4).

The space group is $P2_1$ and the crystal system is monoclinic. However the assignment of the space group was ambiguous due to disorder in the molecule.

The chelate ring of O1-N4 has an amine bond between C3-N4 (1.42 Å). The proton of the α-carbon atom is on the amine face of the chelate ring. This can be compared to the major isomer of $[Co(A_2trien)]^+$ system (**I1**), where the nitrogen-α-carbon bond length is 1.48 Å, and the proton of the α-carbon atom is also located on the amine face of the molecule.

The chelate ring of N13-O16 still retains the imine bond, as shown by the bond distance between N13-C14 (1.287 Å). This bond length is analogous to the imine bond length of 1.28 Å of the $[Co(Aim_2trien)]^+$ system.

2.3.5 SEPARATION AND IDENTIFICATION OF THE MINOR ISOMERS

2.3.5.1 SPECTROSCOPIC DATA FOR MINOR ISOMERS – BAND 2 (I2)

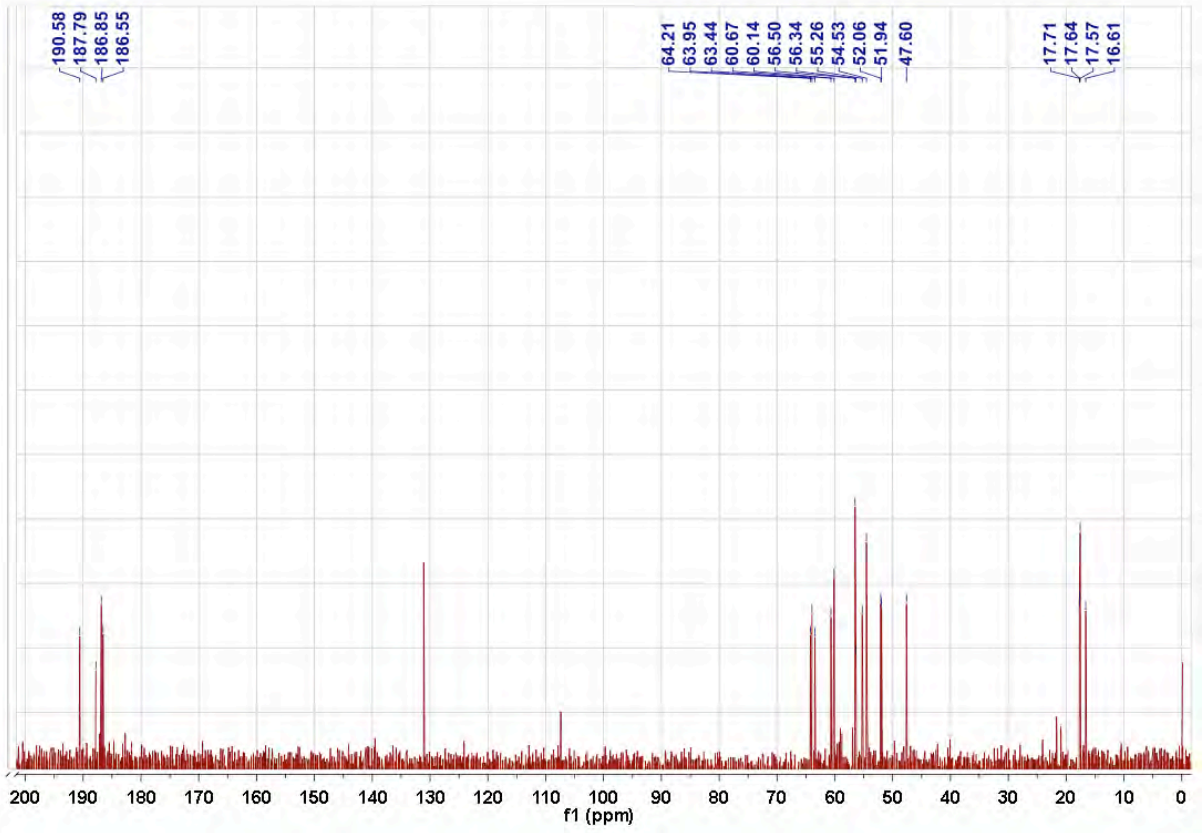

Figure 2-19: $^{13}C\{^{1}H\}$ NMR spectrum of the $[Co(A_2trien)]^+$ (band 2) complexes obtained from column chromatography

A $^{13}C\{^{1}H\}$ NMR spectrum was obtained (Figure 2-19), and multiple resonances in the methyl and carbonyl chemical shift range reveal the presence of multiple isomers in solution. An expansion of the methyl region of the spectrum (δ 16-17 ppm) shows 4 peaks. A $[Co(A_2trien)]^+$ complex may not be a symmetrical molecule; in which case a total of 12 signals would be expected in the $^{13}C\{^{1}H\}$ NMR spectrum, with 2 signals predicted in the methyl region. The band could therefore be a mixture of 2 asymmetric isomers, 4 symmetrical isomers, or some combination of both.

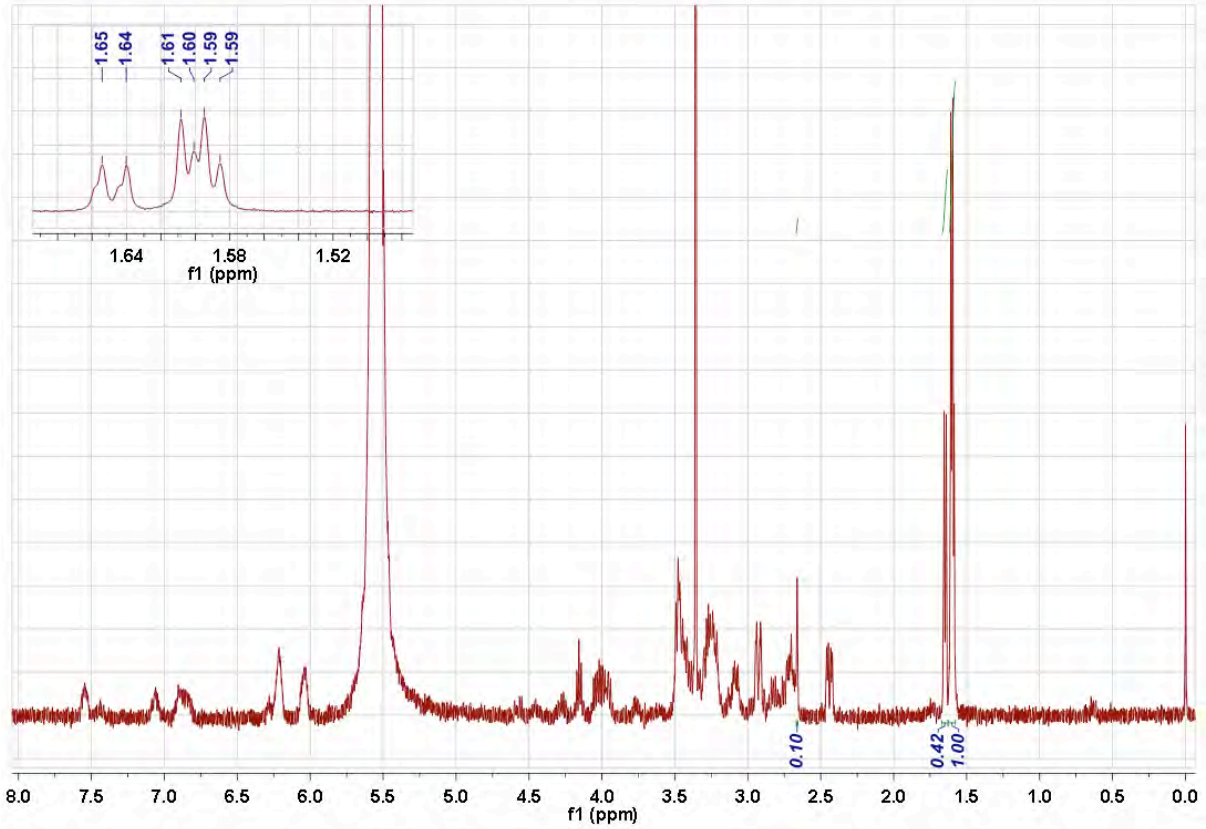

Figure 2-20: ^{1}H NMR spectrum of [Co(A$_2$trien)]$^{+}$ - (band 2). Note the expansion of the methyl region in the top left hand corner

The ^{1}H NMR spectrum (Figure 2-20) of **I2** shows that the methyl region in the ^{1}H NMR spectrum has three sets of doublets. In an asymmetrical molecule, such as this, it could be predicted that the methyl groups (which are in two different environments) would appear as two sets of doublets, of equal height. However, there appears to be another set of doublets at δ 1.59 and δ 1.60 ppm. The ^{13}C{^{1}H} spectrum of band 2, described previously, may account for the multiple resonances seen.

I2 accounts for 14.5% of the total yield from all bands, based on mass isolated.

2.3.5.2 CRYSTAL STRUCTURE – [Co(A$_2$trien)]Cl – MINOR ISOMER (I2a) (BAND 2) (2.14)

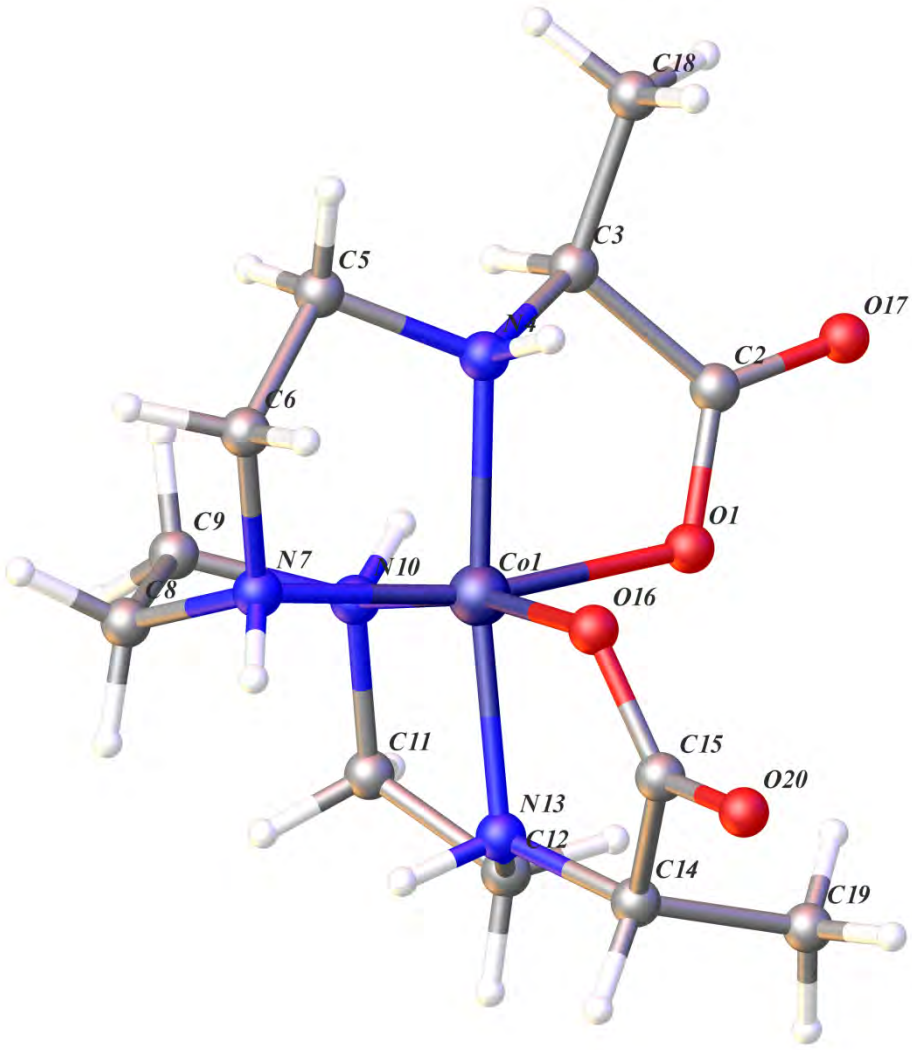

Figure 2-21: [Co(A$_2$trien)]Cl - minor isomer (I2a) (solvent molecules and counter-ion omitted for clarity)

$^{13}C\{^{1}H\}$ data of **I2** material showed the product to be a mixture of isomers. Crystals of the **I2** material (**I2a**) were grown by removal of solvent *in vacuo*. This crystal structure is, therefore, only one of the components found in solution. Attempts to characterise another single crystal by capillary NMR had limited success, as the crystal used for that experiment was disordered over one of the methyl positions.

Selected atomic distances (Å): Co1-O1, 1.927(8); Co1-N4, 1.932(10); Co1-N7, 1.957(10); Co1-N10, 1.968(11); Co1-N13, 1.935(11); Co1-O16, 1.905(8); N4-C3, 1.502(14); N13-C14, 1.496(16); C2-O17, 1.224(14); Other Nitrogen-Carbon bond lengths 1.449(16)-1.51(2).

Selected bond angles (°): O16-Co1-O1, 91.3(4); O1-Co1-N4, 83.4(4); N4-Co1-N7, 85.5(5); N7-Co1-N10, 86.9(5); N13-Co1-N10, 85.9(5); O16-Co1-N13, 84.9(4); N4-Co1-N13, 171.9(4); C5-N4-C3, 117.9(10).

Selected torsion angles (°): H-N4-C3-H, 167.28; H-N13-C14-H, 25.98.

The R_1 factor for this structure is poor, due to unassigned and/or unrefined electron density in the difference map. However, the core structure has been unambiguously assigned.

The orientation of the hydrogen atoms on N13-C14 are in the *anti* conformation, resulting in the N-H proton placed on the carboxylate face, and the α-C-H proton placed on the amine face of the meridional ligand fragment. This feature is seen also in the major isomer. However the position of the hydrogen atoms on N4-C3 are in the *syn* conformation. The hydride attack on this fragment of the molecule still occurs on the amine face, resulting in the α-C-H proton placed on the amine face of the meridional ligand fragment, while the N-H proton is also placed on the amine face of the molecule.

2.3.5.3 *SPECTROSCOPIC DATA FOR MINOR ISOMERS – BAND 3 (I3)*

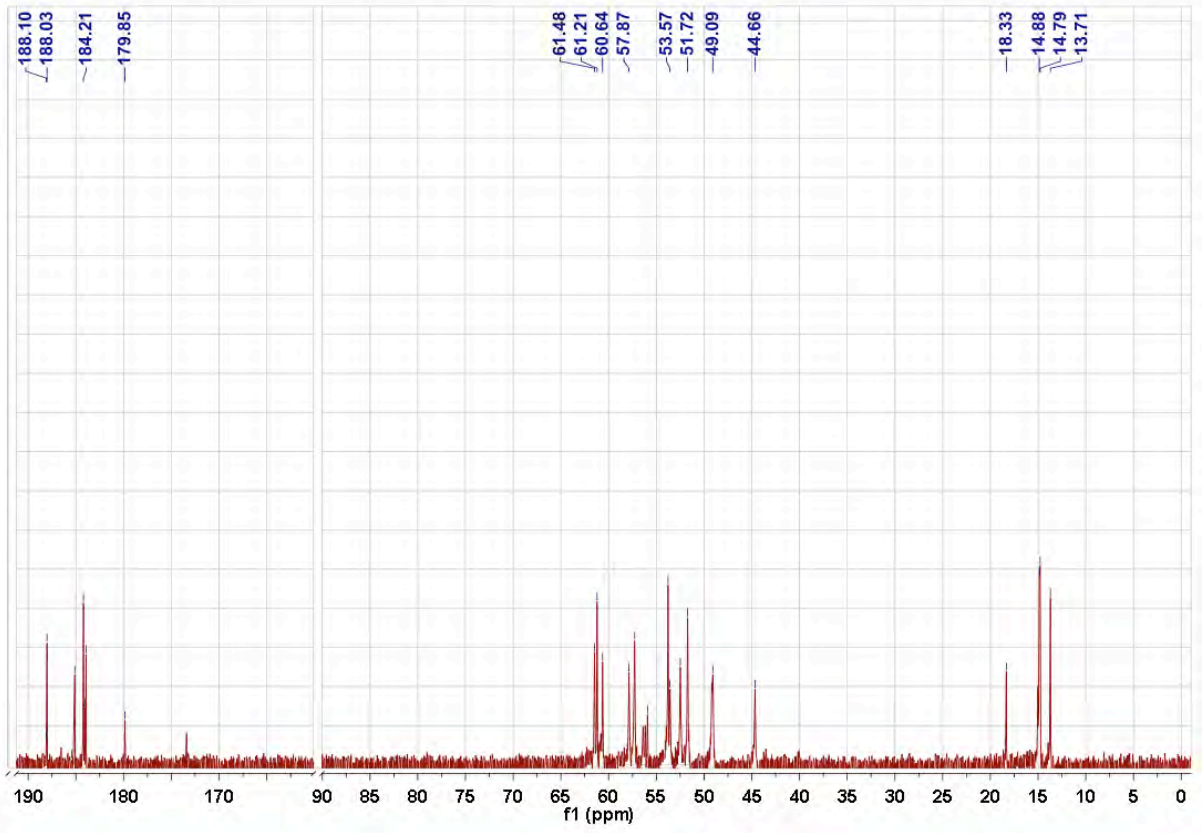

Figure 2-22: $^{13}C\{^1H\}$ NMR spectrum of the $[Co(A_2trien)]^+$ - band 3 obtained from column chromatography

A $^{13}C\{^1H\}$ NMR spectrum was obtained (Figure 2-22), and multiple resonances in the methyl and carbonyl chemical shift range reveal the presence of multiple isomers in solution. It may be assumed that this band of the $[Co(A_2trien)]^+$ complex, like **I2**, could be an asymmetric molecule; so a total of 12 signals would be expected in the $^{13}C\{^1H\}$ NMR spectrum, with 2 signals predicted in the methyl region. An expansion of the methyl region of the spectrum (δ 13-20 ppm) shows 5 peaks. There may be 5 symmetrical isomers present, or a mixture of symmetrical and asymmetric isomers.

I3 accounts for only 0.5% of the total yield from all bands based on mass isolated.

2.3.6 UV-VISIBLE AND INFRA-RED DATA FOR THE COMPLEXES

Complex	UV-visible data λ_{max} nm,(ε_{max} $M^{-1}cm^{-1}$)	Infra-red (cm^{-1})
[Co(A_2trien)]Cl – **I1**	486 nm, (26 $M^{-1}cm^{-1}$)	1664 cm^{-1}, 1487 cm^{-1}
[Co(A_2trien)]Cl – **I2**	486 nm (154 $M^{-1}cm^{-1}$)	1623 cm^{-1}, 1461 cm^{-1}
[Co(cpgim$_2$trien)]Cl	465 nm (216 $M^{-1}cm^{-1}$)	3216 cm^{-1}, 1587 cm^{-1}
[Co(Eim$_2$trien)]Cl	456 nm (144 $M^{-1}cm^{-1}$)	3062 cm^{-1}, 2880 cm^{-1}, 1677 cm^{-1}

Table 2: UV-visible and Infra-Red spectroscopic data for the imino and amino acid complexes

2.4 DISCUSSION

2.4.1 ASSIGNING THE $^{13}C\{^1H\}$ AND ^1H NMR DATA

Signals in the $^{13}C\{^1H\}$ NMR spectra, such as methyl, carbonyl and imine peaks can be assigned to specific chemical shifts. Complete assignment of the $^{13}C\{^1H\}$ NMR spectra was not possible for all complexes, as insufficient data was available.

The ^1H NMR spectra for the imino-acid complexes were useful for characterisation, particularly for the pyruvate derived complexes where the methyl group occurs as a singlet peak at approximately δ 2.6 ppm. This signal splits into a doublet and changes the chemical shift in the resulting amino acid complexes to approximately δ 1.6 ppm.

In some cases, the methylene protons occurred as broad multiplets in the ^1H spectra. This may be due to the adjacent protons causing multiplicity, as well as the inequivalent methylene groups of the polyamine backbone, contributing to overlapping signals in the spectra. In these cases, complete assignment of ^1H NMR spectra was difficult.

2.4.1.1 $[Co(Aim_2trien)]^+$ AND $[Co(A_2trien)]^+$ NMR DATA

The first peak to be assigned in the $^{13}C\{^1H\}$ NMR spectrum of the $[Co(Aim_2trien)]^+$ complex was the methyl group, which was introduced upon condensation of pyruvate with the trien complex. The methyl group was also the first to be assigned in the $^{13}C\{^1H\}$ NMR spectra for the separated $[Co(A_2trien)]^+$ isomers

The $^{13}C\{^1H\}$ NMR spectrum of $[Co(Aim_2trien)]^+$ has already been previously described and assigned.[3]

2.4.2 FORMATION OF THE IMINE PRODUCTS

The synthesis of the polydentate imino acid products in this section of work was *via* a double intramolecular condensation reaction between the polydentate cobalt(III) complex and an α-keto acid.

2.4.2.1 $[Co(Aim_2trien)]_2[ZnCl_4]$

This complex was prepared according to a literature preparation[3] with comparable yields. It was taken directly to the reduction reaction.

2.4.2.2 $[Co(Eim_2trien)]Cl$ AND OTHER AMINO ACID DERIVATIVES

The synthesis of the $[Co(Eim)_2trien]Cl$ complex resulted in crystals of X-ray quality after purification.

Because of the charge of the $[Co(Eim)_2trien]Cl$ complex (due to the carboxylic acid groups), a reduction reaction under the conditions used, would be unsuccessful. Protecting these groups as methyl esters would circumvent this problem, but this is left to a future project.

Other keto acid derivatives could be used in the intramolecular condensation reaction, such as phenylpyruvic acid and LiBKPA. The nature of the side chain may have an effect on stereo and regioselectivity. However, it was beyond the scope of this thesis to investigate these reactions.

2.4.2.3 $[Co(Aimtetraen)][ZnCl_4]$

The $[Co(Aimtetraen)][ZnCl_4]$ complex was prepared according to a literature preparation[3] with comparable yields. It was taken directly to the reduction reaction.

2.4.2.4 $[Co(cpgimtetraen)][ZnCl_4]$

Work conducted by Julian Browne describes the coordination of an α-keto acid to a pentaamine backbone (Figure 2-23).[11]

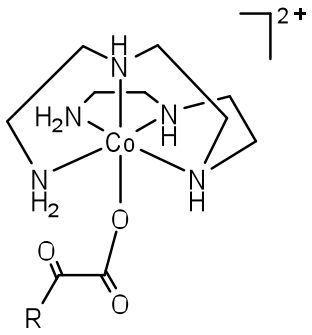

Figure 2-23: An *ffm*-[Co(tetraen)(α-keto acidate)]$^{2+}$ complex

In that example, pyruvic acid and α-ketoglutaric acid were used; however the same principles apply to the system using LiBKPA. The secondary amines on the polyamine backbone are too hindered to react with the keto acid. As noted in the introduction, the formation of the planar imine, as opposed to an angular one, is preferred. Hence, the primary amine *cis* to the coordinated α-keto acid will react to form the imino acid complex (Figure 2-24).

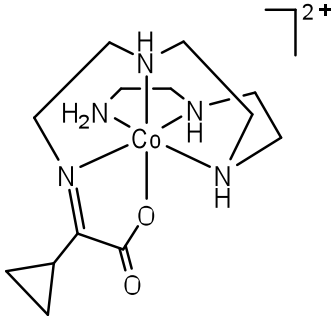

Figure 2-24: The [Co(cpgimtetraen)]$^{2+}$ complex

2.4.3 STEREOISOMERS FORMED FROM THE REDUCTION REACTION

From the borohydride reduction reaction, four stereogenic centres are formed. These stereocentres, as well as the existing stereocentre at the cobalt(III) centre means 2^5 stereoisomers are possible for a molecule with a general polyamine backbone.

However, the polyamine backbone that has been used in these experiments (trien), is symmetrical. Since the sequence of reactions involves modifying both ends of the polyamine, the resulting molecule may retain some symmetry. This will limit the numbers of stereoisomers observed due to the possible retention of a C_2 axis of rotation. For example, take the *ASRSR* isomer shown in Figure 2-25, one enantiomer of the major diastereoisomer, and consider the isomers that result from successive epimerisations.

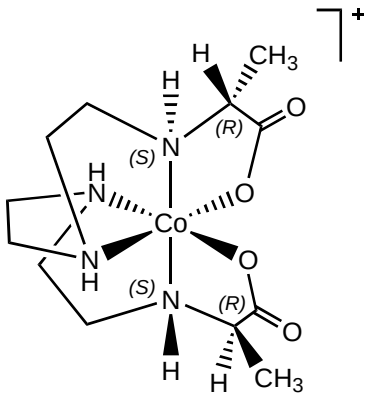

Figure 2-25: The *ASRSR* isomer of $[Co(A_2trien)]^+$. The stereochemistry around the metal centre is 'A'. The top half of the molecule has the stereochemistry 'S' and 'R' around the amine and *α*-carbon atoms respectively. The lower half of the molecule is analogous

If epimerisation of the amine at the top half of the molecule and a C_2 rotation were performed, the following would be created;

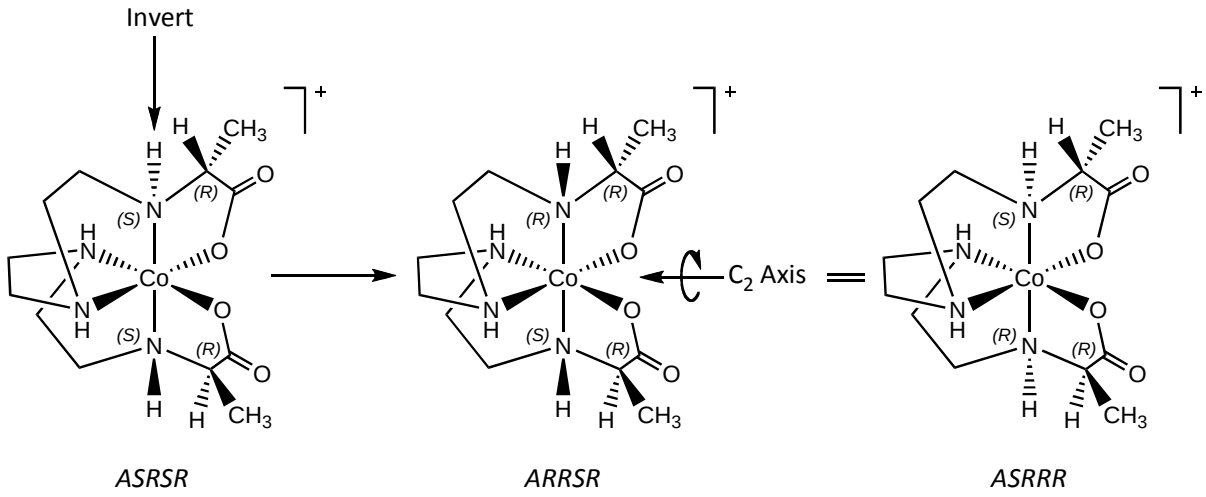

Figure 2-26: N-H epimerisation and rotation of the molecule

However, if the original molecule from Figure 2-25 had the amine proton on the bottom half of the molecule inverted, the same molecule is obtained as shown in Figure 2-26, where the configuration is *ASRRR*.

The original sixteen diastereoisomers that could be produced in the general case from the reduction reaction may be limited to ten, due to the possible presence of a C_2 axis rendering some combinations of absolute configurations equivalent.

2.4.4 REDUCTION REACTIONS

The reduction reactions were performed in a carbonate buffer solution, using sodium borohydride as the reducing agent. The reaction usually involved a ten-fold excess of borohydride being reacted with the imino acid complex for around five minutes. Great care had to be taken in observing the colour changes of the solution as excessive reaction times lead to reduction of the metal ion and decomposition of the complex. The reaction was performed under suction on a Na^+-form Dowex column and washed with excess H_2O, to remove any unreacted borohydride, which could still potentially react with the complex under these conditions.

2.4.4.1 [Co(Atetraen)]$ZnCl_4$ – isomer mixture

Reduction of the $[Co(Aimtetraen)]^{2+}$ complex results in four stereogenic centres (Figure 2-27). Two of the stereogenic centres (the metal ion and meridional secondary amine) were present in the imino acid complex. In all, 2^4 stereoisomers are possible.

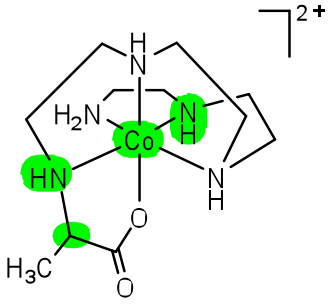

Figure 2-27: [Co(Atetraen)]$^{2+}$ complex. Stereogenic centres are indicated in green

The $^{13}C\{^{1}H\}$ NMR spectrum of the reduced isomers shows that there is a mixture of isomers in solution. Previous study of this system suggested that if the meridional nitrogen atom retains its original configuration (*anti* to the carboxylate group) and if the chirality of the amine adjacent to the α-carbon atom is correlated to that atoms chirality, then only two diastereomers should form.[11] These observations fit the $^{13}C\{^{1}H\}$ NMR spectrum obtained. There are two signals in the carbonyl region.

To achieve separation of the isomers, the material was loaded onto an H^{+}-Dowex column. However, only one band was observed. Separation of the isomers on a different ion-exchange column (SP Sephadex C25) also resulted in one band being observed. Further work in this area is required.

2.4.4.2 [Co(A$_2$trien)]Cl – ISOMER MIXTURE

^{1}H NMR spectroscopy was used to confirm if the reduction reaction had occurred. In the imine product, there is a singlet at δ 2.6 ppm (Figure 2-28). Reduction of the bond results in splitting the signal and a shift of the peaks to approximately δ 1.6 ppm.

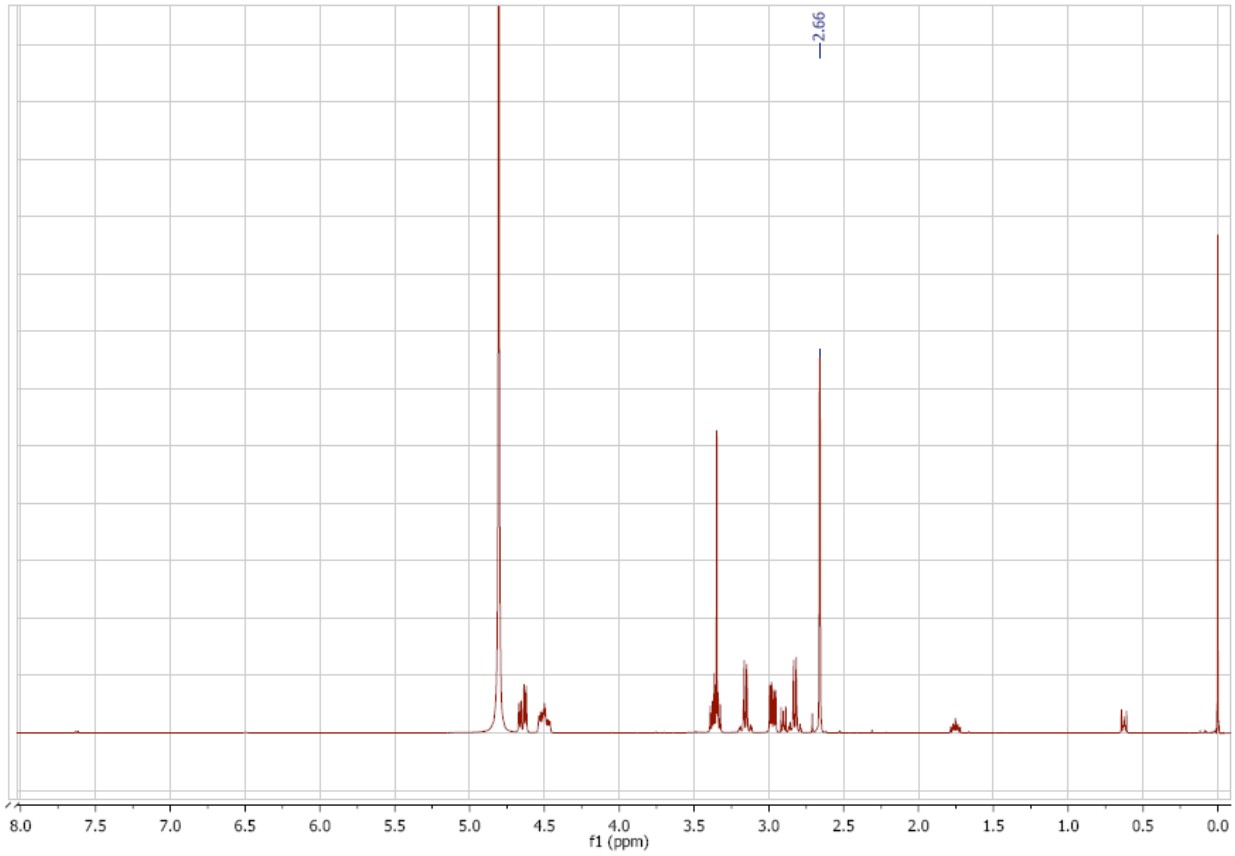

Figure 2-28: ^{1}H NMR spectrum of the [Co(Aim$_2$trien)]$^+$ complex. Note the singlet at δ 2.6 ppm, indicative of the imine functionality in the complex

As previously described, the reduction reaction involving [Co(Aim$_2$trien)]$^+$ results in a isomer mixture. Only a few stereoisomers are formed in significant yield, based on NMR results (Figure 2-8) where the integration of the peaks is an 8:4:1 ratio. The integral of '8' refers to **I1**. The integral '4' refers to **I2**, which appears to be a mixture of two isomers in solution. The final integral '1' refers to **I3**, which is a mixture of isomers. These isomers (**I1**, **I2** and **I3**) were separated *via* ion-exchange chromatography.

2.4.4.3 [Co(A$_2$trien)]Cl – BAND 1 – I1

Due to the symmetry of this isomer, the $^{13}C\{^1H\}$ NMR and ^1H NMR spectra were straightforward to assign. The isomer was typically 80-85% of the total isomers isolated, making this the major isomer of the material. The enantiomer of the isomer is presumably also present.

The absolute configuration of the molecule is *CRSRS*; where *C* is the configuration about the central metal ion; *R* is the configuration about the amine nitrogen atom, and *S* is the configuration about the α-carbon atom. The same configurations are found on the other amine nitrogen and α-carbon atoms. The enantiomer of the complex has the absolute configuration *ASRSR (*where *A* is the configuration about the central metal ion; *S* is the configuration about the amine nitrogen atom, and *R* is the configuration about the α-carbon atom).

Results from the X-Ray crystallographic data show that, on both α-carbon atoms, the proton is located on the amine face of the meridional ligand fragment.

The ^3J coupling constant from the isomer mixture material of the largest doublet is ^3J = 6.9 Hz, which occurs between the methyl group protons and the proton on the α-carbon atom. The ^3J coupling constant from the major isomer ^1H NMR between the methyl group protons and the proton on the α-carbon atom is also ^3J = 6.9 Hz. Band 1, therefore, is the predominant isomer in the isomer mixture material.

2.4.4.4 [Co(AimAtrien)]Cl – HALF REDUCED ISOMER – I4a

In one case, a small amount of 'half reduced' complex was obtained and a crystal structure determined. Positions N1-C2 are joined by an imine bond while positions N4-C9 are joined by an amine bond. Of note, is the position of the protons on N4-C9 – which are in an *anti* configuration, where the hydride attack has occurred on the amine face of the molecule; this results in the N-H proton placed on the carboxylate face, and the α-C-H proton placed on the amine face of the meridional ligand fragment. This is the same configuration seen in the major isomer. The coupling constant of the doublet at 1.63 ppm is ^3J = 6.9 Hz which occurs from the methyl group protons and the proton on the α-carbon atom, and has the same value as **I1**. The enantiomer of this isomer is also present in the crystal structure.

2.4.4.5 [Co(A$_2$trien)]Cl – BAND 2 – I2

As described in section 2.3.5.1, the $^{13}C\{^1H\}$ NMR spectrum of this isomer does not match the predicted results of a single isomer in solution. It would be expected that (due to the unsymmetrical nature of the molecule) that two signals in the methyl and carbonyl regions of the $^{13}C\{^1H\}$ NMR spectrum would be observed. Instead, as shown in Figure 2-19, there are four signals in both regions. Two of each of these signals appears to have the same peak intensity, which could correlate to a single isomer. If **I2** were a mixture of one minor (asymmetric) isomer, as well as the major isomer, it could be assumed that three signals would be observed in the methyl and carbonyl regions (two from the minor isomer, and one from the symmetrical major isomer); this cannot satisfactorily explain the presence of four signals. The presence of two asymmetric isomers, however, correlates with the results in the spectrum.

The ^1H NMR spectrum may also explain the congestion seen in the $^{13}C\{^1H\}$ NMR spectrum. The expansion of the methyl region in Figure 2-20 has a set of overlapping doublets at δ 1.59-1.60 ppm. This also indicates multiple isomers are present in solution.

Results from the X-Ray crystallographic data show for the crystal structure (**I2a**), the proton is located on the amine face of the meridional ligand fragment on both α-carbon atoms. However, the configuration of the proton on the adjacent amine is *anti* for one chelate ring and *syn* for the other chelate ring This result can account for one of the asymmetric isomers, observed in both the $^{13}C\{^1H\}$ and ^1H NMR spectra.

Also seen in the ^1H NMR spectrum is a singlet peak at δ 2.64 ppm. This was an unexpected result, as this peak was assigned (in the $[Co(Aim_2trien)]^+$ complex) as the methyl group attached to the adjacent imine. According to the isomer mixture ^1H NMR spectrum, no unreduced material was present in solution. However, this could be explained by looking at the amount of the fragments present. **I1** accounts for 85% of the isomer mixture. Because the **I1** material is in large excess, small signals, such as the singlet peak at δ 2.64 ppm may not be observed in the isomer mixture ^1H NMR spectrum. Once **I1** has been separated, only 15% of the isomer mixtures remain and signals, previously overwhelmed by **I1**, are now observed. The $^{13}C\{^1H\}$ NMR spectrum of this material has four peaks in the carbonyl chemical shift region, where imine carbon signals also are observed. It is difficult to assess if any of those four signals may indicate an imine carbon signal.

The ^{3}J coupling constant from the isomer mixture material (second major peak) is ^{3}J = 7.0 Hz. Both expected doublets in **I2** also have a ^{3}J coupling constant of ^{3}J = 7.0 Hz.

Further attempts to separate the mixture of isomers were unsuccessful.

2.4.4.6 [Co(A$_2$trien)]Cl – BAND 3 – I3

The $^{13}C\{^{1}H\}$ NMR spectrum of the **I3** material (Figure 2-22) shows that multiple isomers are present in solution. The ^{1}H NMR spectrum for this fraction is extremely congested in the methyl region with approximately five sets of doublets.

It would be expected that, if the molecule was asymmetric, that 12 signals would be predicted in the $^{13}C\{^{1}H\}$ NMR spectrum. An expansion of the methyl and carbonyl regions in Figure 2-22 shows five and four signals in each area respectively. These signals could be explained if five symmetrical isomers are present in solution or a mixture of asymmetric and symmetric isomers are present.

Also present in this spectrum (as for **I2**) is a singlet peak at approximately δ 2.7 ppm. According to the isomer mixture ^{1}H NMR spectrum, no unreduced material was present in solution. As described previously, this may not be unsurprising given the excess of major isomer material in the isomer mixture.

Further separation *via* other ion-exchange chromatographic techniques could be employed to detect the mixture of isomers present in the solution.

2.4.5 PROTON POSITION ON THE α-CARBON ATOMS

In the cases where products of the borohydride reaction have been crystallised, it has been found that the position of the proton on the α-carbon atoms has been on the amine face of the meridional ligand fragment. This configuration would occur only when hydride attack attacks the amine face selectively.

2.5 CONCLUSIONS

A series of imino acid complexes were synthesised by coordination of α-keto acids to a polyamine cobalt(III) complex with the backbone of cobalt di-chlorido *N*,*N'*-bis(2-aminoethyl)ethane-1,2-diamine. The intramolecular condensation reaction between the carbonyl group of the α-keto acid and an amine of the polyamine backbone of the complex led to the formation of an imino acid complex.

Reduction of the imine to the amino acid complex in particular the $[Co(A_2trien)]^+$ system, was extensively investigated. The crude ^1H NMR data showed isomers giving an integral of 8:4:1 were present in solution, and these were separated *via* ion-exchange chromatographic techniques. The major isomer (**I1**) and one minor isomer (**I2a**) were extensively characterised. However the NMR of the third band (**I3**) still showed multiple isomers in solution. A half-reduced isomer (**I4a**) was obtained, and an investigation into the selectivity of hydride attack was also conducted. At this point, it is thought that the predominant hydride attack occurs on the amine face of the molecule, determining the configuration at the α-carbon proton seen in the crystal structures obtained.

2.6 REFERENCES

1 R. M. Hartshorn and S. G. Telfer, *Journal of the Chemical Society-Dalton Transactions*, 1999, 3217.

2 R. M. Hartshorn and S. G. Telfer, *Journal of the Chemical Society-Dalton Transactions*, 1999, 3565.

3 J. M. W. Browne, J. Wikaira, C. M. Fitchett, and R. M. Hartshorn, *Journal of the Chemical Society-Dalton Transactions*, 2002, 2227.

4 L. C. Marsh, 'B.Sc. Hons. Report; Department of Chemistry, University of Canterbury', 2001.

5 D. A. House and C. S. Garner, *Inorganic Chemistry*, 1966, **5**, 2097.

6 A. M. Sargeson and G. H. Searle, *Inorganic Chemistry*, 1967, **6**, 787.

7 H. Plieninger, *Chemische Berichte-Recueil*, 1950, **83**, 271.

8 E. Ohler and U. Schmidt, *Chemische Berichte-Recueil*, 1975, **108**, 2907.

9 G. M. Ksander, J. E. McMurry, and M. Johnson, *Journal of Organic Chemistry*, 1977, **42**, 1180.

10 P. J. Lawson, M. G. McCarthy, and A. M. Sargeson, *Journal of the American Chemical Society*, 1982, **104**, 6710.

11 J. M. Browne, 'Intramolecular condensation reactions of cobalt(III) complexes : a thesis submitted in partial fulfilment of the requirements for the degree of Master of Science in Chemistry at the University of Canterbury', 2000.

CHAPTER THREE

ISOMERISATION STUDIES

3.1 INTRODUCTION

The initial results of the borohydride reduction to form the $[Co(A_2trien)]^+$ complex, have been discussed in Chapter Two. Is the isomer distribution observed due to thermodynamic or kinetic control, or a combination? In this Chapter, the results of proton epimerisation of both the amine and α-carbon atom centres are presented.

Previous studies by Buckingham *et al.* [1] used the $[Co(en)_2(val)]^{2+}$ (val = valinate) and $[Co(en)_2(ala)]^{2+}$ (ala = alaninate) complexes to study α-proton exchange and mutarotation by using optically active ligands, such as amino acids. Williams *et al.* [2] and Terrill *et al.* [3] showed in their work that in aqueous solution the α-carbon proton undergoes base-catalysed exchange, which introduced the possibility of mutarotation of the coordinated amino acids. The mechanism of the exchange may be *via* a coordinated carbanion (Figure 3-1).

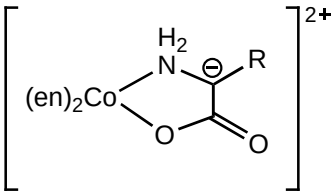

Figure 3-1: $[Co(en)_2(val)]^{2+}$ complex, with the carbanion centre

The carbanion centre may react with solvent water, which could retain or invert the configuration about the α-carbon atom. Buckingham *et al.* found that, in basic solution, the coordinated amino acid complex would mutarotate, but with the configuration at the cobalt(III) centre retained (Figure 3-2).[1]

$$\text{D-}[Co(en)_2(\text{L-ala})]^{2+} \underset{k_2}{\overset{k_1}{\rightleftharpoons}} \text{D-}[Co(en)_2(\text{D-ala})]^{2+}$$

Figure 3-2: Equilibrium diagram for the mutarotation of $[Co(en)_2(val)]^{2+}$ complex. The alaninate complex is analogous

Results from this study established that the rate law for the α-carbon proton exchange in the coordinated amino acid anion is consistent with the nucleophilic attack of OH^- at the proton leaving the coordinated amino acid carbanion. From the kinetic data from the $[Co(en)_2(ala)]^{2+}$ equilibration experiments Buckingham *et al.* proposed the rate determining step as proton removal.[1] The carbanion rearranges and reacts rapidly with solvent water (≈ 10^{10} sec^{-1}), to regenerate both the D and L forms of the amino acid, in approximately equal amounts. The study also proposed a mechanistic pathway to account for their observations (Scheme 1).

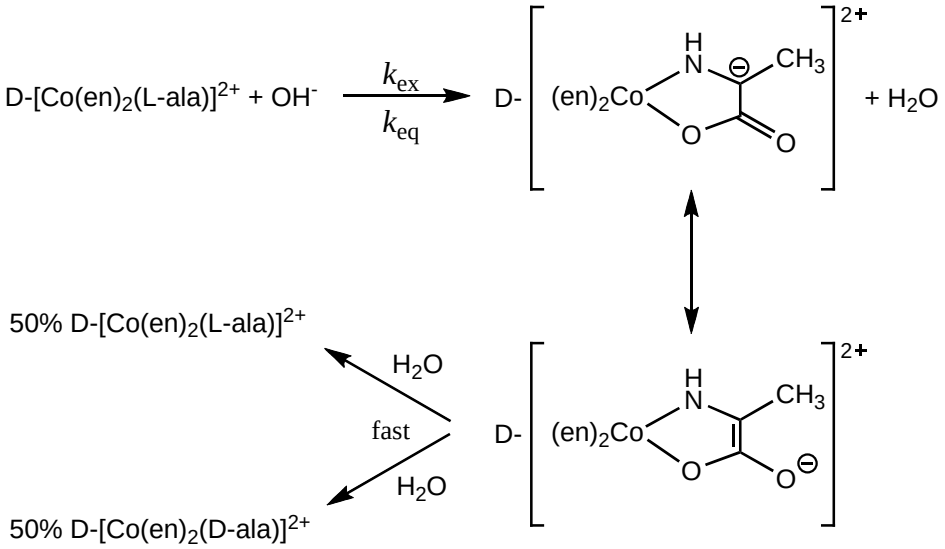

Scheme 1: Proposed mechanism for proton exchange of $[Co(en)_2(ala)]^{2+}$ *via* a carbanion intermediate

A later paper by Buckingham *et al.* expanded on his previous work to include a study of the carbanion intermediate.[4] The study concluded that a single carbanion intermediate is formed, which controls the thermodynamic distribution of epimers (Scheme 2).

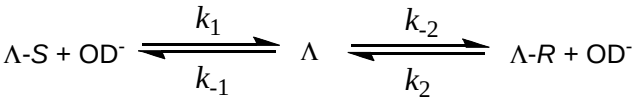

Scheme 2: Mechanism I for the thermodynamic distribution of epimers[4]

For the system $[Co(en)_2(ala)]^{2+}$, there appeared to be some selectivity for reprotonation on a favoured face of the carbanion; this resulted in the Λ-*S* epimer of $[Co(en)_2(ala)]^{2+}$.

The reduction reaction of $[Co(A_2trien)]Cl$, in this work, is performed under mildly basic conditions in carbonate buffer – is it possible that base catalysed inversion of the stereogenic centres can occur under these conditions, with a purified and characterised isomer of $[Co(A_2trien)]^{+}$?

To investigate this question, the major isomer of $[Co(A_2trien)]^{+}$ was dissolved in a basic solution and studied to see if epimerisation occurred, and at which centres. These results may allow examination of whether the isomer distribution from reduction is a result of dynamic equilibrium.

3.2 EXPERIMENTAL

3.2.1 MATERIALS

Reagents and solvents were obtained from Sigma Aldrich or Merck and were of reagent grade or better and were used without further purification, unless stated otherwise.

Dowex 50WX2-200 (cation exchange resin), Dowex 50WX2-400 (cation exchange resin) and SP Sephadex C25 ion exchange resins were obtained from Sigma Aldrich. Column dimensions are given as (height x diameter).

3.2.2 INSTRUMENTATION/MEASUREMENTS

^{1}H, gCOSY and HSQCAD experiments were all recorded on a Varian INOVA 500 spectrometer at 23℃, operating at 500 MHz. The INOVA was equipped with a variable temperature and inverse-detection 5 mm probe or a triple-resonance indirect detection PFG probe. The ^{13}C NMR spectra were recorded on either a Varian UNITY 300 NMR spectrometer equipped with a variable temperature direct broadband 5 mm probe, at 23℃, operating at 75 MHz or on a Varian INOVA 500 spectrometer at 23℃, operating at 125 MHz, using a 5mm variable temperature switchable PFG probe. Chemical shifts are expressed in parts per million (ppm) on the δ scale and were referenced to the appropriate solvent peaks: DMSO-d_6 referenced to $CD_3(C\mathbf{H}D_2)SO$ at δ_H 2.50 (^{1}H) and $(\mathbf{C}D_3)_2SO$ at δ_C 39.6 (^{13}C). As reference in D_2O and DCl (99% D, 35 wt. % in D_2O), 3-(trimethylsilyl)propane-1-sulfonic acid (TMPS) or 3-(trimethylsilyl)propionic acid-d_4 sodium salt was used as an internal standard (δ_H 0 (^{1}H); δ_C 0 (^{13}C)).

Infrared spectra were obtained using a Shimadzu 8201PC Series FTIR using diffuse reflectance method in solid KBr.

High Resolution Electrospray Ionisation Mass Spectra (HRESIMS) were recorded on a Micromass LCT spectrometer using a probe voltage of 3200V, an operating temperature of 150°C and a source temperature of 80°C. The carrier solvent was 50:50 CH_3CN/H_2O at

20 μL/minute. Typically, 10 μL of a 10 μg/mL solution was injected. Leucine enkephalin was used as the lock mass internal standard.

UV-visible spectra were recorded on a Varian CARY Probe 50 UV-vis. spectrophotometer, or a Varian CARY 100 UV-vis. spectrophotometer.

Evaporations were performed using a Büchi rotary evaporator equipped with either a diaphragm vacuum pump or a water aspirator pump (pressure ≈15 torr) and at a temperature of 40°C unless otherwise stated.

Elemental analyses were performed by the Campbell Microanalytical Laboratory at the University of Otago.

3.2.3 PREPARATIONS

3.2.3.1 SMALL SCALE ISOMERISATION

mffm-[Co(A_2trien)]Cl – major isomer – I1 (*ASRSR*/*CRSRS*)

mffm-[Co(A_2trien)]Cl – major isomer (**I1**) (0.0020 g, 5.23×10^{-3} mmol) and Na_2CO_3 (0.0020 g, 0.01 mmol) was added to ≈150μL of D_2O. The sample was mixed on a vortex mixer for 2 minutes. The sample was then loaded into a 3 mm NMR tube and a ^{1}H NMR spectrum obtained. The sample was typically kept for a fortnight at room temperature, during which additional ^{1}H NMR spectra were obtained.

3.2.3.2 LARGE SCALE ISOMERISATION – TWO HOURS

mffm-[Co(A_2trien)]Cl – major isomer (**I1**) (0.10 g, 0.26 mmol) was added to a 0.1M solution of Na_2CO_3 (300 mL; pH = 11.07). The sample was stirred for 2 hours. The sample was then quenched with aqueous HCl (1 M, 500 mL) and the solution was taken to dryness by rotary evaporation at 40°C. The product, according to ^{1}H NMR, was a mixture of isomers. This was then taken directly to the separation experiment.

The product (0.29 g, 0.76 mmol) was dissolved in aqueous HCl (0.05M, 1 L) and loaded onto an H^+-Dowex column (24 x 3 cm). A red/purple band (band 1) was observed along with a red band (band 2) and an orange/brown band (band 3). These were eluted with aqueous HCl (0.1 M, 9 L). The eluates were taken to dryness by rotary evaporation at 40°C.

Band 1 – 0.28 g

Band 2 – 0.07 g

Band 3 – 0.07 g

3.2.3.3 *Large Scale Isomerisation – Two Weeks*

mffm-[Co(A_2trien)]Cl – major isomer (**I1**) (0.10 g, 0.26 mmol) was added to a 0.1M solution of Na_2CO_3 (300 mL; pH = 11.07). The sample was stirred for 2 weeks at room temperature. The sample was then quenched with aqueous HCl (1 M, 500 mL) and the solution was taken to dryness by rotary evaporation at 40°C. The product was a mixture of isomers according to ^{1}H NMR. This was then taken directly to the separation experiment.

The product (0.29 g, 0.76 mmol) was dissolved in aqueous HCl (0.05M, 1 L) and loaded onto an H^+-Dowex column (24 x 3 cm). A red/purple band was observed along with a red band (band 2) and an orange band (band 3). They were eluted with aqueous HCl (0.1 M, 9 L). The eluates were taken to dryness by rotary evaporation at 40°C.

Band 1 – 0.38 g

Band 2 – 0.006 g

Band 3 – 0.073 g

3.2.3.4 *Reduction of mffm-[Co(Aim$_2$trien)]$_2$[ZnCl$_4$] using NaBD$_4$*

mffm-[Co(Aim$_2$trien)]$_2$[$ZnCl_4$] (0.20 g, 0.5 mmol) was dissolved in 250mL of carbonate buffer (2.12 g K_2CO_3 and 2.09 g $KHCO_3$ in 500mL H_2O). $NaBD_4$ (0.22 g 5 mmol) was added and stirred constantly for 10 minutes. The red/orange solution was adsorbed onto a Na^+-form Dowex column (10 x 10 cm) under suction, followed by carbonate buffer (250 mL). The column was initially washed with H_2O (≈3 L), after which the red band was ready to be eluted with aqueous HCl (0.2 M, 1 L; 1 M, 2 L). The red eluate was taken to dryness on a rotary evaporator at 40°C.

Yield: 7.08 g. The crude material was contaminated with NaCl.

3.3 RESULTS

3.3.1 SPECTROSCOPIC DATA FOR THE SMALL SCALE ISOMERISATION EXPERIMENTS

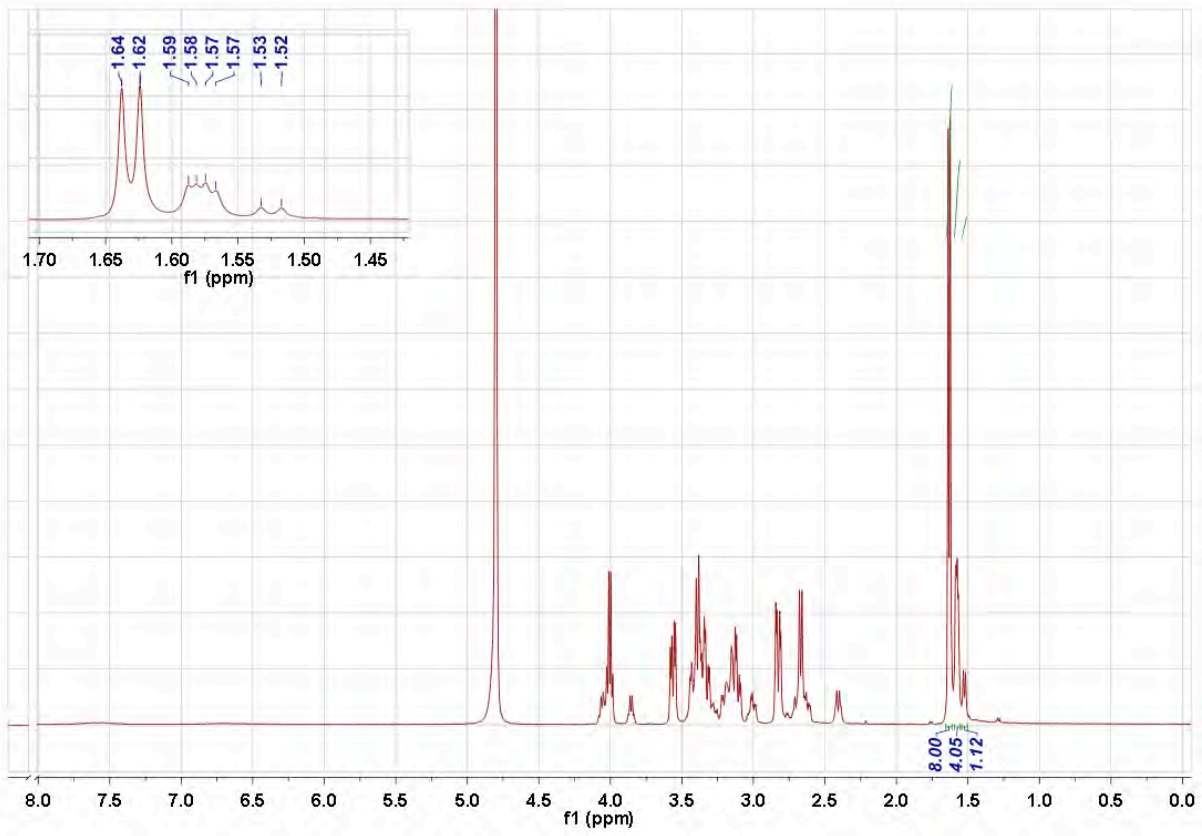

Figure 3-3: ^{1}H NMR spectrum of the [Co(A_2trien)]$^{+}$ major isomer (I1) after the sodium carbonate isomerisation experiment. ^{1}H NMR spectrum was collected immediately after mixing

After base treatment, a mixture of isomers is present in solution, as indicated by the presence of multiple peaks at δ 1.5-1.65 ppm. The integral ratio of these peaks is approximately 8:4:1. There is a loss of signal in the amine proton region (δ 6-7.5 ppm). The α-carbon proton signals are still present (approximately δ 4.0 ppm), along with all other C-H signals. The

peaks at δ 1.57-1.59 ppm (shown in the expansion), appear to be two sets of doublets overlapped.

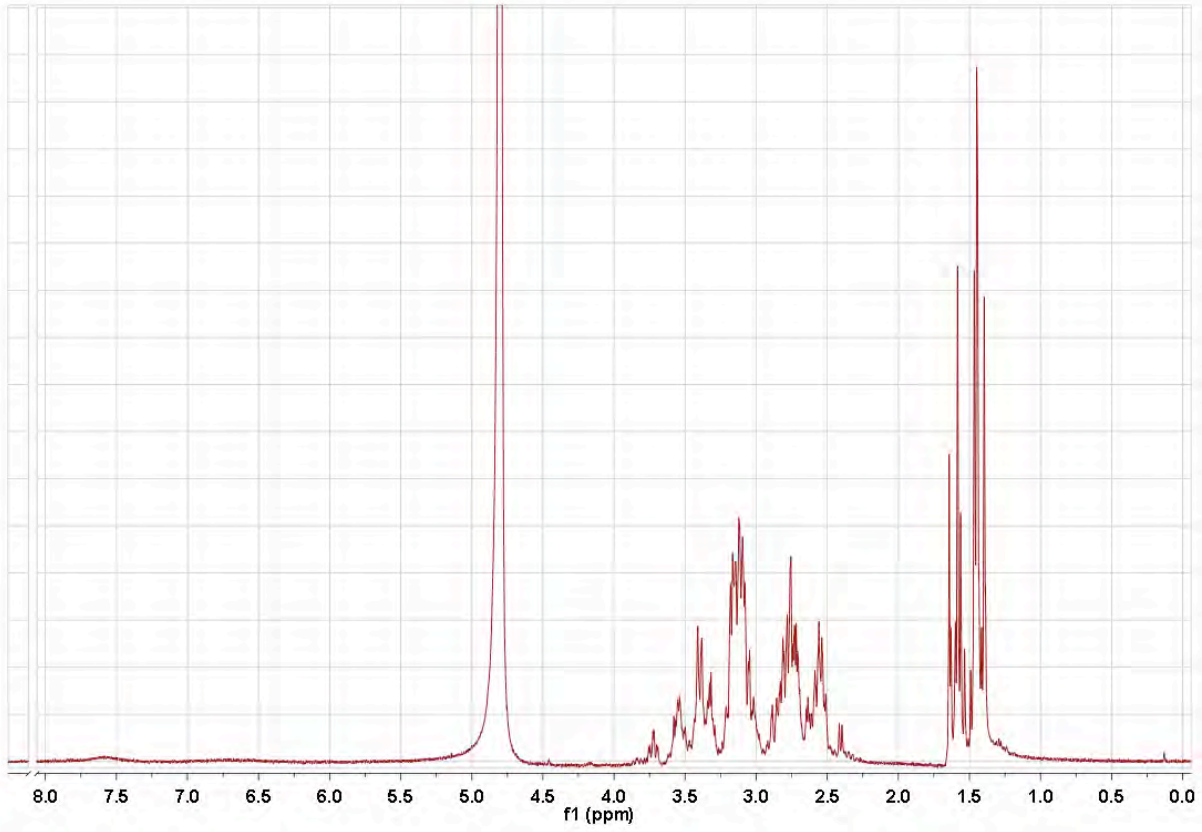

Figure 3-4: ^{1}H NMR spectrum of the [Co(A_2trien)]$^{+}$ major isomer (I1) with sodium carbonate isomerisation experiment. ^{1}H NMR was performed a fortnight after initial mixing

The initial sample was kept to monitor the proton exchange over a period of time. Figure 3-4 is a ^{1}H NMR spectrum taken two weeks after mixing. There is much greater complexity seen in the methyl region of the spectrum (δ 1.40-1.65 ppm), presumably due to multiple isomers being present in solution. There is also loss of signal both in the amine proton and α-carbon proton regions. The resulting peaks in the methyl region are singlets, due to the exchange of α-carbon protons to deuterons.

3.3.2 SPECTROSCOPIC DATA FOR THE ISOMERISATION EXPERIMENTS – LARGE SCALE

The material from the isomerisation experiments was analyzed *via* ^{1}H NMR and again showed a mixture of isomers to be present in solution. The isomers from the two hour experiment were separated *via* ion-exchange chromatography.

3.3.2.1 [Co(A$_2$trien)]Cl – TWO HOUR EXPERIMENT

BAND ONE

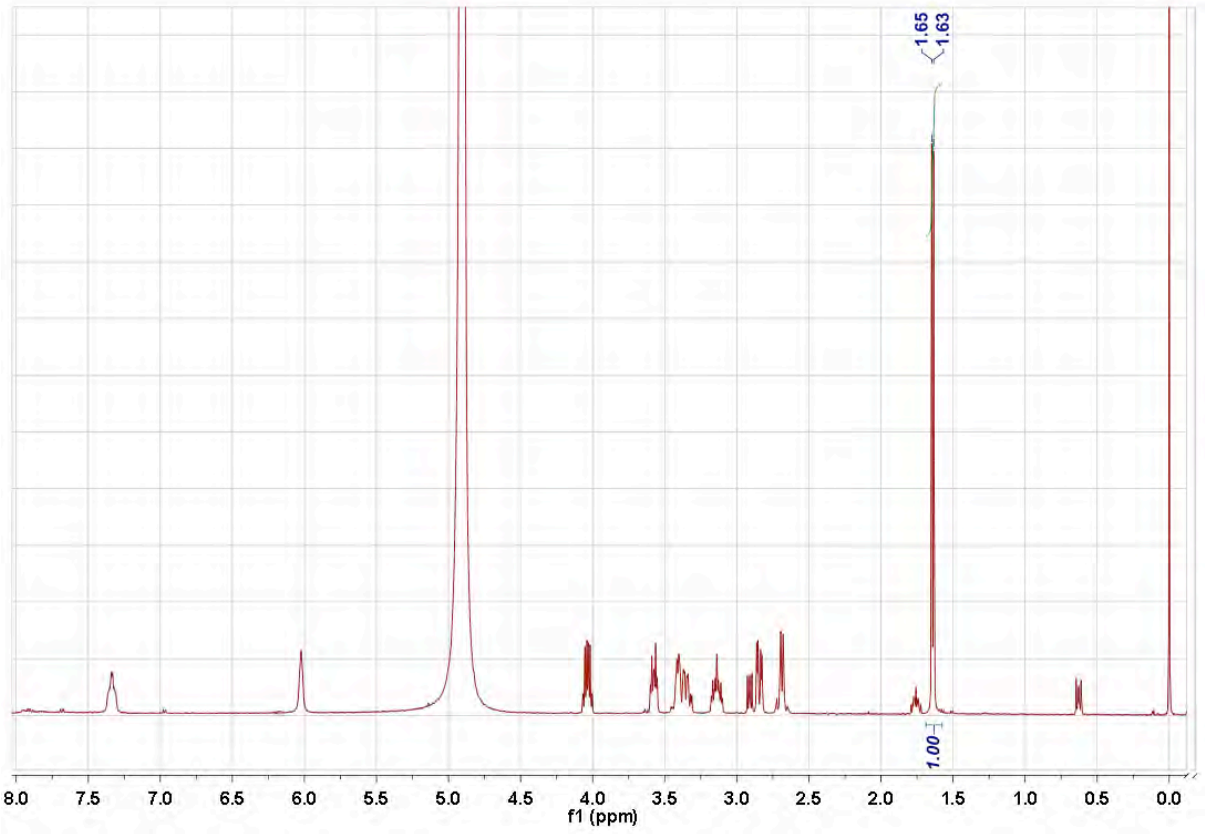

Figure 3-5: ^{1}H NMR spectrum of the [Co(A$_2$trien)]Cl band one product; after the 2 hours isomerisation experiment

The ^{1}H NMR spectrum of first band to be eluted off the H^{+}-Dowex column (Figure 3-5) has a set of doublet peaks at δ 1.63-1.65 ppm. The ^{3}J coupling constant at δ 1.64 ppm is ^{3}J = 6.9 Hz (between the methyl group protons and the proton on the α-carbon atom). The chemical shifts and ^{3}J coupling constant are consistent with the values for the **I1** starting material. This band, it is concluded, is **I1**.

BAND TWO

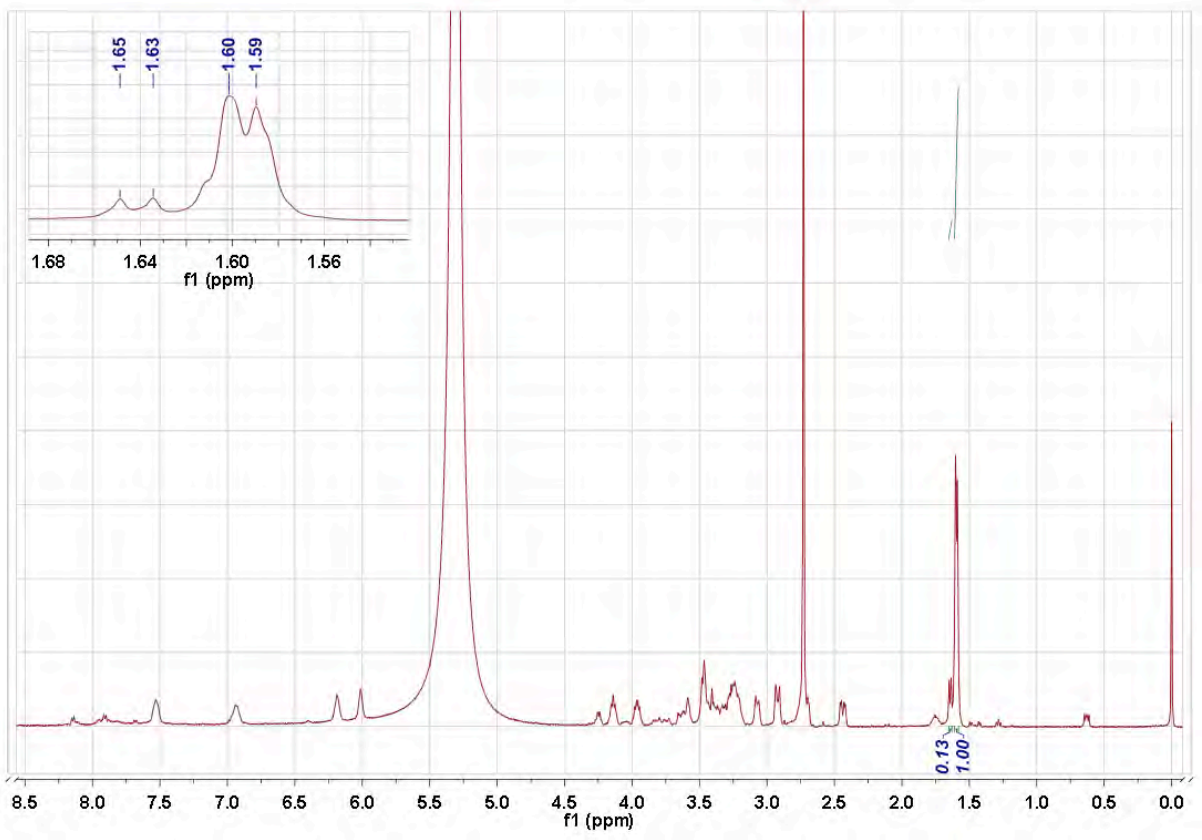

Figure 3-6: ^{1}H NMR spectrum of the [Co(A_2trien)] Cl band two product; after the 2 hours isomerisation experiment

The ^{1}H NMR spectrum of the second band to be eluted off the H^{+}-Dowex column (Figure 3-6) has two sets of doublets (the region is shown in an expansion in Figure 3-6), approximately at δ 1.64 and δ 1.60 ppm, with that at δ 1.60 ppm being somewhat broadened, perhaps due to overlapping resonances. The ^{3}J coupling constant for the doublet at δ 1.64 ppm is ^{3}J = 7.2 Hz. The chemical shift of the minor set of doublets at δ 1.64 ppm and the ^{3}J

coupling constant have values consistent with the **I1** starting material and has been assigned as such. The singlet peak at δ 2.75 ppm has a peak intensity that is too large to be related to the sample and therefore conclude that it is an impurity.

BAND THREE

The third band of this material was unable to be characterised. A ^{1}H NMR spectrum was unable to be obtained, perhaps due to contamination from a paramagnetic species.

3.3.2.2 [Co(A$_2$trien)]Cl – TWO WEEK EXPERIMENT

The material from the isomerisation experiments was analyzed *via* ^{1}H NMR and showed a mixture of isomers in solution. Isomers from the two week experiment were separated *via* ion-exchange chromatography.

BAND ONE

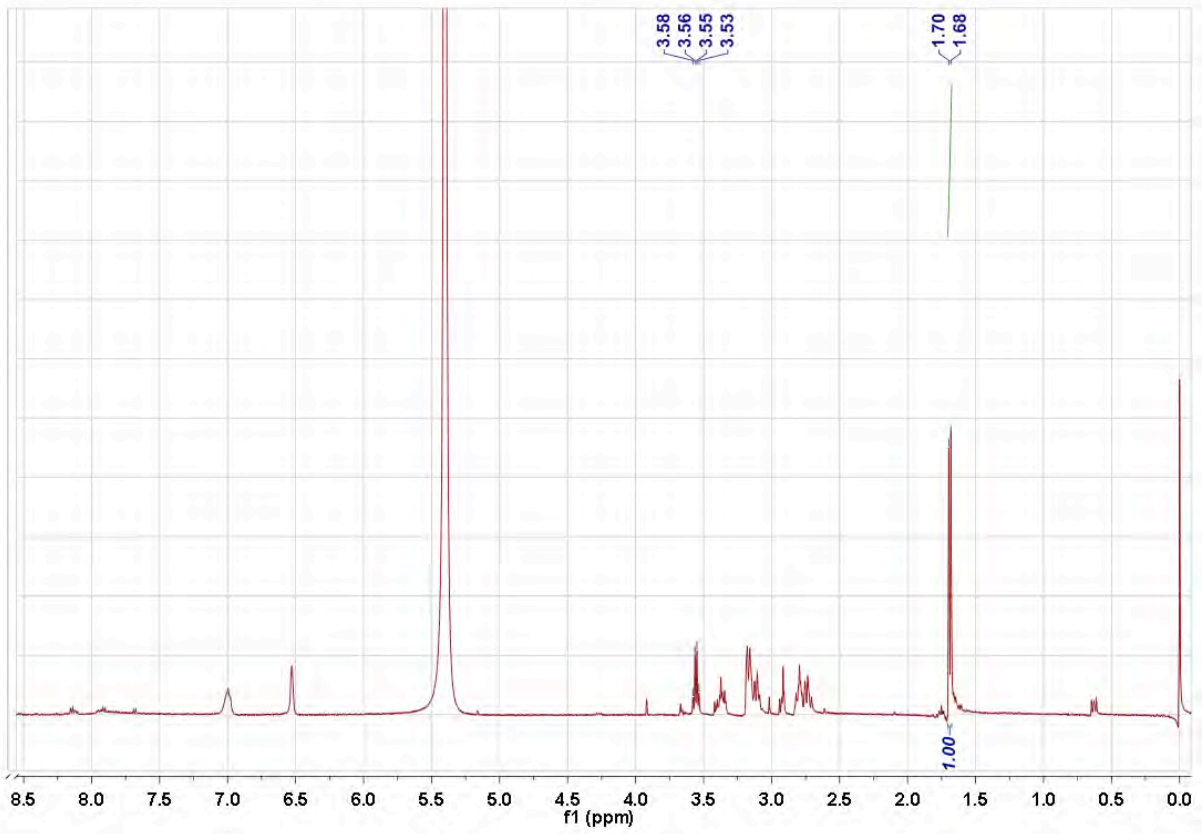

Figure 3-7: ^{1}H NMR spectrum of the two week isomerisation experiment - band one

The ^{1}H NMR spectrum of first band to be eluted off the H^+-Dowex column (Figure 3-7) has a set of doublet peaks at $\delta \approx 1.7$ ppm and the ^3J coupling constant has been measured as ^3J = 7.6 Hz (between the methyl group protons and the proton on the α-carbon atom, located upfield at δ 3.5 ppm). There is no α-carbon proton signal at δ 4.0 -4.5 ppm, therefore this compound is not **I1**. Further NMR spectra (such as $^{13}C\{^1H\}$ NMR and gCOSY) were obtained to characterise this isomer. From the gCOSY (Figure 3-8) the methyl group is

coupling to the quartet at δ 3.5 ppm) which can be attributed to a proton on the α-carbon. From the chemical shifts of the doublet at δ 1.70 ppm, the chemical shifts in the $^{13}C\{^{1}H\}$ NMR, and the coupling constant, it is believed that this material is a new isomer, not previously seen.

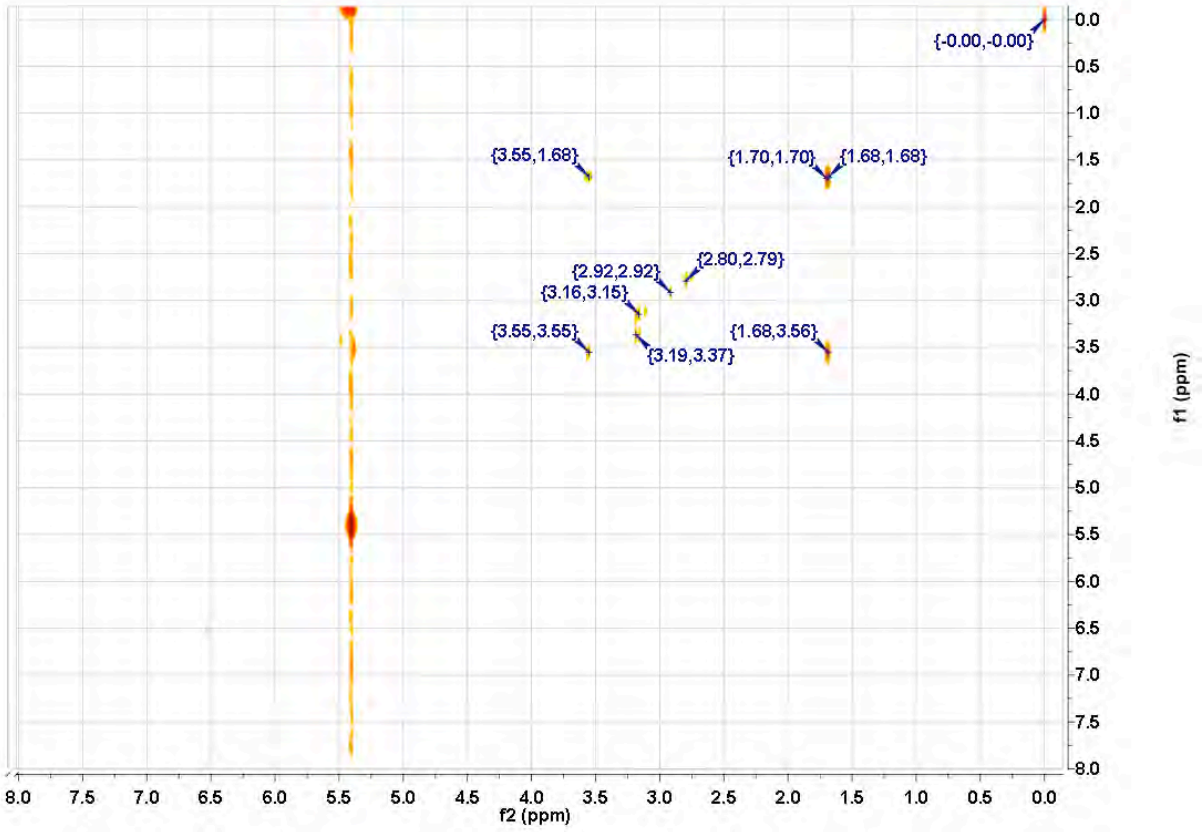

Figure 3-8: gCOSY spectrum of the two week isomerisation experiment - band one

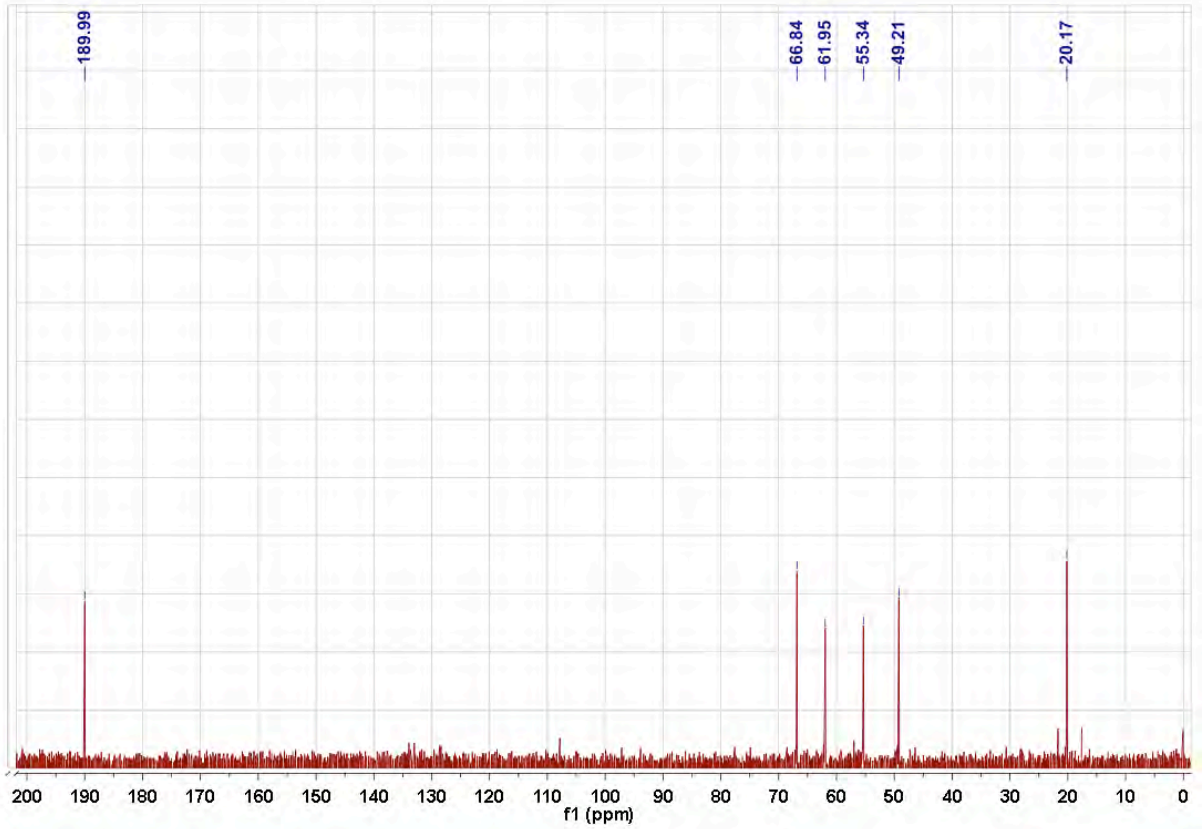

Figure 3-9: $^{13}C\{^{1}H\}$ spectrum of the two week isomerisation experiment - band one

From the $^{13}C\{^{1}H\}$ NMR spectrum (Figure 3-9), it is clear that there are 6 signals present, which indicates that this new isomer is a symmetrical complex. The chemical shifts seen are different to those seen in **I1**, isolated from the reduction experiments. For example, the carbonyl and methyl peaks in this spectrum have a chemical shift of δ 189.9 and δ 20.17 ppm respectively. These peaks in the **I1** spectrum occur at δ 187.0 and δ 17.79 ppm respectively.

BAND TWO

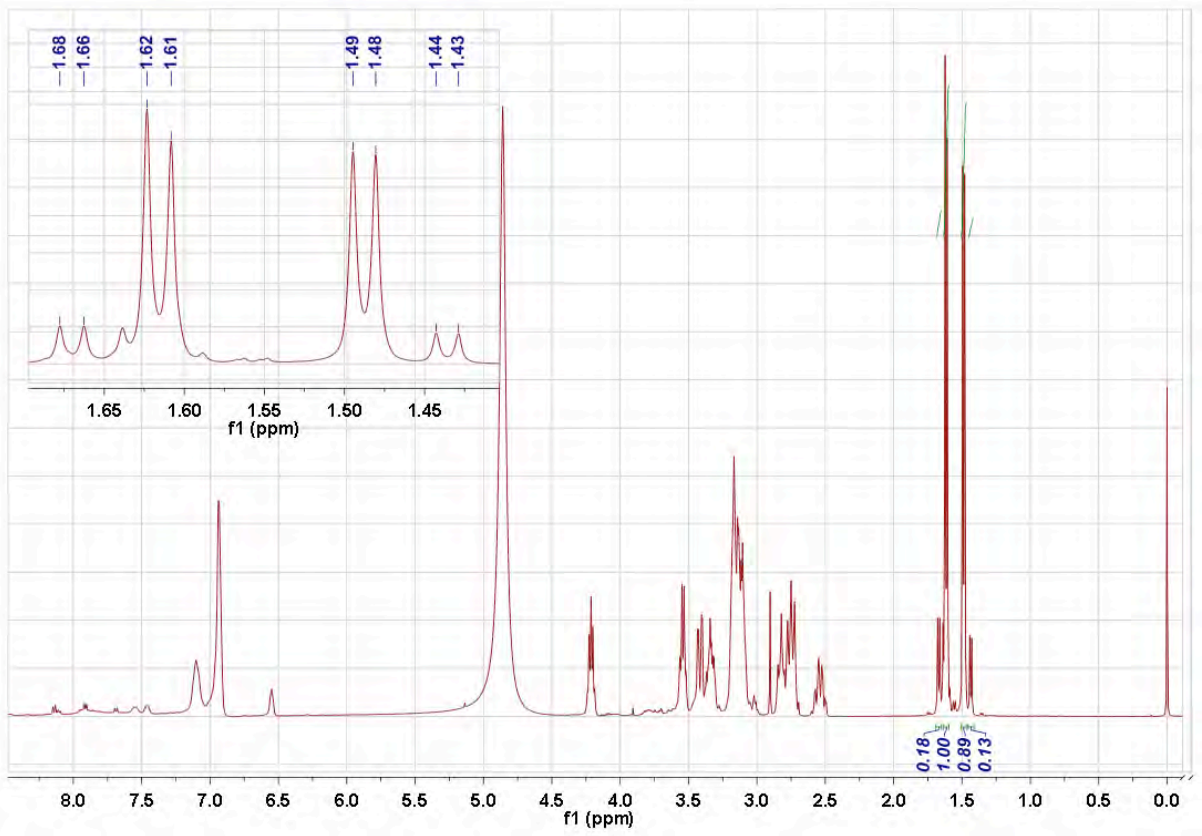

Figure 3-10: ^{1}H NMR spectrum of the two week isomerisation experiment - band two

The ^{1}H NMR spectrum of the second band to be eluted off the H^{+}-Dowex column (Figure 3-10) has four sets of doublet peaks. There are two sets at δ 1.4 ppm and two sets at δ 1.6 ppm. The ^{3}J coupling constants between the methyl group protons and the proton on the α-carbon atom have been measured: δ 1.67 ppm (^{3}J = 7.5 Hz); δ 1.62 ppm (^{3}J = 7.6 Hz); δ 1.49 ppm (^{3}J = 7.1 Hz); δ 1.44 ppm (^{3}J = 6.9 Hz). The peak intensities suggest that one asymmetric isomer is the major component in solution.

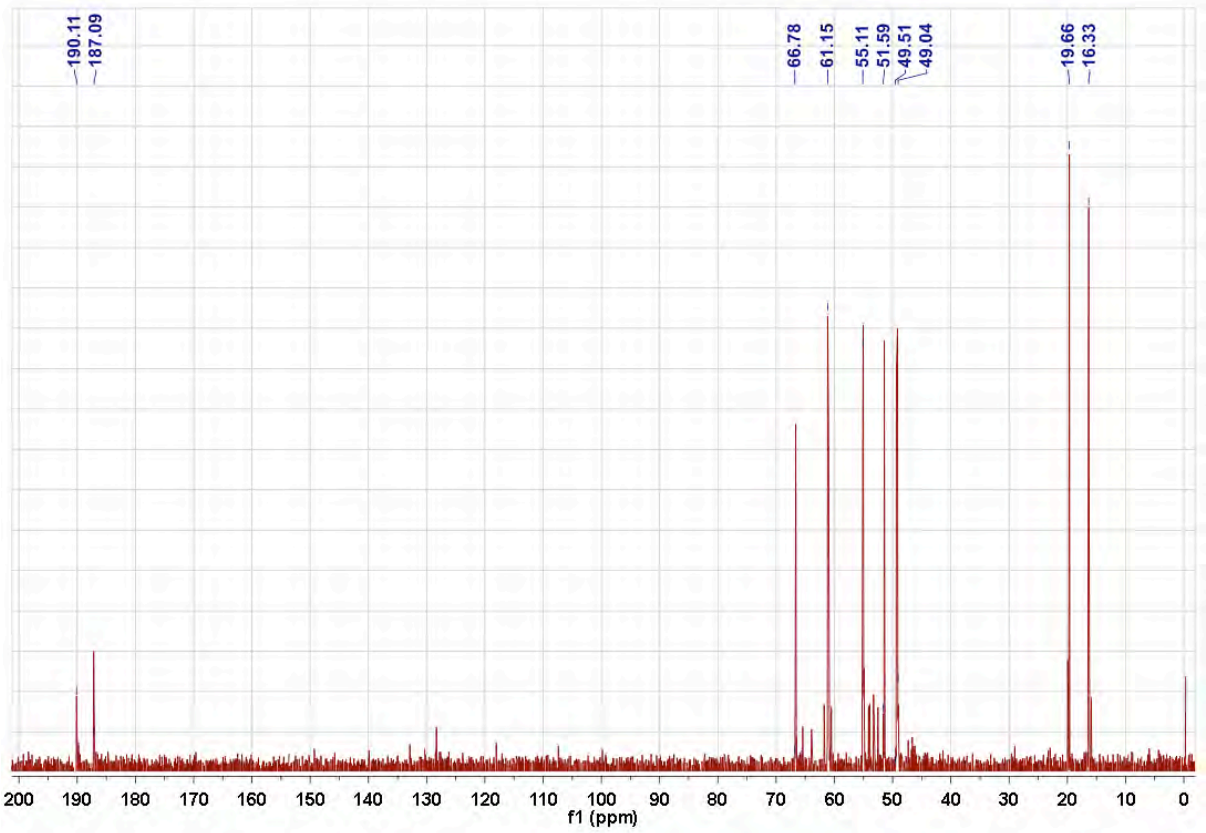

Figure 3-11: $^{13}C\{^{1}H\}$ NMR spectrum of the two week isomerisation experiment - band two

The $^{13}C\{^{1}H\}$ spectrum shows that there are two signals both in the carbonyl and methyl regions (δ 190.1; δ 187.1 and δ 19.6; δ 16.3 ppm respectively), which supports the ^{1}H NMR spectrum (Figure 3-10) assignment which suggests that one asymmetric isomer is the major component in solution.

BAND THREE

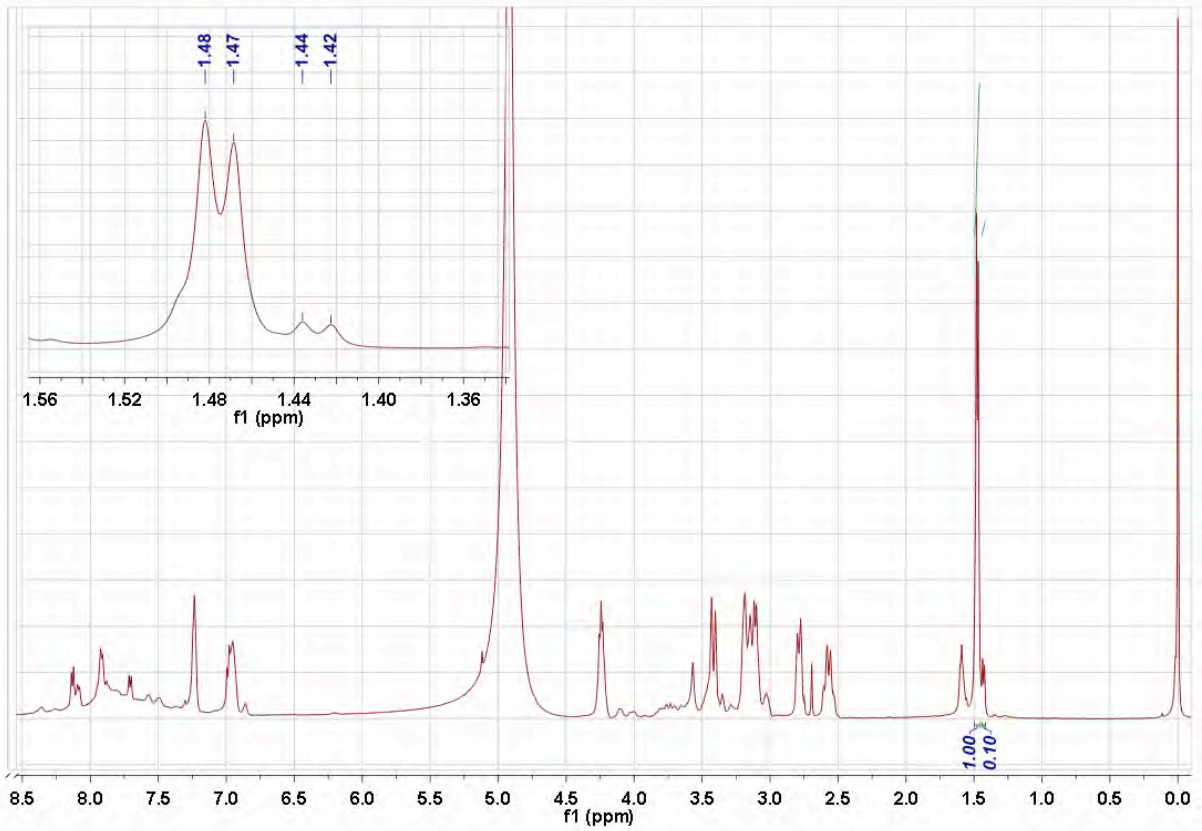

Figure 3-12: ^{1}H NMR spectrum of the two week isomerisation experiment - band three

The ^{1}H NMR spectrum of third band to be eluted off the H^{+}-Dowex column (Figure 3-12) has two sets of doublet peaks. These are located at δ 1.43 ppm and at δ 1.48 ppm. The ^{3}J coupling constants between the methyl group protons and the proton on the α-carbon proton have been measured: δ 1.48 ppm (^{3}J = 6.7 Hz) and δ 1.43 ppm (^{3}J = 6.7 Hz). However, the doublet set at δ 1.48 ppm has a greater intensity, and it is proposed that this doublet set is the major component in solution.

Peaks in the aromatic regions for both the ^{1}H NMR (δ 8.0 ppm) and the ^{13}C{^{1}H} NMR (δ 120-130 ppm (Figure 3-13) result from contamination by excess 2,6-lutidine.

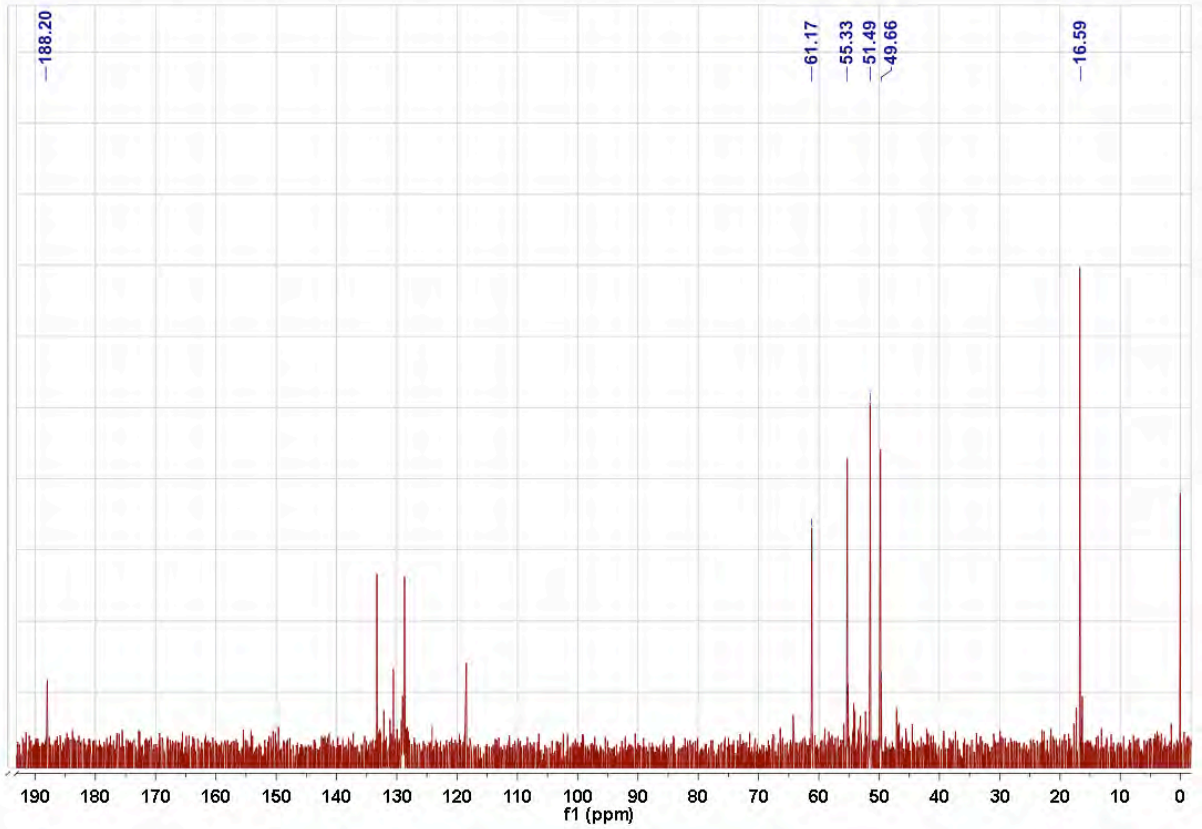

Figure 3-13: $^{13}C\{^{1}H\}$ NMR spectrum of the two week isomerisation experiment - band three

The single peak (δ 188 ppm) in the carbonyl region of the $^{13}C\{^{1}H\}$ NMR spectrum of the material from band three suggests that one symmetrical isomer is the major component in solution. The height of the methyl signal (in comparison to other peaks) is due to the lutidine contamination of the sample.

Further NMR spectra, such as gCOSY were not obtained.

3.3.2.3 *[Co(A$_2$trien)]Cl – REDUCTION USING NaBD$_4$*

A reduction reaction using borodeuteride was performed in order to verify the site of hydride attack and also to examine the methyl group chemical shifts in the when there is a deuteron on the α-carbon atom. This experiment also shows that α-C-H exchange does not occur under the conditions of the reduction experiment and subsequent isomer separation.

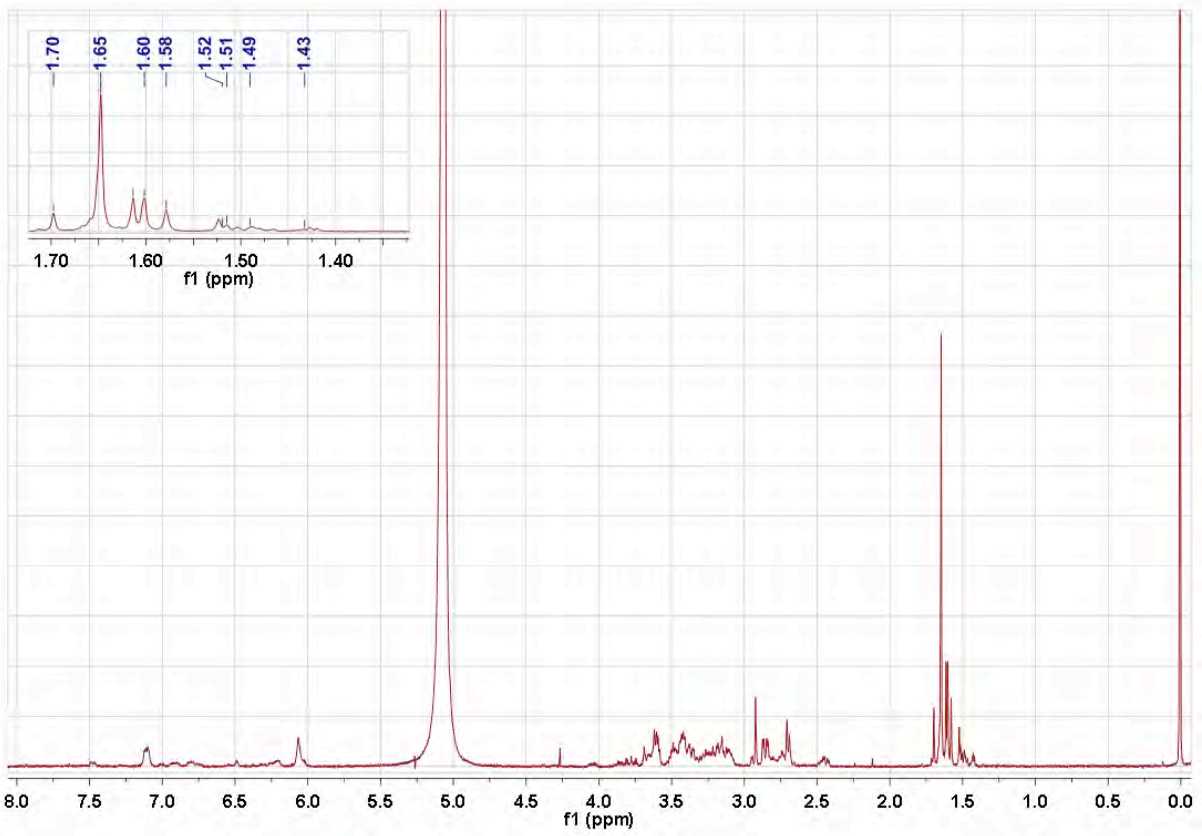

Figure 3-14: $^{13}C\{^1H\}$ NMR spectrum of the $[Co(A_2trien)]^+$ complex with $NaBD_4$ as the reducing agent

There is an absence of peaks at δ 4-4.5 ppm (Figure 3-14) which confirms that the hydride/deuteride attack is at the α-carbon. The presence of singlet peaks in the methyl region is expected (since the adjacent proton is now a deuteron, thus not splitting the signal).

The position of three of the singlets in Figure 3-14 (δ 1.65 ppm, δ 1.58 ppm and δ 1.52 ppm) have the same chemical shift as those doublets seen in the isomer mixture from borohydride reduction of [Co(A$_2$trien)]Cl.

3.4 DISCUSSION

The purpose of these experiments was to subject the well characterised isomer, **I1**, to basic conditions, in order to study base-catalysed epimerisation of the N-H and α-C-H stereogenic centres. The results of such experiments may give insight on whether the isomer distribution initially obtained from borohydride reduction is a result of dynamic equilibrium versus the kinetic product. The isomerisation experiment was performed under basic conditions; the exact pD of the small scale isomerisation experiments was not determined however the pH of the solutions for the large scale isomerisation experiments was typically ≈11 as measured by a calibrated pH probe. It is believed that the basicity of the solutions to be comparable, due to the similarity of the isomer distributions observed, at similar times, both in the small scale and large scale isomerisations.

3.4.1 SMALL SCALE ISOMERISATION EXPERIMENTS – IMMEDIATE MIXING

^{1}H NMR spectroscopy was used as the primary method of following the course of the isomerisation experiments as **I1** is well characterised, and splitting of the methyl signal at δ 1.6 ppm can be easily observed. The exchange of protons with deuterons in the NMR monitored experiments leads to a loss of signal when the amine protons (δ 6-7.5 ppm) and α-carbon proton (δ 4.0 ppm) are exchanged.

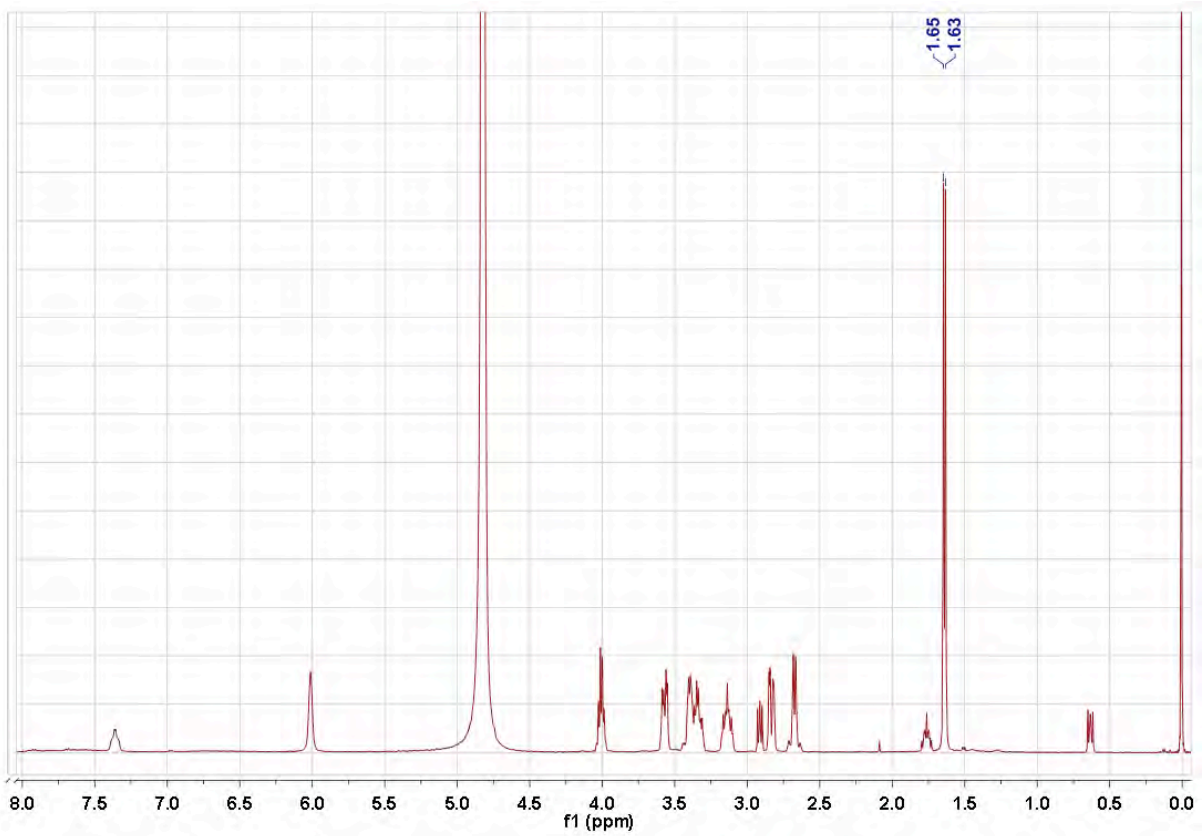

Figure 3-15: ^{1}H NMR spectrum of I1

The ^{1}H NMR spectrum of **I1** (Figure 3-15) clearly shows a doublet at δ 1.64 ppm. This can be confidently assigned as the methyl side chain of the alanine amino acid fragment.

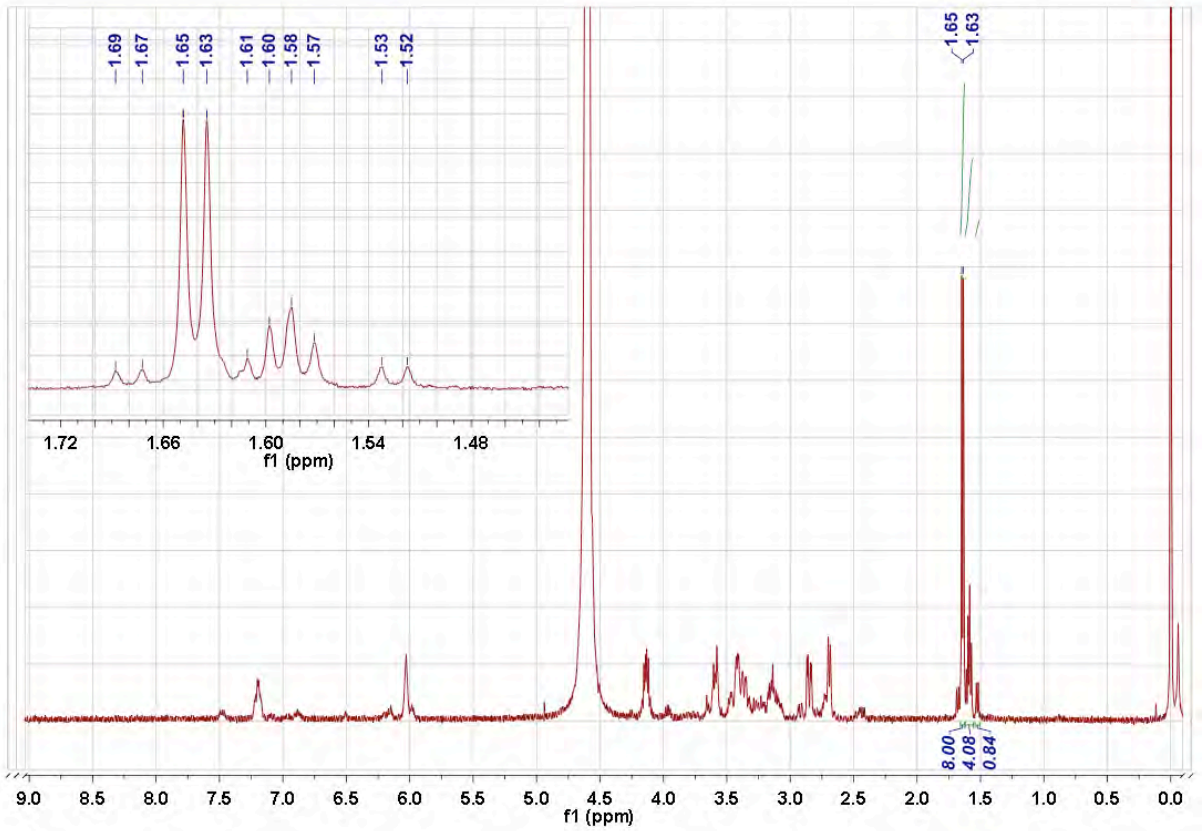

Figure 3-16: ^{1}H NMR spectrum of the isomer mixture of [Co(A$_2$trien)]Cl after borohydride reduction, prior to ion-exchange chromatography, with an expansion of the isomer ratio in the top left of the figure

The spectrum of the material from borohydride reduction is shown in Figure 3-16. The integration of the methyl peaks (δ 1.5-1.7 ppm) is approximately in an 8:4:1 ratio. An expansion of this area is shown in Figure 3-16, with the doublet peaks labelled. From the initial small scale isomerisation results (Figure 3-3), the isomer integral ratio is also 8:4:1. The chemical shifts from both sets of spectra are also comparable.

Also of interest are the coupling constants of the isomers. The coupling constant measured is between the methyl group protons and the proton on the α-carbon proton. In the isomer mixture of [Co(A$_2$trien)]$^{+}$ (shown in Figure 3-16), the doublet at δ 1.64 ppm had a ^{3}J value of ^{3}J = 6.9 Hz; the doublet at δ 1.54 ppm had a ^{3}J value of ^{3}J = 7.7 Hz (while the multiplet at δ 1.61-1.57 ppm was unable to be determined). The values obtained from the small scale ^{1}H NMR spectrum (obtained after immediate mixing) are similar; the doublet at δ 1.63 ppm had a ^{3}J value of ^{3}J = 6.9 Hz; the doublet at δ 1.52 ppm had a ^{3}J value of ^{3}J = 7.7 Hz.

The results of the small scale isomerisation (Figure 3-3) and the comparison to the isomer mixture from borohydride reduction allow some conclusions to be drawn. There is an exchange of amine protons with deuterons in the isomerisation experiment, which results in the loss of the signal in the spectrum at δ 6 ppm and δ 7.5 ppm. The isomerisation of the N-H proton resulted in an isomer distribution similar to that seen in the material from borohydride reduction (Figure 3-16). From this, it may be concluded that the isomer distribution from the reduction reaction appears to be very similar to that produced following amine proton exchange reactions.

The isomerisation experiments used only the single major isomer of [Co(A_2trien)]Cl (**I1**). The position of the proton on the α-carbon atom is on the amine face of the chelate ring on both α-carbon atom centres. Because there has been no exchange of the α-C-H proton in the small scale isomerisation experiment, is can be concluded that all these isomers (or at least the vast majority of them) have the α-carbon atom proton on the amine face of the molecule.

3.4.2 *Small Scale Isomerisation Experiments – Two Weeks*

The initial isomerised sample was kept to monitor the proton exchange over a period of time. ^{1}H NMR experiments were conducted 48 hours after the initial mixing, a week after mixing and finally a fortnight after mixing. The results of the extended isomerisation experiment (two weeks) resulted in the exchange of the α-carbon protons (Figure 3-4) and a greater complexity in the methyl region of the spectrum, compared to that of the original single isomer. It is possible that, in basic conditions, the polyamine backbone is able to rewrap, and so the configuration may no longer be *mffm* in all isomers. There are therefore many more possible isomers.

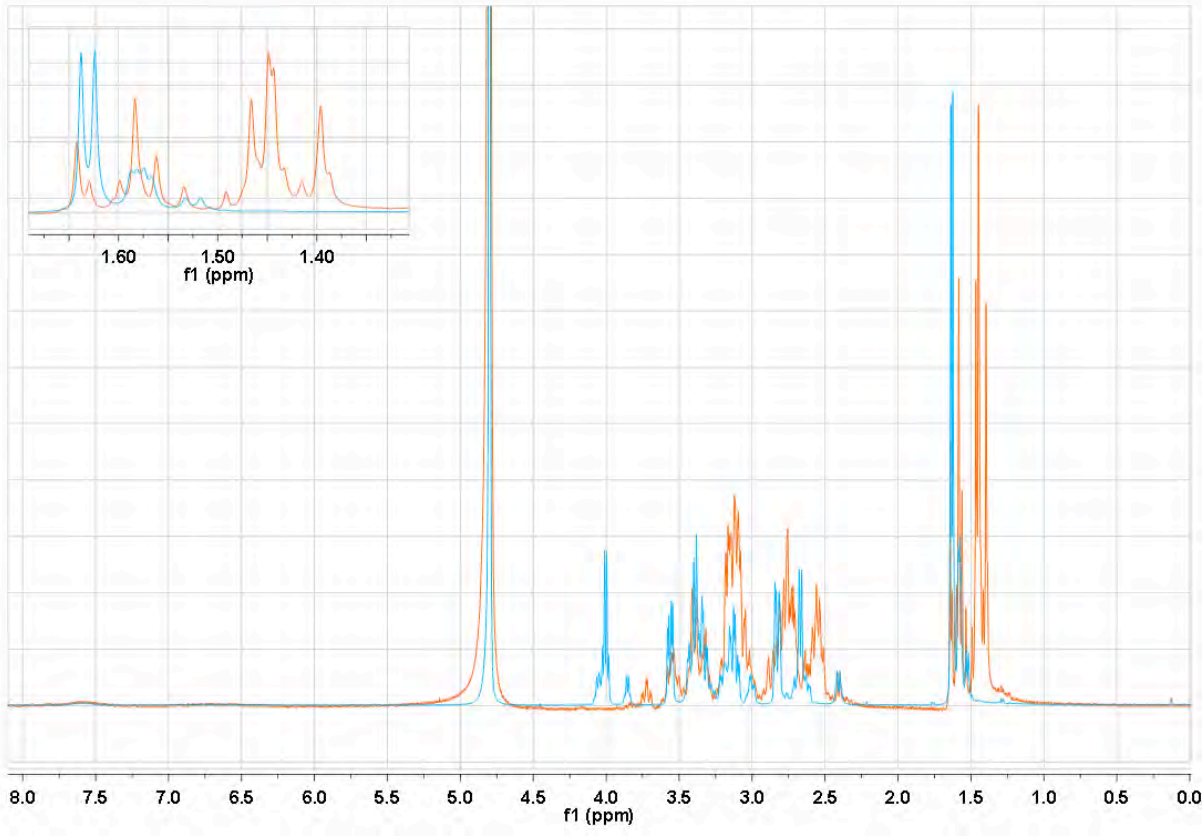

Figure 3-17: Superimposed ^{1}H NMR isomerisation experiments. two hour elapsed time is in blue: two week elapsed time is in orange. Note the distinct clusters of signals in the expansion. Both samples are referenced to D_2O (δ 4.8 ppm)

From Figure 3-17 the effect of isomerisation from the immediate exchange (in blue) and two week exchange (in orange) is clear. The immediate exchange still has signals at δ 4.0 ppm, indicative of the protons on the α-carbon atoms. Because of this, the signals observed in the methyl region of the spectrum are doublets. In the extended (two week) isomerisation experiment, there are no signals in the amine region (δ 6-7ppm) or the α-carbon region. The signals observed in the methyl region are all singlets. There appears to be a distinct cluster of signals when the N-H proton is exchanged (δ 1.50-1.65 ppm) and when there is exchange with the α-C-H protons (δ 1.40-.149 ppm).

Due to the exchange of protons with deuterons (from the solvent), there may be some effect on the chemical shift due of nearby protons. This complicates assignments of peaks due to isomers that have already been characterised. The borodeuteride reduction assists with this.

This can be best observed where the spectra of the borodeuteride reduction (in orange) and two week equilibration (in blue) are compared (Figure 3-18).

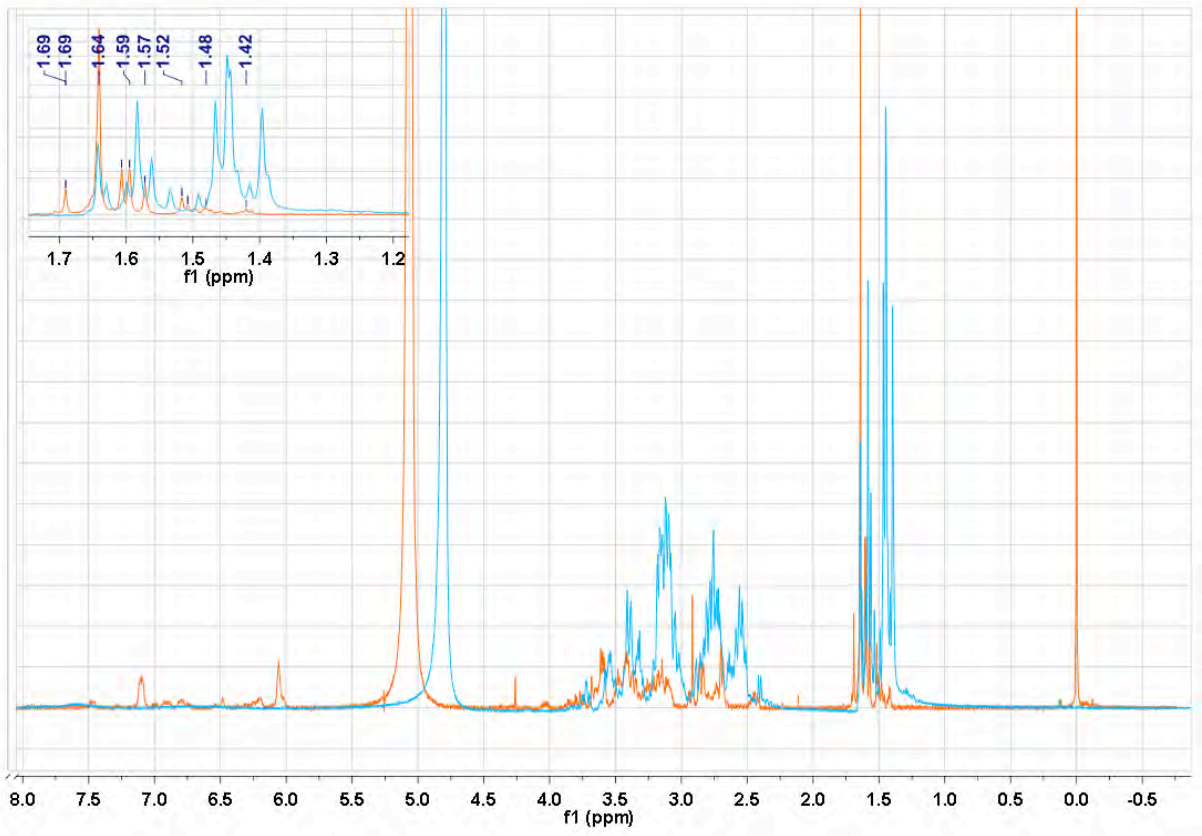

Figure 3-18: Superimposed ^{1}H spectra of [Co(A_2trien)]$^{+}$ isomer mixture from borodeuteride reduction (orange) and [Co(A2trien)]+ major isomer (I1) after two weeks isomerisation – of interest are the signals at δ 4.0, δ 6.0 and δ 7.4 ppm, which are not present in the 2 week solution (blue)

As shown by the expansion in Figure 3-18, there is an overlapping of signals from both sets of experiments (δ 1.52-1.64 ppm). There is a subtle difference in chemical shift (approximately δ 0.01 ppm) downfield observed with the borodeuteride singlets. This difference may be due to there being protons on the nitrogen atom adjacent to the α-carbon atom, creating a different environment from that observed in the two week isomerisation product (where both the α-carbon atom protons and N-H protons have been exchanged for deuterons).

The average chemical shifts of the doublets from the borohydride reduction, is δ 1.64, δ 1.59 and δ 1.53 ppm. These values compare to some of the chemical shifts of the singlets of the borodeuteride reduction where there are signals also seen at δ 1.64, δ 1.59 and δ 1.52 ppm. The only shift observed is δ 0.01 ppm upfield (δ 1.52 ppm) from the original values.

A paper by Jackson [5] described isotopomer effects on chemical shift of carbon atom signals of polyamine ligands in $^{13}C\{^{1}H\}$ spectra. It was observed that the chemical shifts when exchange of protons for deuterons led to an isotopic shift of <1 Hz for carbon α to the exchanging groups or 0.6-2.4 Hz for carbon β to the exchanging groups. These effects are seen in our system, but are smaller than those observed in Jackson's system.

3.4.3 LARGE SCALE ISOMERISATION EXPERIMENTS

The success of the small scale isomerisation led to a large scale experiment to determine if the results were consistent and possibly provide sufficient material to separate and characterise new isomers. An advantage of the larger scale experiment meant that separation and characterisation of the new isomers seen in the extended experiment might be achieved. Initial large scale experiments were set up, again using aqueous sodium carbonate as the base. The first attempts at the experiment were not successful as the pH (pH = ≈9) was not high enough. Once the pH was increased to ≈11, the results that were seen in the NMR experiment were mirrored by that of the large scale equilibration.

The isomers from both the two hour, and two week equilibration experiments were chromatographed *via* ion-exchange techniques.

3.4.3.1 TWO HOUR ISOMERISATION

The results that were seen in the small scale experiment were mirrored by that of the large scale equilibration. Separation of the isomers *via* ion-exchange chromatography was conducted. During the elution on H^+-Dowex, three bands separated out, and characterisation using NMR was performed.

The first band of this material (Figure 3-5) was characterised. The coupling constant for **I1** and also the set of doublet peaks in band 1 is ^3J = 6.9 Hz, where the coupling between the methyl group protons and the α-carbon atom proton is measured. This, and other NMR data, therefore confirms the first band to be the **I1**.

The second band of this material (Figure 3-6) has two sets of doublets in the methyl region. However, the doublet at δ 1.60 ppm is broadened, which may be due to overlapping resonances. The chemical shift of the doublet at δ 1.64 ppm, and the coupling constant, ^3J = 7.2 Hz, is consistent with values of the major isomer and has been assigned as such. From the small scale isomerisation, it can be determined that the only exchange has been on the N-H proton, and not the α-carbon proton. From this analysis, this isomer must be the

same as one of the isomers from band 2 (**I2**) of the original [Co(A_2trien)]Cl separation, discussed in Chapter Two. In that isomer (**I2a**), one amino acid fragment has the protons of the amine and α-carbon atom in an *anti* conformation, and the other half of the fragment in a *syn* conformation (Figure 3-19) but both α-C-H protons are on the amine face of the chelate ring.

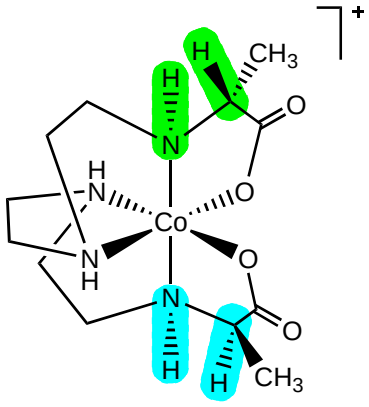

Figure 3-19: Schematic of the [Co(A_2trien)]$^+$ molecule with protons in an *anti* configuration in green, and protons in a *syn* configuration in blue

The third band of this material was unable to be characterised by NMR techniques due to contamination from a paramagnetic species.

3.4.3.2 Two Week Isomerisation

As noted in the section on the NMR equilibration experiments, the prolonged exposure of **I1** to base resulted in isomers not previously seen. During the elution on H^+-Dowex, three bands separated out, and characterisation using NMR was performed.

It is believed that the first band is a new isomer and has been isolated. Characterisation of the material has been *via* NMR techniques. One method to establish the identity of the new isomer is by using coupling constants. Due to the quadrupolar nature of the amine nitrogen, the signal is broadened, and therefore rather difficult to extract any useful data. However, the doublet peak at $\delta \approx 1.7$ ppm is not affected and the coupling constant has been measured as ^3J = 7.6 Hz between the methyl group protons and the proton on the α-carbon atom. This is compared to that of the major isomer where ^3J = 6.9 Hz. The $^{13}C\{^1H\}$ NMR spectrum

shows 6 signals, which suggests the isomer is symmetrical. From the discussion in Section 2.1, the number of symmetrical isomers can be limited to three diastereoisomers, where Figure 3-20 shows **I1** along with the three symmetrical diastereoisomers.

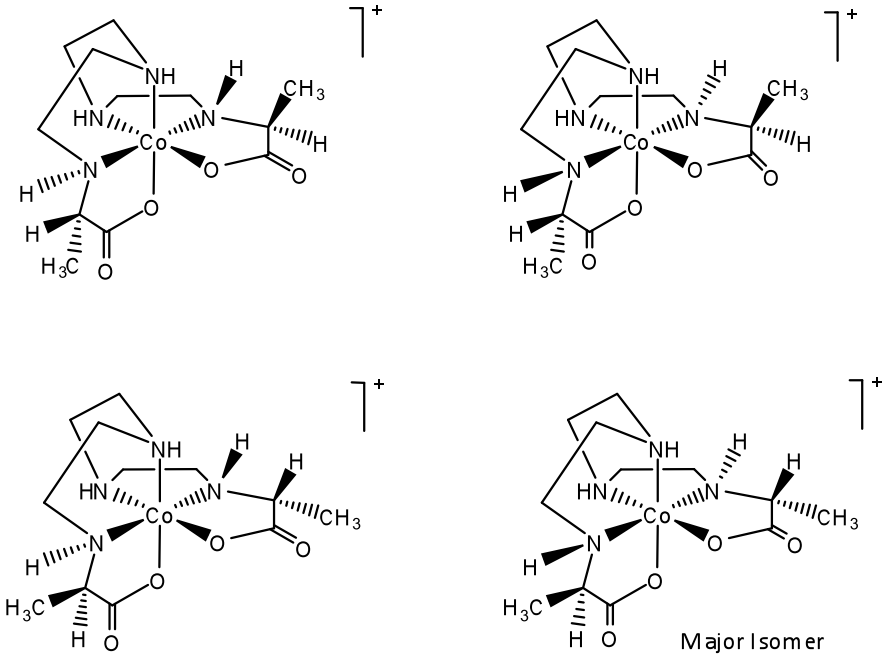

Figure 3-20: The four diastereoisomers of [Co(A_2trien)]$^+$ - the major isomer (I1) is labelled

The peaks in the $^{13}C\{^1H\}$ NMR spectrum have different chemical shift signals to that of the major isomer, which confirms that these isomers are not the same. Unfortunately crystals of X-ray quality have not been obtained.

The second band (band 2) appears to have a mixture of isomers in solution; two sets of doublets of similar intensity (δ 1.61 and δ 1.49 ppm) and a set of doublets 'shouldered' onto either terminal side of the 'major' peaks (δ 1.67 and δ 1.44 ppm). The coupling constants of each set of doublets have been measured. δ 1.61 ppm ^3J = 7.5 Hz; δ 1.49 ppm ^3J = 7.1 Hz; δ 1.67 ppm ^3J = 7.5 Hz and δ 1.44 ppm ^3J = 6.9 Hz. Separation of these isomers could be achieved by use of a longer column, a different ion-exchange resin, or milder elution conditions. The small amount of material precludes such studies at this time.

The third band (band 3) also appears to have a mixture of isomers in solution. However, the major component has a doublet at δ 1.47 ppm, and the coupling constant has been measured at ^3J = 6.7 Hz.

3.4.4 *ISOMER DISTRIBUTION*

From the results of both the small and large scale isomerisation experiments, the question of whether the isomer distribution is a result of thermodynamic control (dynamic equilibrium), kinetic control or a combination of both can be addressed. It is important to note that the initial conditions of the borohydride reduction, discussed in Chapter Two are milder than that of the small and large scale isomerisations

In the small scale experiment (after immediate mixing) and the two hour large scale experiment, a ^{1}H NMR spectrum was obtained. The integral ratio of the isomers were comparable with the spectrum obtained from the initial borohydride reduction. Because of the absence of protons in the small scale isomerisation experiment, it can be inferred that the equilibration of the N-H protons in the conditions for all three experiments determines the isomer distribution as a result of dynamic equilibrium. However, at this point, there is no exchange of the protons on the α-carbon atom. The rate of exchange, compared to that of the amine proton, is very slow. The conditions of the experiments are not sufficiently harsh to allow equilibration of the proton to occur within short times. It is not until the reaction has been proceeding for two weeks that epimerisation of the α-C-H centre is observed. It can be concluded from this that under the initial conditions for borohydride reduction (and the short term small scale and large scale isomerisations) that the selectivity of addition of the hydride to the α-carbon atom is under kinetic control.

3.4.5 *SELECTIVITY OF HYDRIDE ATTACK*

From these results and the results from Chapter Two, it appears that there is significant selectivity in the stereoisomers formed. The hydride may attack from either one of two faces of each imine, and the face chosen determines the configuration at the α-carbon atom in the initial product. Results from the borodeuteride reduction prove that hydride (or deuteride) attack is at the α-carbon atom and that the initial configuration at the α-C-H/D is retained through to isolation. There is facial selectivity occurring in this reaction.

The initial isomer distribution from the borohydride reduction is an integral ratio from the ^{1}H NMR spectrum of 8:4:1 (Figure 3-16). From the results of NMR characterisation and single crystal x-ray crystallography, it has been shown that **I1** (NMR integral ratio = 8) has the

hydride on the α-carbon atom located on the amine face of the molecule. From similar characterisation, it has been shown that one of the two stereoisomers in band 2 (**I2a**) of the original reduction (from the NMR integral ratio = 4) also has the hydride on the α-carbon atom located on the amine face of the molecule. From NMR data, the final isomer (**I3**) (with the NMR integral ratio = 1) will have the hydride on the α-carbon atom located on the amine face of the molecule. Hence 11/13 of the possible isomers (based on the NMR integrals) result from hydride attack on the amine face (≈85%). The facial selectivity is higher based on amounts isolated rather than NMR integrals. Because the hydride attack occurs twice (as there are two imine bonds to reduce), the facial selectivity for any individual reduction step is higher. Where, for two sequential reductions, each with a selectivity *x*, the overall selectivity will be *x* x *x* and approximates 85%; therefore:

$$x^2 = 0.85$$

$$x = \sqrt{0.85}$$

$$x = 0.92$$

This is a very high level of selectivity (92%). What is causing such selectivity?

The study by Pearce *et al.* [6] of conversion of α-imino acids (Figure 3-21) to amino acids by borohydride also investigated the distribution of products.

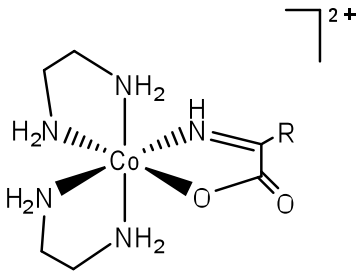

Figure 3-21: An example of an α-iminoacidato ligand, chelated to cobalt(III)

In this study, a range of imino-acidate ligands were used, derived from amino acids (glycine, alanine and valine). When the reduction using borohydride was performed on the bis(1,2-ethanediamine) complex, there was some selectivity for the Λ*R*,Δ*S* diastereoisomers.

This amounted to attack of the borohydride on the more hindered face of the imino-acidato ligands.

Previous work in this area also provided some evidence of selectivity for the Λ*R*,Δ*S* diastereoisomers during imine bond reduction by various hydride reagents.[7] It was thought that increasing the bulk of the reducing agent would change the selectivites observed for the systems used, shown in Figure 3-22.

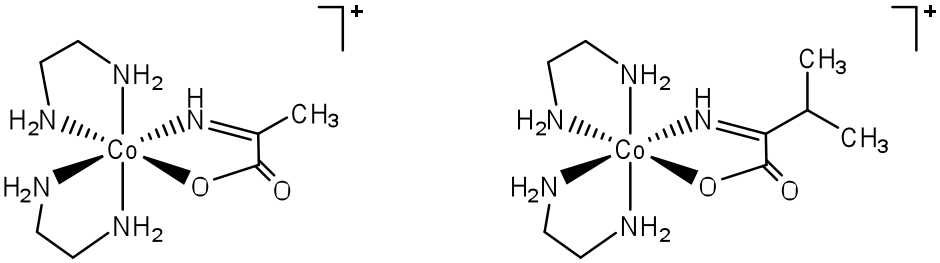

Figure 3-22: Schematic of the complexes used by Hartshorn [7] to investigate selectivity in hydride reduction reactions

However, in all cases, the selectivity stayed the same (Λ*R*,Δ*S*:Λ*S*,Δ*R* = 6:4), regardless that hydride delivery came from the more hindered face. One rationalisation of this result was that some of the reducing agents used (BH_4^-, NH_3BH_3 and $N(CH_2CH_2OH)_3BH_3$) have similar steric bulk.[7]

It is possible, from the results of the crystal structure determinations and the results from the Pearce *et al.* study [6], that there is another interaction that may cause such selectivity in both the systems examined by this thesis, and the previous work described above.

We suggest that a di-hydrogen bonding interaction occurs between the amine proton of the polyamine backbone adjacent to the imine, and a hydride on the BH_4^-. This would allow the hydride to be delivered from the amine face preferentially (Figure 3-23).

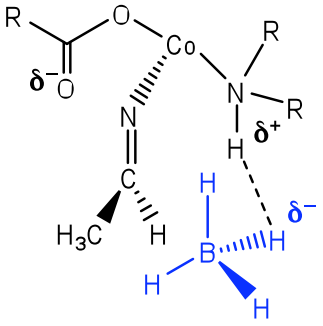

Figure 3-23: Schematic of hydride delivery in the reduction reaction on the imino acid complex. Hydride attack on the amine face is in blue

The delivery of the hydride occurring from the carbonyl face (Figure 3-24) may be hindered due to the electrostatic repulsion between the two δ^- fragments.

The crystal structures of **I1** and **I2a** have the proton on the α-carbon atom on the amine face of the molecule, which lends support to this hypothesis.

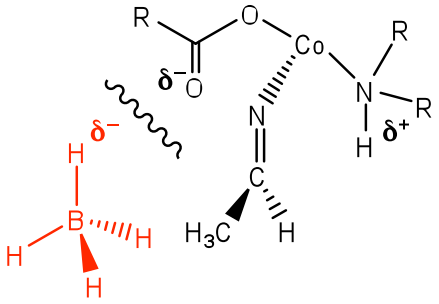

Figure 3-24: Schematic of hydride delivery in the reduction reaction on the imino acid complex. Hydride attack on attack on the carbonyl face is in red

3.5 CONCLUSIONS

It has been demonstrated, both on the small and large scale, that the major isomer of $[Co(A_2trien)]^+$ complex (**I1**) undergoes proton exchange reactions under basic conditions. Immediate exchange of the amine protons leads to an isomer distribution very similar to that of the crude isomer mixture material from borohydride reduction. Extended reaction time leads to exchange of the α-carbon protons, and to a range of isomers not previously seen.

From the results of the initial isomerisation experiments (where there is no epimerisation of the α-carbon proton) and the original isomer distribution, as seen in Chapter Two, it may be concluded that there is a high selectivity of hydride attack on the amine face of the molecule (calculated to be at least 92% in the borohydride reduction of the complex).

From these results it is proposed that hydride attack may be directed due to a di-hydrogen bonding interaction between the hydride and amine proton of the complex.

It has also been shown that under the initial basic conditions, N-H epimerisation is a result of dynamic equilibrium, but the addition of hydride is under kinetic control.

The separation and characterisation of the isomers seen in both the short and extended isomerisation experiments were attempted. New isomers have been found but have yet to be crystallographically characterised.

Furthermore, it would be of interest to establish whether the minor isomer **I2a** exhibits similar patterns of isomer distribution to **I1**.

3.6 REFERENCES

[1] D. A. Buckingham, L. G. Marzilli, and A. M. Sargeson, *Journal of the American Chemical Society*, 1967, **89**, 5133.

[2] D. H. Williams and D. H. Busch, *Journal of the American Chemical Society*, 1965, **87**, 4644.

[3] J. B. Terrill and C. N. Reilley, *Inorganic Chemistry*, 1966, **5**, 1988.

[4] D. A. Buckingham, I. Stewart, and P. A. Sutton, *Journal of the American Chemical Society*, 1990, **112**, 845.

[5] W. G. Jackson, *Inorganic Chemistry*, 1991, **30**, 1570.

[6] D. A. Pearce, R. M. Hartshorn, and A. M. Sargeson, *Journal of the Chemical Society-Dalton Transactions*, 2002, 1747.

[7] R. M. Hartshorn, 'Reactions of chelated ligands : a thesis submitted for the degree of Doctor of Philosophy in the Australian National University', 1989.

CHAPTER FOUR

EXTENDING THE CHEMISTRY – THE SYNTHESIS OF NOVEL POLYAMINE AMINO ACID COMPLEXES

4.1 INTRODUCTION

In Chapter Two, the major isomers produced from the borohydride reduction of [Co(Aim$_2$trien)]Cl were separated and characterised. The isomers produced from that system largely resulted from hydride attack on the imine bond occurring on the amine face of the imine. The major isomer of $[Co(A_2trien)]^+$ (**I1**) was then subjected to isomerisation experiments to determine whether the isomer distribution was a result of dynamic equilibrium. Results from these experiments show that, under the basic reduction conditions, the amine proton is equilibrating, however the α-carbon proton is not.

The initial results from the two hour isomerisation experiments showed that there is exchange only with the amine proton adjacent to the α-carbon atom, and no exchange with the proton on the α-carbon atom. The ratio of isomers being produced during this experiment was similar to that seen in the original crude isomer mixture from the borohydride reduction. From these results it is inferred that the vast majority of these isomers have the α-carbon proton on the amine face of the molecule. Only with extended reaction time in the carbonate buffer is exchange of the protons on the α-carbon atom observed, which results in isomers not previously seen.

In Chapter Three, the hypothesis of di-hydrogen bonding directing hydride attack was presented. It is thought that electrostatic bonding between the hydride and the proton on an amine may occur to direct the hydride attack (Figure 4-1).

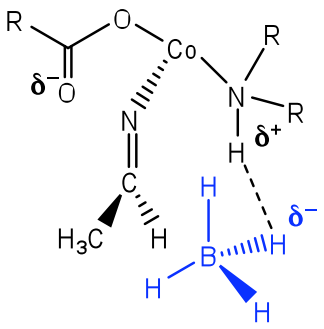

Figure 4-1: Schematic of hydride delivery in the reduction reaction on the imino acid complex. Hydride attack on the amine face is in blue

To test this hypothesis, imino acid complexes with varying tetraamine backbones were synthesised. This would change the locations and orientations of the protons on the amine relative to the imine bond being reduced. This could affect the possible di-hydrogen bonding interactions between the proton and hydride and so affect the facial selectivity of the reduction reaction.

A further test of the system was to produce a borohydride derivative. By replacing three of the hydrides with a bulky substituent (such as acyl groups), does facial selectivity in the reduction reaction still occur? Are there possible electrostatic interactions between the amine proton and carbonyl groups?

Are the same isomer distributions observed as those in the $[Co(A_2trien)]^+$ system? These systems were synthesised and tested.

4.2 EXPERIMENTAL

4.2.1 MATERIALS

Reagents and solvents were obtained from Sigma Aldrich or Merck and were of reagent grade or better and were used without further purification, unless stated otherwise. Distilled H_2O was used unless stated otherwise.

The preparation of $NaB(OAc)_3H$ was prepared according to literature methods, however toluene, rather than benzene, was used as the solvent.[1]

trans-[Co(2,3,2-tet)Cl_2]ClO_4[2, 3] and *trans*-[$CoCl_2$(2,2,3-tet)]ClO_4[4, 5] compounds were provided by Professor D. A. House.

Dowex 50WX2-200 (cation exchange resin), Dowex 50WX2-400 (cation exchange resin) and SP Sephadex C25 ion exchange resins were obtained from Sigma Aldrich. Column dimensions are given as (height x diameter).

4.2.2 INSTRUMENTATION/MEASUREMENTS

^{1}H, gCOSY and HSQCAD experiments were all recorded on a Varian INOVA 500 spectrometer at 23°C, operating at 500 MHz. The INOVA was equipped with a variable temperature and inverse-detection 5 mm probe or a triple-resonance indirect detection PFG probe. The ^{13}C NMR spectra were recorded on either a Varian UNITY 300 NMR spectrometer equipped with a variable temperature direct broadband 5 mm probe, at 23°C, operating at 75 MHz or on a Varian INOVA 500 spectrometer at 23°C, operating at 125 MHz, using a 5mm variable temperature switchable PFG probe. Chemical shifts are expressed in parts per million (ppm) on the δ scale and were referenced to the appropriate solvent peaks: DMSO-d_6 referenced to $CD_3(C\mathbf{H}D_2)SO$ at δ_H 2.50 (^{1}H) and $(\mathbf{C}D_3)_2SO$ at δ_C 39.6 (^{13}C). As reference in D_2O and DCl (99% D, 35 wt. % in D_2O), 3-(trimethylsilyl)propane-1-sulfonic acid (TMPS) or 3-(trimethylsilyl)propionic acid-d_4 sodium salt was used as an internal standard (δ_H 0 (^{1}H); δ_C 0 (^{13}C)).

Infrared spectra were obtained using a Shimadzu 8201PC Series FTIR using diffuse reflectance method in solid KBr.

High Resolution Electrospray Ionisation Mass Spectra (HRESIMS) were recorded on a Micromass LCT spectrometer using a probe voltage of 3200V, an operating temperature of 150°C and a source temperature of 80°C. The carrier solvent was 50:50 CH_3CN/H_2O at 20 μL/minute. Typically, 10 μL of a 10 μg/mL solution was injected. Leucine enkephalin was used as the lock mass internal standard.

UV-visible spectra were recorded on a Varian CARY Probe 50 UV-vis. spectrophotometer, or a Varian CARY 100 UV-vis. spectrophotometer.

Evaporations were performed using a Büchi rotary evaporator equipped with either a diaphragm vacuum pump or a water aspirator pump (pressure ≈15 torr) and at a temperature of 40°C unless otherwise stated.

Elemental analyses were performed by the Campbell Microanalytical Laboratory at the University of Otago.

4.2.3 PREPARATIONS

***CAUTION*: Perchlorate salts of metal complexes containing organic ligands are potentially explosive and should be handled with care and in small quantities.**

4.2.3.1 SYNTHESIS OF THE IMINES

[Co(Aim$_2$2,3,2-tet)][ClO$_4$]

trans-[Co(2,3,2-tet)Cl$_2$]ClO$_4$ (0.97 g, 2.5 mmol), pyruvic acid (0.88 g, 10 mmol), 2,6-lutidine (1.07 g, 10 mmol) and 250 mL of methanol were heated at reflux for 18 hours. Methanolic ZnCl$_2$ (ZnCl$_2$ (0.34 g, 2.5 mmol), LiCl (0.10 g, 2.5 mmol) in 10 mL of methanol) was added dropwise to the hot solution and heated at reflux for a further 30 minutes. The solution was cooled to room temperature during which time a precipitate developed. The red/orange product was filtered and dried under suction.

Yield: 1.68 g, (147.2%). Anal. Calcd. for $C_{13}H_{22}ClCoN_4O_8 \cdot ½CH_3OH \cdot ½H_2O$: C, 33.66; H, 5.23; N, 11.63. Found: C, 33.77; H, 5.00; N, 11.75. Absorption spectrum λ_{max}, (ε_{max}): 476 nm, (190 M^{-1} cm^{-1}). IR (str) 1647 cm^{-1}, 1462 cm^{-1}. HRESIMS: *m/z* = 357.2 ($[M\text{-}ClO_4]^+$ 100%), 358.3 ($[M\text{-}ClO_4]^+$ 35%), 359.2 ($[M\text{-}ClO_4]^+$ 3%). $^{13}C\{^1H\}$ NMR (ppm); 177.3 (C=N), 171.7 (C=O), 53.2, 51.1, 46.5 (CH_2NH_2), 22.5 (methylene CH_2), 16.4 (CH_3).

[Co(Aim$_2$2,2,3-tet)][ClO$_4$]

trans-[Co(2,2,3-tet)Cl$_2$]ClO$_4$ (0.97 g, 2.5 mmol), pyruvic acid (0.88 g, 10 mmol), 2,6-lutidine (1.07 g, 10 mmol) and 250 mL of methanol were heated at reflux for 18 hours. Methanolic ZnCl$_2$ (ZnCl$_2$ (0.34 g, 2.5 mmol), LiCl (0.10 g, 2.5 mmol) in 10 mL of methanol) was added dropwise to the hot solution and heated at reflux for a further 30 minutes. The solution was cooled to room temperature during which time a precipitate developed. The pink/red product was filtered and dried under suction.

Yield: 0.993 g, (86.8%). Anal. Calcd. for $C_{13}H_{22}ClCoN_4O_8$: C, 34.19; H, 4.86; N, 12.27. Found: C, 34.20; H, 5.06; N, 12.15; Absorption spectrum λ_{max}, (ε_{max}): 479 nm, (175 M^{-1} cm^{-1}). IR (str) 1682 cm^{-1}, 1649 cm^{-1}, 1465 cm^{-1}, 1428 cm^{-1}.

HRESIMS: *m/z* = 357.2 ($[M\text{-}ClO_4]^+$ 100%), 358.3 ($[M\text{-}ClO_4]^+$ 30%), 359.2 ($[M\text{-}ClO_4]^+$ 3%). $^{13}C\{^1H\}$ NMR (ppm); 180.9, 179.8 (C=N), 172.3, 171.2 (C=O), 53.2, 51.1, 46.5 (CH_2NH_2), 22.5 (methylene CH_2), 16.4 (CH_3).

4.2.3.2 REDUCTION OF THE IMINE COMPLEXES

Reduction of [Co(Aim$_2$2,3,2-tet)][ClO$_4$]

[Co(Aim$_2$2,3,2-tet)]ClO$_4$ (0.50 g, 1.09 mmol) was dissolved in 250 mL of carbonate buffer (2.12 g K_2CO_3 and 2.09 g $KHCO_3$ in 500 mL H_2O). $NaBH_4$ (0.41 g, 10.8 mmol) was added and stirred constantly for 5 minutes. The pink solution was adsorbed onto a Na^+-form Dowex column (10 x 10 cm) under suction, along with the remaining carbonate buffer (250 mL). The column was initially washed with H_2O (3 L), after which the red band was ready to be eluted with aqueous HCl (0.1 M, 2 L; 3 M, 2 L). The red eluate was taken to dryness on a rotary evaporator at 40°C. The product was a mixture of components (by $^{13}C\{^1H\}$ NMR).

Yield: 6.64 g. (There is contamination due to the presence of NaCl.)

Reduction of [Co(Aim$_2$2,2,3-tet)][ClO$_4$]

[Co(Aim$_2$2,2,3-tet)]ClO$_4$ (0.50 g, 1.09 mmol) was dissolved in 250mL of carbonate buffer (2.12 g K_2CO_3 and 2.09 g $KHCO_3$ in 500mL H_2O). $NaBH_4$ (0.41 g, 10.8 mmol) was added and stirred constantly for 5 minutes. The pink/red solution was adsorbed onto a Na^+-form Dowex column (10 x 10 cm) under suction, along with the remaining carbonate buffer (250 mL). The column was initially washed with H_2O (3 L), after which the red band was ready to be eluted with aqueous HCl (0.1 M, 2 L; 3 M, 2 L). The red eluate was taken to dryness on a rotary evaporator at 40°C. The product was a mixture of components (by $^{13}C\{^1H\}$ NMR).

Yield: 5.02 g. (There is contamination due to the presence of NaCl.)

4.2.3.3 ATTEMPTED ISOLATION OF THE ISOMERS FROM 4.2.3.2

[Co(A$_2$2,3,2-tet)]Cl

[Co(A$_2$2,3,2-tet)]Cl **(**2.00 g, 5.04 mmol) was dissolved in acidified H_2O (0.05 M, pH ≈ 3, 1 L) and adsorbed onto a H^+-Dowex column (30 x 3 cm). The column was eluted with aqueous HCl (0.1 M, 10 L; 1 M, 1 L) where, during the elution only one band (pink/orange) was observed. The eluate was taken to dryness on a rotary evaporator at 40°C.

Yield: 0.03 g

[Co(A$_2$2,2,3-tet)]Cl

[Co(A$_2$2,2,3-tet)]Cl **(**2.00 g, 5.04 mmol) was dissolved in acidified H_2O (0.05 M, pH ≈ 3, 1 L) and adsorbed onto a H^+-Dowex column (30 x 3 cm). The column was eluted with aqueous HCl (0.1 M, 17 L; 1 M, 1 L) where, during the elution, two bands developed. The first band (orange/pink) and the second band (pink) were collected. The eluates were taken to dryness on a rotary evaporator at 40°C.

Yield – Band 1: 0.25 g

Yield – Band 2: 0.8 g

4.2.4 CRYSTAL STRUCTURE DETERMINATIONS

Information on the setup of the X-Ray system can be found in Appendix I. Reference numbers (*e.g.* **4.10**, **4.11** etc) for each structure are provided, referring to the tables in Appendix I

[Co(Aim$_2$2,3,2-tet)][ClO$_4$] (4.10)

Crystals of [Co(A$_2$2,3,2-tet)][ClO$_4$] (red blocks) were grown by vapour diffusion of ethanol into a solution of [Co(A$_2$2,3,2-tet)][ClO$_4$] in aqueous hydrochloric acid (0.2 M)

Crystal Data:

$C_{13}H_{22}ClCoO_{12}N_4$, M =456.73, Monoclinic, a = 7.7569(4) Å, b = 18.9498(10) Å, c = 12.5721(6) Å, α = 90, β= 97.362(3)°, γ = 90, U = 1832.76(16) Å^3, T = 296(2), space group P2$_1$/n (no. 14), Z = 4, μ(Mo-Kα) = 1.133, 20261 reflections measured, 3222 unique (R_{int} = 0.0396) which were used in all calculations. The final $wR(F_2)$ was 0.1642 (all data). R_1 = 0.0518 (Final R indexes [I>2σ (I)]).

[Co(Aim$_2$2,2,3-tet)][ClO$_4$] (4.11)

Crystals of [Co(A$_2$2,2,3-tet)][ClO$_4$] (red blocks) were grown by vapour diffusion of ethanol into a solution of [Co(A$_2$2,2,3-tet)][ClO$_4$] in aqueous hydrochloric acid (0.2 M)

Crystal Data:

$C_{13}H_{22}ClCoO_8N_4$, M =456.73, Orthorhombic, a = 13.722(3) Å, b = 14.333(6) Å, c = 18.494(8) Å, α = 90, β= 90, γ = 90, U = 3637(2) Å^3, T = 296(2), space group Pbca (no. 61), Z = 8, μ(Mo-Kα) = 1.141, 19953 reflections measured, 3144 unique (R_{int} = 0.1172) which were used in all calculations. The final $wR(F_2)$ was 0.1871 (all data). R_1 = 0.0647 (Final R indexes [I>2σ (I)]).

4.3 RESULTS

4.3.1 SPECTROSCOPIC DATA FOR THE IMINE COMPLEXES

$^{13}C\{^{1}H\}$ NMR DATA

Complex	C=N (ppm)	CO_2Co (ppm)	CH_3 (ppm)	CHRNR'R"	Methylene CH_2
$[Co(Aim_2 2,3,2\text{-tet})]^+$	177.3	171.7	16.4	53.2, 51.1, 46.5	22.5
$[Co(Aim_2 2,2,3\text{-tet})]^+$	180.9, 179.8	172.3, 171.2	16.4	53.2, 51.1, 46.5	22.5

Table 3: $^{13}C\{^{1}H\}$ NMR data for the imine complexes

For the $[Co(Aim_2 2,3,2\text{-tet})]^+$ system, the presence of a C_2 axis of symmetry reduces the number of signals observed in the NMR spectra.

The $[Co(Aim_2 2,2,3\text{-tet})]^+$ complex is asymmetric and so the presence of two imine signals, and two carbonyl signals in the $^{13}C\{^{1}H\}$ NMR is expected.

Comparisons between both systems can be made, however. The chemical shift of the methyl group of the amino acid side chain occurs at $\delta \approx 16$ppm. The carbonyl signals for both systems also occur at a similar chemical shift ($\delta \approx 171\text{-}172$ ppm). The tetraamine backbone for both systems have secondary amine chemical shifts that are identical.

4.3.1.1 ^{1}H NMR Spectra for the Imino Acid Complexes

[Co(Aim$_2$2,3,2-tet)]$^{+}$

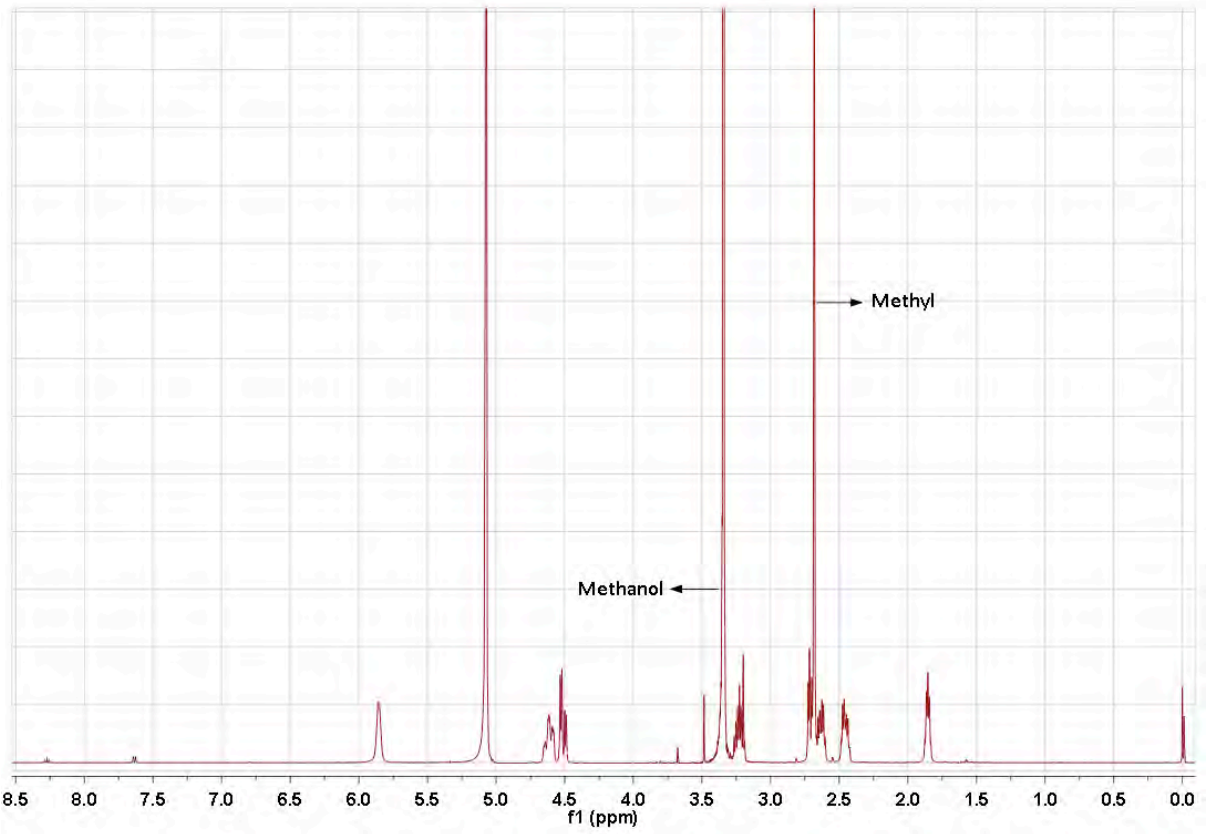

Figure 4-2: ^{1}H NMR spectrum of the [Co(Aim$_2$2,3,2-tet)]$^{+}$ complex

The first signal to be assigned was the methyl peak at δ 2.68 ppm. Due to the symmetric nature of the complex, only one methyl peak would be observed, (as shown in Figure 4-2). Comparisons with the [Co(Aim$_2$trien)]$^{+}$ systems can be made. The broad peak at δ 5.8 ppm is the proton on the amine on the polyamine backbone. The peak at approximately δ 1.8 ppm is the methylene protons on the polyamine backbone. All other multiplet peaks are protons on the carbon atoms of the polyamine backbone, which are inequivalent (where the peaks at δ 4.5 ppm are the methylene protons closest to the imine bond).

[Co(Aim$_2$2,2,3-tet)]$^+$

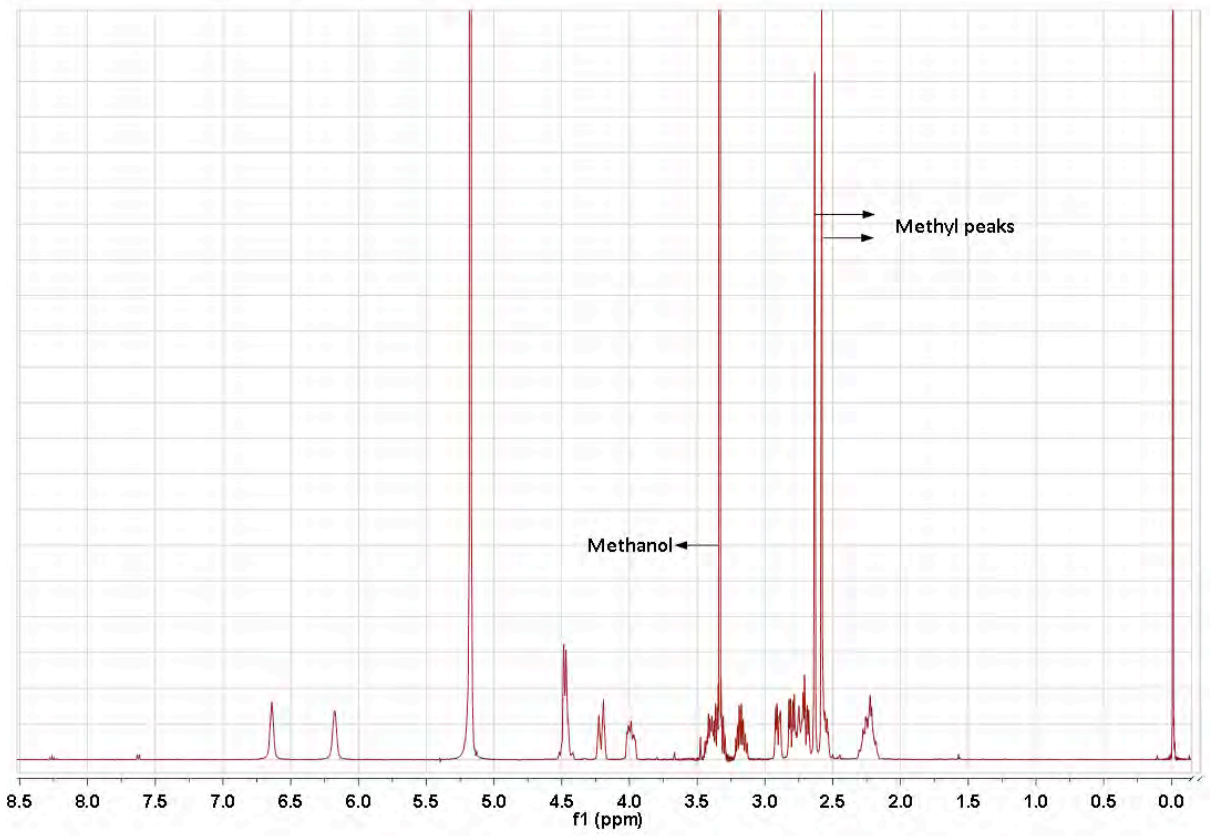

Figure 4-3: ^{1}H NMR spectrum of the [Co(Aim$_2$2,2,3-tet)]$^+$ complex

The first signals to be assigned were the methyl peaks at δ 2.58 and δ 2.63 ppm respectively. Due to the asymmetric nature of the complex, two methyl peaks would be observed, (as shown in Figure 4-3). Other peaks that can be assigned are the broad peaks at δ 6.2 and 6.6 ppm, which are the protons on the secondary amines of the polyamine backbone. The broad multiplet at δ 2.3 ppm are the protons of the methylene group. All other multiplet peaks are protons on the carbon atoms of the polyamine backbone, which are inequivalent.

4.3.2 UV-VISIBLE AND INFRA-RED DATA FOR THE IMINE COMPLEXES

Complex	UV-visible data (λ_{max} nm, ε_{max} $M^{-1}cm^{-1}$)	Infra-red (cm^{-1})
$[Co(Aim_2 2,3,2\text{-tet})]^+$	476 nm, (190 M^{-1} cm^{-1})	1647 cm^{-1}, 1462 cm^{-1}
$[Co(Aim_2 2,2,3\text{-tet})]^+$	479 nm, (175 M^{-1} cm^{-1})	1682 cm^{-1}, 1649 cm^{-1}, 1465 cm^{-1}, 1428 cm^{-1}

Table 4: UV-visible and Infra-Red data for the imine complexes

4.3.3 CRYSTAL STRUCTURES

4.3.3.1 [Co(Aim$_2$2,3,2-tet)]ClO$_4$ (4.10)

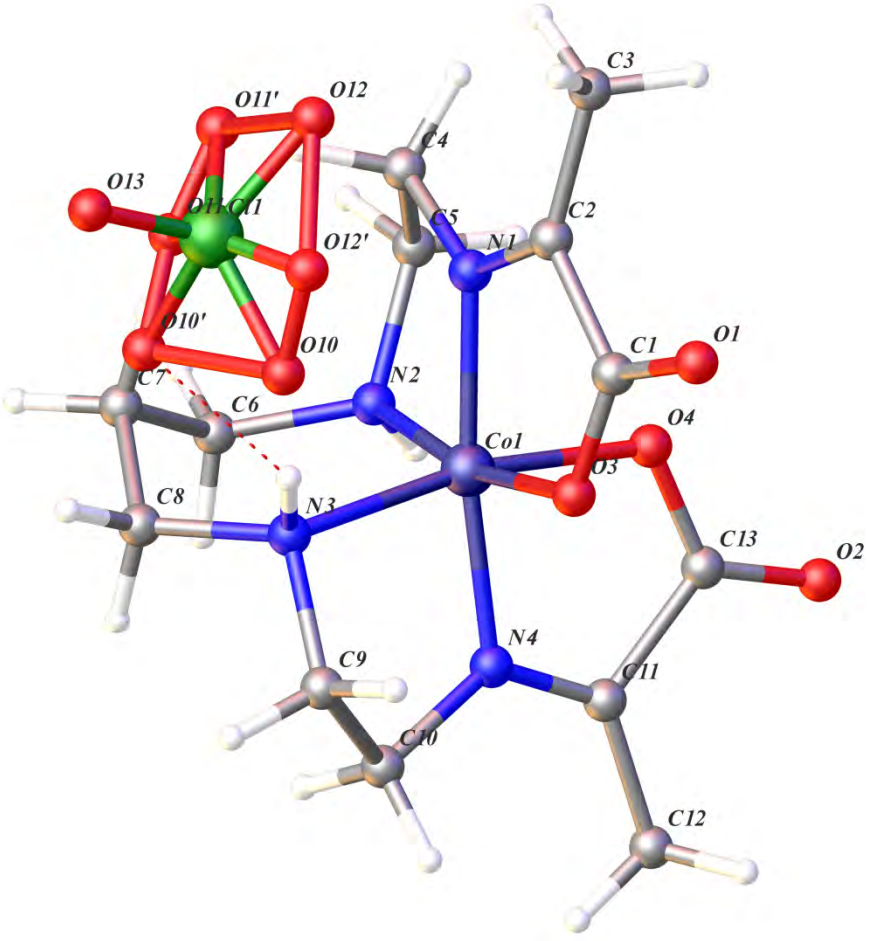

Figure 4-4: X-ray crystal structure of [Co(Aim$_2$2,3,2-tet)]ClO$_4$ (solvent molecules omitted for clarity)

Selected atomic distances (Å): Co1-N1, 1.883(4); Co1-N2, 1.953(4); Co1-N3, 1.988(4); Co1-O3, 1.923(3); Co1-O4, 1.924(3); N1-C2, 1.275(6); N4-C11, 1.258(7); C2-C3, 1.486(6); Other Nitrogen-Carbon lengths, 1.486(8)-1.498(7).

Selected bond angles (°): O4-Co1-O3, 91.98(15)l N1-Co1-O3, 83.13(14); N1-Co1-N2, 86.20(16); N2-Co1-N3, 98.10(17); N4-Co1-N3, 85.8(2); N4-Co1-O4, 83.71(17); N4_Co1-N1, 172.58(17); C2-N1-C4, 126.6(4).

Selected torsion angles (°): C4-N1-C2-C3, 1.59; C4-N1-C2-C1, 174.16

The space group is $P2_1/n$ and the crystal system is monoclinic.

The presence of imine bonds are confirmed by comparison of the bond lengths of C2-N2 (1.27 Å) and N5-C11 (1.26 Å) with other nitrogen-carbon bond lengths (≈1.49 Å). These values are comparable to the values found for an analogous system $[Co(Aim_2trien)]^+$ system ,where the imine bond was measured as 1.28 Å and other nitrogen-carbon bond lengths (1.47-1.51 Å).[6]

The imine appears to be planar as the torsion angles around the imine bond are approximately 180° for *trans* substituents and approximately 0° for *cis* substituents. These values are also analogous for the $[Co(Aim_2trien)]^+$ system.

The ClO_4^- is disordered over two occupancies, with the dominant occupancy of 80%. There is a hydrogen bonding interaction in the lesser occupancy to one of the N-H hydrogen atoms.

4.3.3.2 [Co(Aim$_2$2,2,3-tet)]ClO$_4$ (4.11)

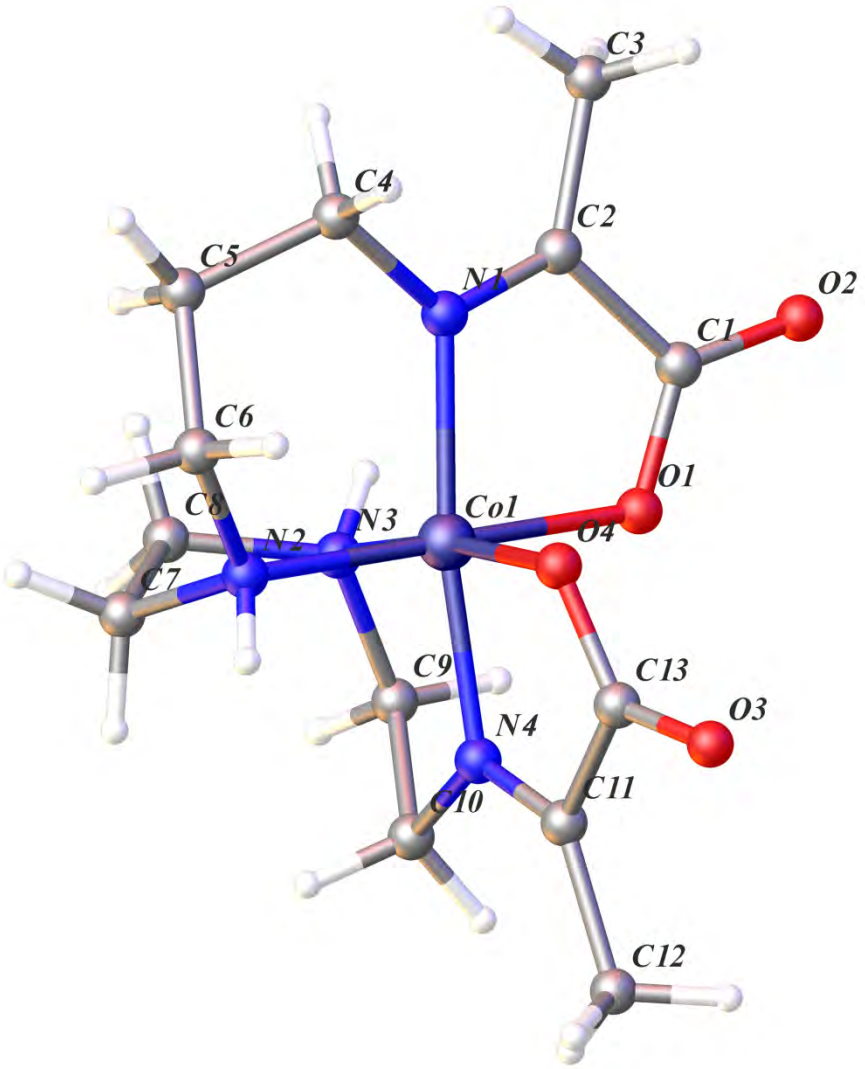

Figure 4-5: X-Ray crystal structure of [Co(Aim$_2$2,2,3-tet)]$^+$ (counter-ion omitted for clarity)

Selected atomic distances (Å): Co1-O1, 1.906(4); Co1-N1, 1.935(6); Co1-N2, 1.945(6); Co1-N3, 1.925(5); Co1-N4, 1.881(6); Co1-O4, 1.918(4); C2-N1, 1.264(9); C1-O2, 1.216(8); Other Nitrogen-Carbon lengths, 1.476(8)-1.499(9).

Selected bond angles (°): O4-Co1-O1, 88.5(2); O1-Co1-N1, 84.1(2); N1-Co1-N2, 96.4(2); N3-Co1-N2, 88.2(2); N4-Co1-N3, 86.6(2); N4-Co1-O4, 83.9(2); N4-Co1-N1, 172.2(2); C2-N1-C4, 120.2(6).

Selected torsion angles (°):C4-N1-C2-C3, 3.41; C4-N1-C2-C1, 177.20

The space group is Pbca and the crystal system is orthorhombic.

The presence of imine bonds are confirmed by comparison of the bond lengths of C2-N1 (1.26 Å) and N4-C11 (1.26 Å) with other nitrogen-carbon bond lengths (≈1.49 Å). These values are comparable to the values found for an analogous system $[Co(Aim_2trien)]^+$ system ,where the imine bond was measured as 1.28 Å and other nitrogen-carbon bond lengths (1.47-1.51 Å).[6]

The imine appears to be planar as the torsion angles around the imine bond are approximately 180° for *trans* substituents and approximately 0° for *cis* substituents. These values are also analogous for the $[Co(Aim_2trien)]^+$ system.

4.3.4 SPECTROSCOPIC DATA FOR THE REDUCED PRODUCTS

4.3.4.1 $[Co(A_2 2,3,2\text{-tet})]^+$ - ISOMER MIXTURE

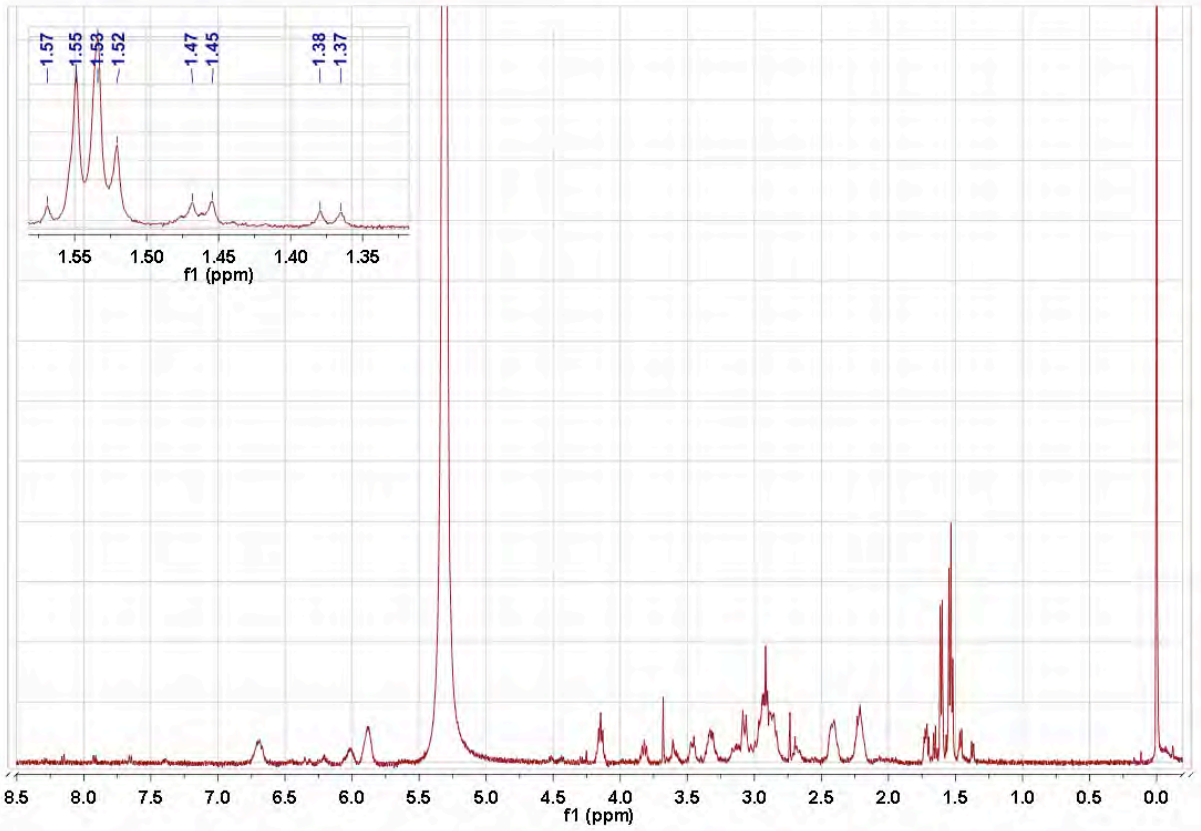

Figure 4-6: ^{1}H NMR spectrum of the isomer mixture of [Co($A_2$2,3,2-tet)]+ complex

There is a loss of the singlet peak at δ 2.68 ppm, which was assigned previously as the methyl peak adjacent to the imine bond, indicating that the reduction reaction has occurred. The presence of methyl doublets at δ 1.37-1.57 ppm indicates that there are multiple isomers in solution. Due to the similarity of this complex to that of the $[Co(A_2trien)]^+$ some comparisons may be made. The two peaks at ≈6 ppm, are the amine protons on the polyamine backbone. The peak at ≈6.5 ppm is the amine proton adjacent to the α-carbon atom. The peaks from δ ≈2.2-4.2 ppm are the protons on the carbon atoms of the polyamine backbone. These chemical shifts are comparable to those of the $[Co(A_2trien)]^+$ system. The expansion of the methyl region shown in Figure 4-6 shows clearly a set of doublets at δ 1.52-1.57 ppm with an

intensity greater than the two sets of doublets at δ 1.38 and δ 1.46 ppm. Based on our understanding of the $[Co(A_2trien)]^+$ system, it can be speculated that the set of doublets at δ 1.54 ppm would be the major isomer present in solution.

4.3.4.2 [Co($A_2$2,2,3-tet)]$^+$ - ISOMER MIXTURE

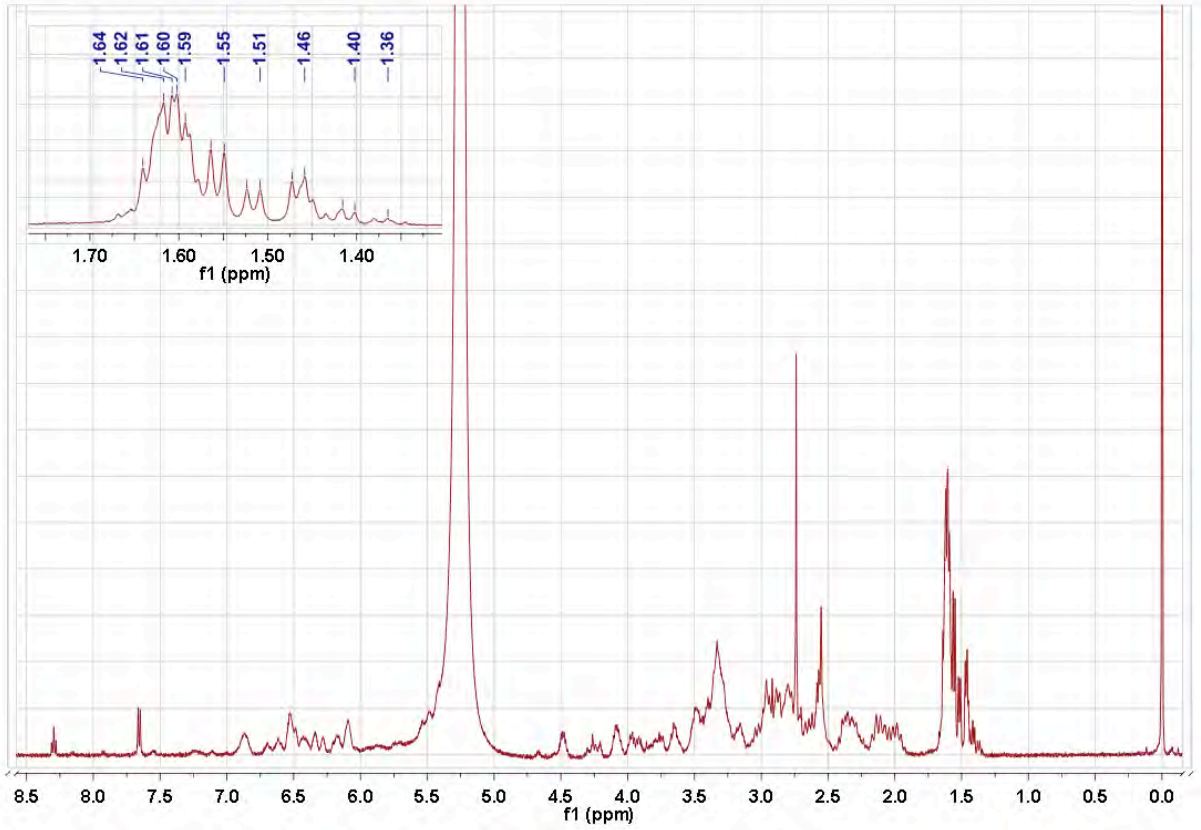

Figure 4-7: ^{1}H NMR spectrum of the isomer mixture of [Co($A_2$2,2,3-tet)]$^+$ complex

Due to the asymmetric nature of the $[Co(A_2$2,2,3-tet)]$^+$ molecule and also the chemical shift of the methylene protons (δ 1.60 ppm), the reduction of the imine to an amine results in the methyl signals being extremely congested at δ 1.36-1.64 ppm. An accurate ratio of isomers present in solution cannot be determined due to such congestion.

A $^{13}C\{^1H\}$ spectrum of the isomer mixture was obtained, but the signal to noise ratio impaired assignment. However, the methyl region showed 4 signals of strong intensity compared to the baseline. It would be expected that a single isomer of this complex would have two methyl signals (as they occur in different chemical environments), therefore the

presence of four methyl signals in the $^{13}C\{^{1}H\}$ spectrum may indicate that two isomers are present in solution.

4.3.5 SPECTROSCOPIC DATA FOR THE ISOLATED PRODUCTS

4.3.5.1 $[Co(A_2 2,2,3\text{-tet})]^+$ - BAND ONE

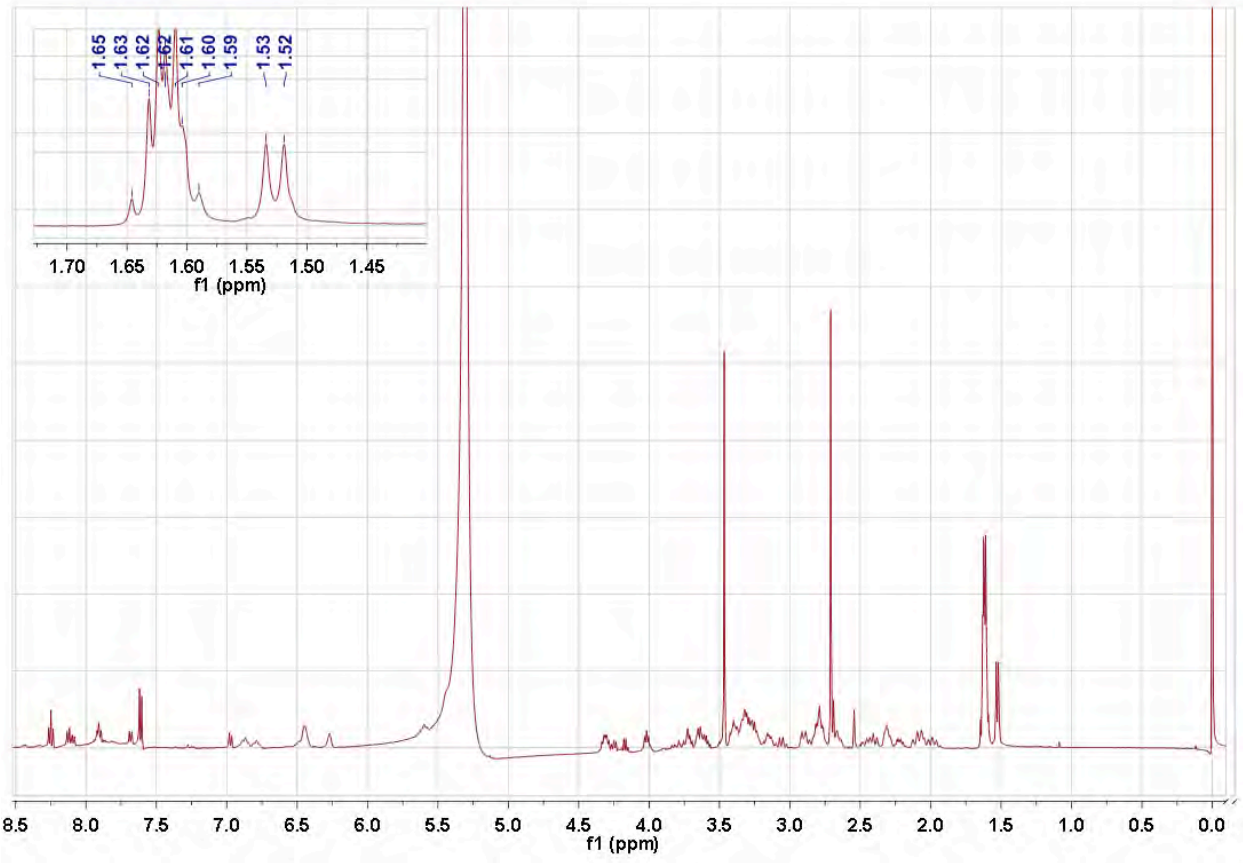

Figure 4-8: ^{1}H NMR spectrum of the $[Co(A_2 2,2,3\text{-tet})]^+$ complex - band one. An expansion of the methyl chemical shift region is located in the top left of the figure

The ^{1}H NMR spectrum (Figure 4-8) of band one shows that there is a broad multiplet located at δ 1.60 ppm and a doublet at δ 1.53 ppm. Because the isomer is asymmetric, multiple methyl signals are expected. However the broad multiplet at δ 1.60 ppm may indicate that multiple isomers are present in solution. The occurrence of sharp signals in the aromatic region of the spectrum also indicates that the sample has been contaminated in some way.

A $^{13}C\{^{1}H\}$ NMR spectrum of this sample was obtained, however the signal to noise ratio made it difficult to completely assign. However, 5 peaks in the methyl chemical shift were

assigned. This leads us to believe that at least two isomers are present in solution. Further chromatographic techniques may separate these isomers, but this is left to a future project.

4.3.5.2 [Co($A_2$2,2,3-tet)]$^+$ - BAND TWO

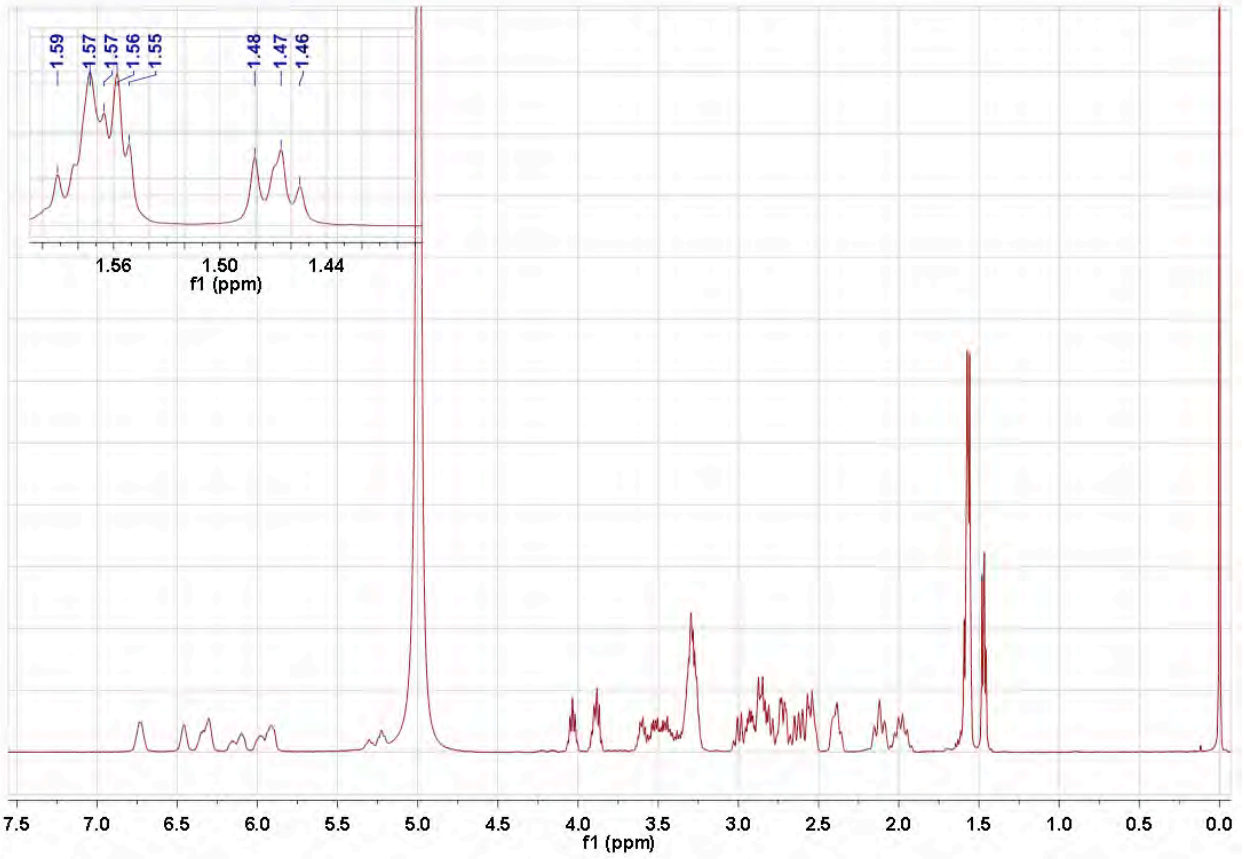

Figure 4-9: ^{1}H NMR spectrum of the [Co($A_2$2,2,3-tet)]$^+$ complex - band two. An expansion of the methyl chemical shift region is located in the top left of the figure

The ^{1}H NMR spectrum (Figure 4-9) shows two sets of doublets in the methyl region of the spectrum. An expansion of this area shows that there are overlapping peaks, which may indicate there are multiple isomers present in solution. A ^{13}C{^{1}H} spectrum was obtained to confirm how many isomers may be present in solution.

The peak heights observed in the spectrum against the baseline made it difficult to assign, however 4 distinct peaks in the methyl region were assigned (approximately δ 17-18 ppm). This may account for two isomers observed in solution. This assignment may be confirmed also by the presence of two methylene peaks assigned in the spectrum also at δ 25 ppm.

4.4 DISCUSSION

4.4.1 SYNTHESIS OF THE IMINO-ACID COMPLEXES

The formation of the imino acid complexes used a general synthetic strategy; intramolecular condensation reactions. Previous research identifies that the amines located *cis* to the coordinated carbonyl fragment of the keto acid are the site for coordination and condensation to occur.[7] The steric crowding of the keto acid used, also prevents secondary amines attacking the carbonyl group. As discussed in the introduction, the geometry of the imine bond is planar. Hence, although the starting materials for these syntheses used the *trans*-dichloridopolyaminecobalt(III) complex, they rearrange to the *cis* configuration at some stage in the reaction sequence.

4.4.1.1 [Co(Aim$_2$2,3,2-tet)][ClO$_4$] AND [Co(Aim$_2$2,2,3-tet)][ClO$_4$]

The initial synthesis of both imino acid complexes used the *trans*-dichlorido tetraamine starting material. Precedents shown in the literature show that the condensation reaction can only occur if the ligand undergoes rearrangement to form the 'planar' imine (as discussed in Chapter One).[7]

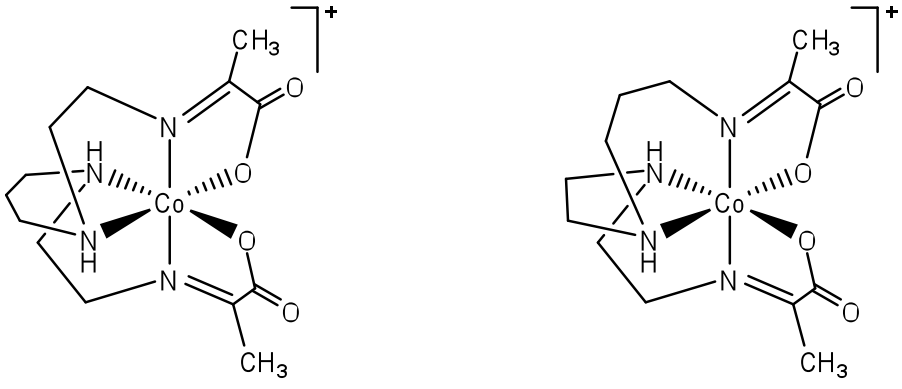

(1) (2)

Figure 4-10: The imino acid complexes; [Co(Aim$_2$2,3,2-tet)]$^+$ (1) and [Co(Aim$_2$2,2,3-tet)]$^+$ (2)

Crystal structures for both these complexes were obtained and confirmed the planarity of the imines for both; as the torsion angles were approximately 180° for *trans* substituents and approximately 0° for *cis* substituents. The polyamine portion of the final ligand is now in an *ff*-wrap as opposed to the *mm* (trans) wrap of the starting material.

Since the complexes isolated contained a perchlorate counter-ion (ClO_4^-), an improved synthesis would add a perchlorate salt, instead of zinc chloride (as $ZnCl_4$).

4.4.2 SYNTHESIS OF THE AMINO-ACID COMPLEXES – REDUCTION REACTION

The conditions of the reduction reaction have been previously described in Section 2.4.4, and these conditions for the reduction reaction were also used in these sets of experiments.

4.4.2.1 [Co(A$_2$2,3,2-tet)]Cl – isomer mixture

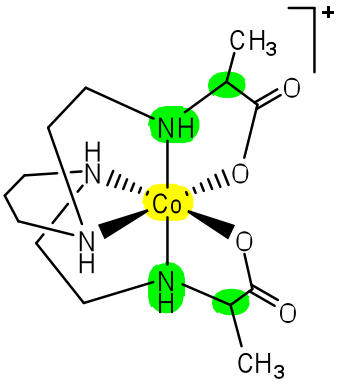

Figure 4-11: [Co(A$_2$2,3,2-tet)]$^+$ with new stereogenic centres highlighted in green

The reduction of [Co(Aim$_2$2,3,2-tet)]$^+$ with borohydride produces four new stereogenic centres (Figure 4-11). This, along with the pre-existing stereogenic centre of the metal ion (highlighted in yellow in Figure 4-11) could result in 2^5 stereoisomers. However, this system is analogous to the system [Co(A$_2$trien)]$^+$ described in Section 2.4.3. Due to the symmetrical nature of the molecule, the sixteen diastereoisomers thought to originate from the reduction

reaction in the general case are limited due to the presence of a C_2 axis, rendering some combinations of absolute configurations equivalent.

If borohydride reduction is facially selective (on the amine face of the meridional ligand fragment), as proposed, then three stereoisomers would be produced (where the protons are *anti* to each other in both halves of the molecule; where one half of the molecule has the protons in an *anti* relationship, while the other half has them in a *syn* relationship; and where the protons are *syn* to each other in both halves of the molecule). The ^{1}H NMR spectrum of the isomer mixture (Figure 4-6) has 3 sets of doublets at $\delta \approx 1.40$ -1.55 ppm, which may indicate the presence of three stereoisomers in solution.

4.4.2.2 [Co(A$_2$2,2,3-tet)]Cl – isomer mixture

The reduction of [Co(A$_2$2,2,3-tet)]$^+$ will produce four new stereogenic centres (Figure 4-12). Including the pre-existing stereogenic centre of the metal ion (highlighted in yellow), 2^5 stereoisomers are possibly formed.

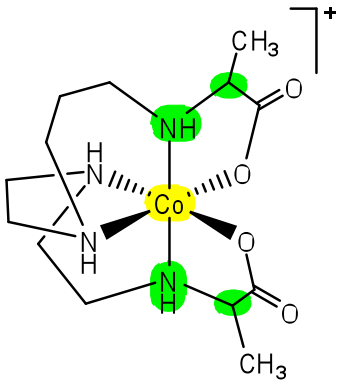

Figure 4-12: [Co(A$_2$2,2,3-tet)]$^+$ complex. New stereogenic centres are indicated in green

Due to the asymmetric nature of the molecule, two methyl signals should be observed in a ^{13}C{^{1}H} NMR spectrum for a single isomer. A ^{13}C{^{1}H} NMR spectrum of the reduced material indicates a mixture of isomers in solution; the methyl region of the spectrum is particularly congested.

The ^{1}H NMR spectrum of this material is particularly congested. Since the methyl signals are not equivalent (due to the asymmetric nature of the molecule), and it is possible that some of

these signals overlap, this may add to the congestion seen, making the spectrum difficult to analyse. If hydride attack is selective on the amine face of the imine, then at least four diastereoisomers would be formed; 1) where the protons are *anti* to each other in both halves of the molecule; 2) where the protons are in an *anti* relationship closest to the '3' section of the backbone, while the protons closest to the '2' section of the backbone are in a *syn* relationship; 3) where the protons are in an *anti* relationship closest to the '2' section of the backbone, while the protons closest to the '3' section of the backbone are in a *syn* relationship; and 4) where the protons are *syn* to each other in both halves of the molecule.

The elution of the complex *via* ion-exchange chromatography resulted in two bands being separated. However, for both bands, ^{1}H and $^{13}C\{^{1}H\}$ NMR spectra indicated multiple isomers were present in solution. Separation of these isomers by other chromatographic techniques could be employed, but this is left to a future project.

4.4.3 [Co(A$_2$trien)]$^+$ - REDUCTION USING NaB(OAc)$_3$H

A reduction of [Co(Aim$_2$trien)]Cl involving an acyl borohydride derivative has been performed. It had an initial reaction time of six hours. This caused some reduction of the imine bond being observed, but the singlet peak at δ 2.67 ppm in the ^{1}H NMR spectrum indicates that full reduction of the complex has not occurred. However, only one isomer is present in solution. The ^{3}J coupling constant has been calculated at ^{3}J = 7.3 Hz. It is unclear whether this isomer is fully or half reduced, however the presence of the singlet peak at δ 2.67 ppm and the chemical shifts of the doublet at δ 1.58 ppm suggest that it is a half reduced isomer only.

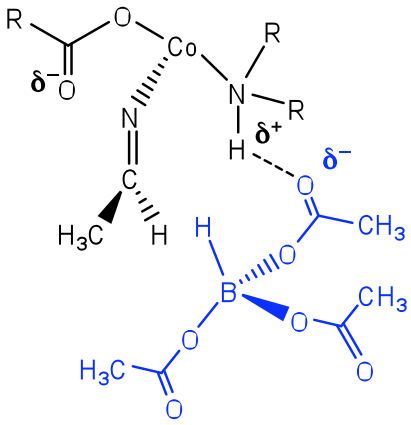

Figure 4-13: Schematic of possible hydride attack using an acyl-borohydride derivative as the reducing agent. Possible hydride delivery from the amine face is shown in blue

The di-hydrogen bonding opportunities are not available in an acyl-borohydride derivative. However it is possible that hydrogen bonding may occur with a carbonyl group (Figure 4-13). This interaction may allow similar types of facial selectivity that is observed in the borohydride reduction reaction.

Delivery from the carbonyl face may be hindered due to electrostatic repulsion of the two carbonyl groups (Figure 4-14).

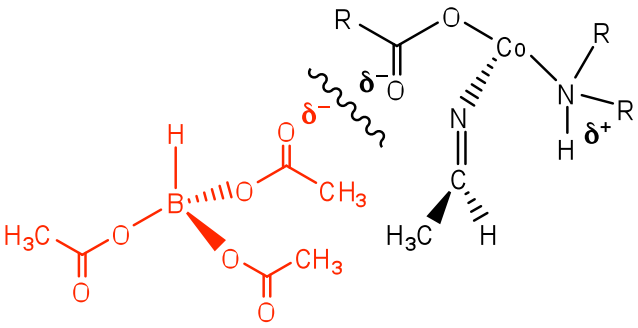

Figure 4-14: Schematic of possible hydride attack using an acyl-borohydride derivative as the reducing agent. Possible hydride delivery from the carbonyl face is shown in red

4.5 CONCLUSIONS

A range of new imino acid complexes with varying tetraamine backbones were synthesised using intramolecular condensation reactions. The borohydride reduction reaction was performed on these new complexes, resulting in new amino acid complexes. Data from $^{13}C\{^{1}H\}$ NMR spectra indicate that multiple isomers are formed in solution. Ion-exchange chromatographic techniques were employed to try and separate the isomers. In some cases a different medium may be required to achieve separation.

^{1}H NMR spectra of the [Co($A_2$2,3,2-tet)]Cl and [Co($A_2$2,2,3-tet)]Cl isomer mixtures showed a mixture of isomers in solution. However, in the case of the [Co($A_2$2,2,3-tet)]Cl system, the methyl region was too congested to determine the isomer distribution. However, if the reduction is facially selective, then at least four diastereoisomers would be formed. The [Co($A_2$2,3,2-tet)]Cl system is also congested, but initial results appear to suggest that at least three diastereoisomers are present in solution.

Those amino acid isomer mixtures that were separated were characterised using NMR techniques. To characterise these isomers more fully, more material is needed. Proton exchange on these systems, such as described in Chapter Three, would provide more evidence for (or lack) of hydride selectivity, and the opportunity for new stereoisomers, not previously seen, to be formed.

4.6 REFERENCES

[1] P. Marchini, G. Liso, A. Reho, F. Liberatore, and F. M. Moracci, *Journal of Organic Chemistry*, 1975, **40**, 3453.

[2] H. G. Hamilton and M. D. Alexander, *Inorganic Chemistry*, 1966, **5**, 2060.

[3] H. G. Hamilton and M. D. Alexander, *Journal of the American Chemical Society*, 1967, **89**, 5065.

[4] D. A. House and J. Svensson, *Inorganica Chimica Acta*, 1998, **278**, 24.

[5] G. R. Brubaker, F. H. Jarke, and I. M. Brubaker, *Inorganic Chemistry*, 1979, **18**, 2032.

[6] J. M. Browne, 'Intramolecular condensation reactions of cobalt(III) complexes : a thesis submitted in partial fulfilment of the requirements for the degree of Master of Science in Chemistry at the University of Canterbury', 2000.

[7] J. M. W. Browne, J. Wikaira, and R. M. Hartshorn, *Journal of the Chemical Society-Dalton Transactions*, 2001, 3513.

CHAPTER FIVE

FUTURE WORK

5.1 FUTURE WORK

The work completed in this thesis is by no means an exhaustive investigation into the stereochemistry of amino acid containing polydentate cobalt(III) complexes. The results reported in Chapter Four of this thesis, which were particularly fruitful, occurred in the latter stages of research.

Suggested future work includes;

Amino acid side chains; By varying the side chain (indicated 'R') on the keto acid, it could be expected that the characteristics of the resulting amino acids (*i.e.* polarity, steric bulk) will change, and also allow further study of the stereochemistry of these systems, and what constraints upon the system different side chains may impose (*e.g.* re-wrapping of the tetraamine ligands and/or impact on the geometry and bond lengths of the metal ion). Analysis of the complexes formed may allow insight into possible patterns that occur when the side chains are polar/non-polar, big/small or acidic/basic.

Another area for investigation is the use of different reductants on the system. Previous work involving the reduction of α-imino acids to amino acids used dithionite. This could also be used to investigate systems mentioned in this thesis.

Hydrogenation of the imine bond using colloids is another reductant that could be investigated. If there is stereoselectivity towards reduction of the imine (and not the metal centre itself), this may lead to higher stereo and regioselectivity.

Further investigation into hydride attack would be useful to understand the selectivity of this reaction better. More bulky substituents in an $NaB(R)_3H$ system would prove useful.

Since the systems investigated are all cobalt(III) derivates it could be interesting to investigate the similarities and differences if other transition metals were used.

The separation of both the second (**I2**) and third bands (**I3**) from the $[Co(A_2trien)]Cl$ system has still resulted in multiple isomers in solution. It may be possible that the use of chiral salts

may separate the enantiomers from **I2**. It is also possible that single crystals of such systems may be analysed using capillary NMR techniques.

The third band of $[Co(A)_2trien]^+$ (**I3**) contains multiple isomers in solution. Subjecting the material to different types of columns and constant elution may separate these out.

The synthesis of new polydentate imino and amino acid complexes described in Chapter Four have not been thoroughly investigated. Is the ratio of isomers present in the isomer mixture solution comparable to that of the original 'trien' system? Can the symmetric and asymmetric systems be compared? It would be interesting to observe if hydride attack is preferential in these systems, as they appear to be in the *N*,*N'*-bis(2-aminoethyl)ethane-1,2-diamine systems. Similar isomerisation studies could also be performed on single isomers of these complexes.

APPENDIX I

X-RAY CRYSTALLOGRAPHIC DATA

Tables A1 and A2 list the crystal data and X-ray experimental details for seven crystal structures discussed in this thesis. Throughout the text, selected bond lengths and angles are discussed and listed under the appropriate figures, while the remaining distances and angles, as well as atomic coordinates are available on request from the Department of Chemistry, University of Canterbury.

The data for the crystal structures in this thesis was collected on a Bruker-Nonius APEX II system using graphite monochromatised Mo Kα (λ = 0.71073 Å) radiation at the temperature indicated in the following tables. The data collection, cell determination and data reduction were all performed with the APEX software. All structures had intensities corrected for Lorentz and polarization effects and for adsorption using SAINT. All structures were solved by direct methods using SHELXS and refined on F^2 using all data by full-matrix least squares procedures using SHELXL-97. Unless otherwise stated all non-hydrogen atoms were refined with anisotropic displacement parameters. Hydrogen atoms were included in calculated positions with isotropic displacement parameters 1.2 and 1.5 times the isotropic equivalent of their carrier carbon atoms. Some of the refinements reported may change a little upon preparation for final publication. The crystal structure pictures were generated using Olex[2] [1].

[1] O. V. Dolomanov, L. J. Bourhis, R. J. Gildea, J. A. K. Howard, and H. Puschmann, *Journal of Applied Crystallography*, 2009, **42**, 339.

Table A1. Crystal data and structure refinement for **2.10**, **2.11**, **2.12**, **2.13**

Compound	**2.10**	**2.11**	**2.12**	**2.13**
Empirical formula	C16 H27.80 Cl Co N4 O9.90	C13 H26 Cl4 Co N5 O2 Zn	C12 H28 Cl Co N4 O6	C10 H10 Cl Co N6 O6
Formula weight	529	550.49	418.76	404.62
Temperature (K)	296(2)	112(2)	293(2)	296(2)
Wavelength	0.71073	0.71073	0.71073	0.71073
Crystal system	Monoclinic	Monoclinic	Monoclinic	Monoclinic
Space group	C2/c	$P2_1/n$	$P2_1/c$	$P2_1$
Unit cell dimensions: a(Å)	23.5815(11)	9.5754(3)	10.2882(17)	10.4102(6)
b(Å)	13.5077(5)	13.1438(4)	12.738(2)	12.7755(6)
c(Å)	14.2947(6)	16.1929(5)	13.267(2)	13.0729(6)
α (°)	90	90	90	90
β (°)	105.8310(10)	95.9850(10)	96.273(6)	95.9870(10)
γ (°)	90	90	90	90
Volume ($Å^3$)	4380.6(3)	2026.88(11)	1728.2(5)	1729.15(15)
Z	8	4	4	4
Density (calculated) Mg/m^3	1.604	1.804	1.609	1.554
Absorption coefficient mm^{-1}	0.966	2.548	1.184	1.185
F(000)	2200	1120	880	816
Crystal size mm^3	0.54 x 0.32 x 0.09	0.52 x 0.38 x 0.18	0.4 x 0.2 x 0.1	Unknown
Theta range for data collection (°)	2.45 to 25.00	2.53 to 25.05	2.22 to 25.05	1.57 to 27.50
Reflections collected	21713	9019	8167	28026
Independent reflections [R(int)]	3855 [0.0588]	3295 [0.0208]	2983 [0.0776]	7965 [0.0412]
Completeness to theta = 25.05° (%)	0.999	0.916	0.976	0.999
Data / restraints / parameters	3855 / 9 / 316	3295 / 5 / 250	2983 / 4 / 243	7965 / 1 / 434
Goodness-of-fit on F^2	1.088	1.061	0.961	0.801
Final R_1 indices [I>2sigma(I)]	0.0456	0.0218	0.048	0.0397
wR_2 (all data)	0.1215	0.055	0.1188	0.1213
Largest diff. peak and hole ($e.Å^{-3}$)	1.738 and -1.504	0.486 and -0.327	0.729 and -0.655	0.980 and -0.705
Flack parameter where applicable				

Table A2. Crystal data and structure refinement for **2.14**, **4.10**, **4.11**

Compound	**2.14**	**4.10**	**4.11**
Empirical formula	C12 H 26 Cl Co N4 O4	C13 H22 Cl Co N4 O8	C13 H22 Cl Co N4 O8
Formula weight	416.75	456.73	456.73
Temperature (K)	296(2)	118(2)	132(2)
Wavelength	0.71073	0.71073	0.71073
Crystal system	Monoclinic	Monoclinic	Orthorhombic
Space group	$P2_1/n$	$P2_1/n$	Pbca
Unit cell dimensions: a(Å)	7.5702(12)	7.7569(4)	13.722(3)
b(Å)	21.160(3)	18.9498(10)	14.333(6)
c(Å)	12.3205(19)	12.5721(6)	18.494(8)
α (°)	90	90	90
β (°)	96.930(8)	97.362(3)	90
γ (°)	90	90	90
Volume ($Å^3$)	1959.1(5)	1832.76(16)	3637(2)
Z	4	4	8
Density (calculated) Mg/m^3	1.413	1.655	1.668
Absorption coefficient mm^{-1}	1.044	1.133	1.141
F(000)	872	944	1888
Crystal size mm^3	0.36 x 0.28 x 0.04	Unknown	0.48 x 0.12 x 0.03
Theta range for data collection (°)	1.92 to 24.99	1.96 to 25.05	2.66 to 25.05
Reflections collected	36332	20261	19953
Independent reflections [R(int)]	3430 [0.1258]	3222 [0.0396]	3144 [0.1172]
Completeness to theta = 25.05° (%)	0.999	0.991	0.978
Data / restraints / parameters	3430 / 0 / 246	3222 / 0 / 289	3144 / 2 / 250
Goodness-of-fit on F^2	1.083	1.134	1.007
Final R_1 indices [I>2sigma(I)]	0.1203	0.0518	0.0647
wR_2 (all data)	0.3425	0.1642	0.1871
Largest diff. peak and hole ($e.Å^{-3}$)	1.843 and -1.286	1.154 and -1.042	1.064 and -0.915
Flack parameter where applicable			